MASTERARBEIT / MASTER'S THESIS

Titel der Masterarbeit / Title of the Master's Thesis

„Cultivation of *Nostoc commune* utilizing periodical desiccation-rehydration"

verfasst von / submitted by

Dipl.-Ing. Alexander M. Bürger, BSc BSc

angestrebter akademischer Grad / in partial fulfilment of the requirements for the degree of

Master of Science (MSc)

Wien, 2023/ Vienna, 2023

Studienkennzahl lt. Studienblatt / degree programme code as it appears on the student record sheet:	UA 066 832
Studienrichtung lt. Studienblatt / degree programme as it appears on the student record sheet:	Masterstudium Botanik
Betreut von / Supervisor:	Ao. Univ.-Prof. Mag. Dr. Michael Schagerl

Kurzfassung

Nostoc commune, ein Cyanobakterium mit kosmopolitischer Verbreitung, kommt auf einer Vielzahl von Substraten wie Sandböden, Wiesen und Felsen vor. Es bildet makroskopische Kolonien, die im feuchten Zustand gallertartig und braun-grün sind. Dieses Cyanobakterium ist Austrocknung gegenüber sehr tolerant und kann lange Trockenperioden überleben. Wenn die Kolonien durch Regen wieder hydratisiert werden, erholen sie sich schnell und die Zellen nehmen die Photosynthese wieder auf. Terrestrische *Nostoc*-Arten produzieren zahlreiche chemische Stoffe, die hohes Potenzial für verschiedene Anwendungen in Bereichen wie der Lebensmittelindustrie und Pharmazie aufweisen. *Nostoc* wächst jedoch sehr langsam und es gibt bisher keine wirtschaftlich praktikable Kultivierungsmethode. In dieser Studie wurde die Chlorophyllfluoreszenz von Kolonien im Freiland gemessen, um den physiologischen Zustand von Kolonien an zwei unterschiedlichen Standorten zu vergleichen und Rückschlüsse auf günstige Wachstumsbedingungen zu ziehen. Außerdem wurden zwei neu entwickelte automatische Bewässerungsmethoden unter verschiedenen Bedingungen anhand im Feld gesammelten Materials getestet. Es zeigte sich, dass eine periodische Austrocknung für eine erfolgreiche Kultivierung entscheidend ist. Die neu entwickelte Lift-Methode, bei der die Proben alle 24 Stunden für 20 Minuten in ein stickstofffreies BG11-Medium eingetaucht wurden, erzielte den höchsten Trockenmassenzuwachs (durchschnittlich über 500 % nach 21 Tagen Kultur), der fünfmal höher ausgefallen ist als für permanent submers kultivierte Proben. Sowohl kürzere als auch längere Austrocknungsintervalle führten zu geringeren Wachstumsraten. Darüber hinaus deuten die Ergebnisse darauf hin, dass sich Stickstoff negativ auf das Wachstum und die Performance der *N. commune*-Kolonien auswirkt. Der in dieser Studie entwickelte Ansatz bietet eine effiziente Methode für die Kultur von *N. commune*, die für die großflächige Kultivierung von terrestrischen *Nostoc*-Kolonien entscheidend sein könnte.

Schlagwörter: *Nostoc commune*, Kultivierung, Austrocknung, Rehydrierung, Stickstoff, Chlorophyllfluoreszenz

Abstract

The cosmopolitan cyanobacterium *Nostoc commune* is found on various substrates such as sandy soils, meadows, and rocks. In its hydrated state, it forms macroscopic gelatinous colonies with a brownish-greenish appearance. The species is highly tolerant against desiccation and survives long drought periods. When rehydrated, the cells quickly recover and perform photosynthesis again. Terrestrial *Nostoc* species produce many valuable compounds with high potential for various applications in the food industry and pharmacy. However, *Nostoc* grows very slowly and no economically feasible cultivation method has yet been established. We compared the chlorophyll fluorescence colonies growing in two contrasting sites to draw conclusions about favorable growth conditions. Based on this information and on literature surveys, we tested a newly developed automatic irrigation system and provided different settings to collected field material. We were able to demonstrate that periodic dehydration is crucial for successful cultivation. The newly developed lift method, which was programmed to submerge the samples every 24 hours for 20 minutes into nitrogen-free BG11 medium, achieved the highest dry mass gains (over 500 % on average after 21 days), about five times higher compared to samples permanently submerged. Both shorter and longer desiccation intervals resulted in lower biomass yield. Additionally, our findings highly suggest that nitrogen supply adversely affects the growth and health status of *N. commune* colonies. The approach developed in this study provides an efficient method for growing *N. commune*, which might pave the way for large-scale cultivation of terrestrial *Nostoc* colonies.

Keywords: *Nostoc commune,* cultivation, desiccation, rehydration, nitrogen, chlorophyll fluorescence

Acknowledgements

I want to express my sincere gratitude to my supervisor, Professor Michael Schagerl (Team Phycology, Department of Functional and Evolutionary Ecology, University of Vienna), for his invaluable guidance and support throughout my research. His expertise and insights have been instrumental in shaping my understanding of the fascinating world of algae. I am also grateful for making it possible for me to conduct my field study at the WasserCluster Lunz and for providing me with all the necessary devices.

Furthermore, I would like to thank my colleague Anna Broschek for sharing her expertise with *Nostoc* with me, as well as my colleagues Alexander Kaptejna and Rainer Siedler, who helped me in the laboratory whenever I had a question.

My heartfelt appreciation goes to my family, whose unwavering support has been my anchor throughout my educational career and has always encouraged my scientific and biological interests. I am incredibly grateful to my mother, who has always been there for me with her invaluable love, advice and support. I would like to extend my deepest thanks to my father for his unyielding support. I want to express special thanks to my grandparents, who took me on countless trips to botanical gardens, natural history museums, zoos and special nature sites from an early age. These experiences ignited my passion for nature and inspired me to pursue a career in the field.

I want to extend my gratitude to Professor Ille C. Gebeshuber (Research Unit of Atomic and Plasma Physics at the Institute of Applied Physics, TU Wien) for her mentorship and for being a scientific role model for me.

Furthermore, I must express my gratitude to Friederike Grabner, my elementary school teacher, who recognized and supported my interest in the field of biology. Her encouragement and guidance were pivotal in shaping my academic path.

Table of Contents

Introduction

Nostoc

The genus *Nostoc* (*Nostoc*aceae, Cyanobacteria) consists of uniseriate and isopolar trichomes without branching; heterocytes and akinetes are usually present (Komárek, 2013). The name *Nostoc* derives probably from the portmanteau **Nostoch,** which was created by Paracelsus and is composed of the Old English "**Nost**hryl" (today nostril) and the German "Nasenl**och**", both words for the same anatomical part of the nose (Potts, 1997). Paracelsus observed that *Nostoc* seems to appear out of nowhere after precipitation events. He explained it as a fiery excretion shot from a purifying star that turns to slime when it touches the earth (Paracelsus, 1566). This is probably why Paracelsus coined the term "Nostoch", seeing it as a kind of sputum expelled from the nostrils of purifying stars. The genus comprises around 250-300 described species, which, however, will need further revision as it is rather heterogenous (Komárek, 2013). *Nostoc* species are found worldwide and colonize various habitats, from terrestrial over freshwater to marine (Fidor et al., 2020; Potts M, 2000). While *N. flagelliforme* occurs in arid deserts, *N. punctiforme* was even found in the abyssal benthos of Lake Baikal at a depth of 890 m (X. Gao et al., 2012; Hu et al., 2012; Tikhonova et al., 2017). Because *Nostoc* species are diazotrophic, they also established symbiotic relationships over a wide range of organisms, for example, bryophytes such as hornworts (e.g., *Anthoceros*) and liver mosses (e.g., *Blasia*), pteridophytes (e.g., *Azolla*) and spermatophytes (Meeks et al., 1988; Meeks & Elhai, 2002; Rodgers & Stewart, 1977). *Nostoc* species were even found in symbiosis with gymnosperms, namely in the coralloid roots of several Cycads species in eleven genera (De Philippis et al., 1996; Margheri & Allotta, 1993; Meeks & Elhai, 2002). Particularly noteworthy, endosymbiosis with angiosperms was found in *Gunnera*, which produces specialized stem glands through which the cyanobacteria can enter the cell tissue. In this way, the plant profits from the N2-fixation abilities of *Nostoc.* This is the only known symbiosis between an angiosperm and a cyanobacterium (Bergman et al., 1992; Guevara et al., 2002). In addition, *Nostoc* is commonly found as photobionts in lichens (Rikkinen, 2013). Furthermore, a unique endosymbiosis with the arbuscular mycorrhiza fungus *Geosiphon pyriformis* is known; it is only found in a few locations in Germany and Austria. The fungus incorporates *Nostoc* cells via endocytosis into its hyphae and forms characteristic bladder structures in which the cyanobacterial cells divide and become physiologically active. As the fungus depends on the cyanobacterium, it is classified as an obligate symbiont. Such an endosymbiosis is not regarded as lichen per definition (Kluge et al., 2002; Schüßler et al., 2007; Schüßler & Kluge, 2001; Schüßler & Wolf, 2005).

Like most cyanobacteria, *Nostoc* is phototrophic, but some species are able to shift to a heterotrophic lifestyle (especially symbiotic taxa). Inside the host tissue, the light supply is often limited due to self-shading. The specimens use exogenous sugars provided by the host via a homoacetic fermentation under dark anaerobic conditions, which is a remarkable trait within cyanobacteria (De Philippis et al., 1996; Khoja & Whitton, 1975; Margheri & Allotta, 1993; Stal & Moezelaar, 1997). Moreover, dissociated cells from *N. flagelliforme* were successfully grown for seven days under dark heterotrophic conditions, feeding on xylose and glucose (Jia et al., 2012; Yu et al., 2009).

Nostoc commune

- **Phylum:** Cyanobacteria
    - **Order:** *Nostoc*ales
        - **Family:** *Nostoc*aceae
            - **Genus:** *Nostoc*
                - **Species:** *Nostoc commune*

Figure 1 Systematic position on *Nostoc commune*.

Nostoc commune is a cosmopolitan species found on every continent in a wide range of habitats from tropical islands to the deglaciated areas of Antarctica (Novis et al., 2007a; Potts M, 2000; Tripathi et al., 1970). This taxon lives subaerophytic on various substrates such as sandy/clay soils and bedrock. The habitats range from semideserts, edges of ways to meadows and moist soils (Komárek, 2013; Mollenhauer et al., 1999). In the dry state, *N. commune* can tolerate temperatures from -269 to 70 °C for 36 h with only a slightly reduced metabolic rate after rehydration. In addition, the colonies can tolerate salinities up to 20 *g/kg* NaCl and a pH range from 3 to 10 (Sand-Jensen & Jespersen, 2012).

One individuum consists of barrel- to spherical-shaped cells aligned in uniseriate trichomes (Figure 2 d). Often, trichomes possess terminal or intercalary heterocytes for fixation of atmospheric N_2 (Komárek, 2013). The single filaments are packed together in an extracellular polysaccharide (EPS) matrix, forming macroscopic lobate colonies, which can build layers up to 20 cm (Mollenhauer et al., 1999; Potts M, 2000). Hydrated colonies have a gelatinous to cartilaginous texture and show mostly an olive-green color or are yellow-brown in different shades (Figure 2 a & b). Desiccated colonies are papery to leathery and are often dark brown with a green tone, sometimes appearing nearly black (Figure 2 c).

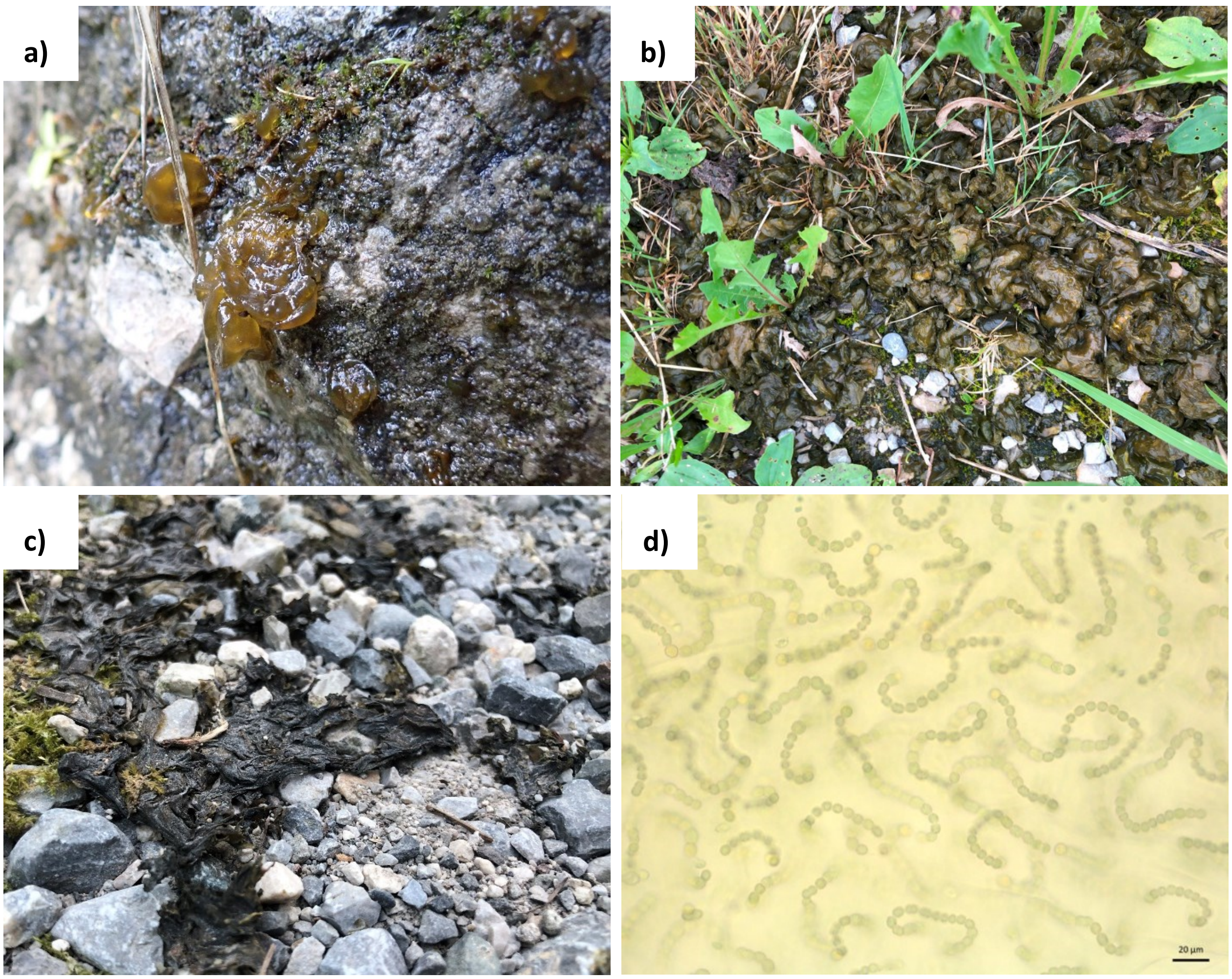

Figure 2 Pictures of *Nostoc commune*: hydrated colonies on a) carbonate rock, b) old gravel road, c) desiccated colonies and d) microscopic image of a colony. ©Alexander M. Bürger

The production of EPS and its composition of monosaccharides varies with different environmental conditions such as pH, nitrogen and CO_2 availability (Z. Huang et al., 1998; Otero & Vincenzini, 2003). The outermost layer of the EPS matrix is rich in silica and calcium.

Interestingly, it was observed that although various microorganisms colonized the outer surface, hardly any were able to penetrate this outer layer (Hill, Peat, et al., 1994). Analysis of the EPS showed that it also includes scytonemin and mycosporine-like amino acids (Hill, Hladuns, et al., 1994; Inoue-Sakamoto et al., 2018; Sakamoto et al., 2019). In addition, a diversity of water stress proteins is found in the gelatinous matrix, which are supposed to play a key role in desiccation tolerance (Sakamoto et al., 2019).

The desiccation tolerance of *N. commune* is remarkable. Studies showed that dried colonies rehydrated after 87 years and after 107 years were still viable (Cameron, 1962; Lipman, 1941). The exact mechanisms of how *Nostoc* can survive such long periods of desiccation and regain activity after rehydration are still unknown. However, *N. commune* cells lack organelles encompassed by membranes, which would be easily damaged during desiccation/rehydration and ice crystal formation (Davey, 1989). It was found that EPS play an essential role in desiccation and stress tolerance (Tamaru et al., 2005). Shirkey et al. (2003) showed that long-term desiccation induces DNA modifications to prevent degradation, damage from radicals in the dry state and loss of cell viability. During rehydration, these modifications are removed. Due to the EPS layers, *N. commune* can take up water 23 times its dry mass during rehydration, which happens in nature primarily by rain (Satoh et al., 2002). This enables *N. commune* to stay photochemical active after rain ceases for a certain period, for example, in Arctic hydro-terrestrial environments for up to two weeks (Kvíderová et al., 2011).

N. commune is closely related to *N. sphaeroides*, *N. flagelliforme* and *N. punctiforme* (X. Gao et al., 2011) and the former two are sometimes referred to as varieties of *N. commune* (Dvořák et al., 2020; Han et al., 2013; Huo et al., 2021; Potts M, 2000; Yang et al., 2011).

Potential use cases for terrestrial *Nostoc*

The terrestrial species *Nostoc commune*, *N. flagelliforme* and *N. sphaeroides* are edible and yield high nutritional value (Han et al., 2013; Liang et al., 2022). In particular, the hair-like *N. flagelliforme* has a long culinary history, as it was already consumed as early as the Jin Dynasty (265-317 AD) (K. Gao, 1998). Sources document its use in traditional Chinese medicine over 400 years ago (Han et al., 2013). *N. flagelliforme* is called ‘Fat Choy’ in Cantonese or ‘FaCai’ in

Mandarin, both names referring to the hair-like structure of the colonies (Pui-Hay But et al., 2002). From 1970 to 2000, *N. flagelliforme* sites were heavily exploited because it is a demanded delicacy in China. As the colonies show only a 6 % growth rate per year, the population decreased drastically, thus yielding heavy soil erosion in this area (X. Gao et al., 2016). Consequently, collecting this taxon was prohibited in China in 2000 to set a measure against the desertification of the northern Chinese regions (Pui-Hay But et al., 2002).

When fed to rats, *N. flagelliforme* did not exhibit toxic effects (Takenaka et al., 1998). In addition, *N. sphaeroides* (in the study referred to as *N. commune* var. *sphaeroides*) showed no significant toxic effects at long-term diet supplementation of up to 5 % (Yang et al., 2011). However, Dvořák et al. (2020) identified the neurotoxic amino acid β -N-methylamino-L-alanine in some *N. flagelliforme* strains. As different strains of the same species could show intraspecific differences in the composition of secondary metabolites, health assessments are highly recommended before using a particular strain as a food supplement.

Besides the nutritional value of *N. commune*, it possesses a manifold of chemical compounds with pharmaceutical potential (Z. Li & Guo, 2018; Nowruzi et al., 2018). For example, its consumption decreased serum cholesterol in rats (Hori et al., 1994). Furthermore, a substance called noscomin exhibited antibacterial activity (Jaki et al., 1999). Nostocine, a chemical compound isolated from *N. commune*, inhibits the growth of *Propionibacterium acnes* and reduces inflammation caused by this bacterium, which is the leading cause of acne vulgaris (Itoh et al., 2014). Nostoflan, an acidic polysaccharide isolated from *N. flagelliforme,* was reported to be a potential anti-herpes agent (Kanekiyo et al., 2007). The water stress protein WSP1 expressed antitumor activities against colon cancer (Guo et al., 2015). EPS extracts of *N. commune* exhibit a wound-healing effect and are anti-allergic (Tseng et al., 2021). Moreover, the polysaccharides show high moisture retention capacity, are antioxidative and positively affect the gut microbiota (H. Li et al., 2011, 2021).

In addition, the EPS could be potentially used for coatings or membranes in biomedical applications (Rodriguez et al., 2017). Polysaccharides gained from *N. commune* can also be used as a thickening additive for food and beverages (Torres-Maza et al., 2020).

Further applications could be soil restoration as *N. commune* can pioneer on unfavorable grounds and can fixate N_2 and CO_2, thus increasing soil fertility. Furthermore, it increases the water retention capacity and reduces the soil albedo (Román et al., 2018; Roncero-Ramos, Román, et al., 2019). Therefore, it facilitates the colonization of other organisms, such as mosses and higher plants (Sand-Jensen & Jespersen, 2012). Moreover, *N. commune* shows the potential for remediation of radioisotopes from polluted soils (Katoh et al., 2012). *Nostoc* could also be a potential candidate for Mars colonization as it could tolerate Mars-like environments, including high UV radiation, low temperatures and drought (Ye et al., 2021). Furthermore, *N. commune* biofilms could serve as a habitat for other bacteria on Mars (Jänchen et al., 2016). It can even be used as a plant substrate, which acts simultaneously as a fertilizer through its N_2 fixation ability, which would be suitable for space agriculture (Katoh et al., 2012).

To sum up, *N. commune* and the other terrestrial species have many applications in the food industry, cosmetics, habitat restoration, phytoremediation and pharmacy. Therefore, the cultivation of these cyanobacteria is of very high interest.

Former cultivation approaches

Plenty of promising use cases of terrestrial *Nostoc* species make cultivation very in demand, but so far, no method could be established to grow *N. commune* efficiently. Mostly, the cultivated colonies deviate from their natural shape, have a slow growth rate and tend to disintegrate (Han et al., 2013; Scherer & Zhong, 1991). CO_2 diffusion in air is much higher than in water. Therefore, Sand-Jensen (2014) described the optimal habitat as wet soils, where inorganic carbon and nutrients are supplied from the substrate while the colony can still take up CO_2 from the air.

To our knowledge, only a few studies focused on culturing *Nostoc commune*. The closely related species *Nostoc flagelliforme* (formerly referred to as *N. commune var. flagelliforme* has been a primary interest of several studies as this species is a delicacy in some provinces of China, but a successful cultivation method of macroscopic colonies could not be established (Cui et al., 2017; K. Gao et al., 1998; Han et al., 2013; Scherer & Zhong, 1991). It was reported that *N. flagelliforme* colonies cannot survive permanent hydration (Scherer & Zhong, 1991). One suggested explanation is that bacteria disintegrate the gelatinous colonies if no periodical desiccation occurs that inhibits their growth (K. Gao & Ye, 2003). Nevertheless, it was managed to establish liquid cultures of free-living individuals/microcolonies mainly for extracellular polysaccharide production (K. Gao & Ye, 2003; Jia et al., 2012; Yu et al., 2010). Visible colonies from these microcolonies were susceptible to desiccation and high irradiation and unsuitable for restoring the natural populations (X. Gao et al., 2015, 2016). There have been several attempts to cultivate *N. flagelliforme* without submergence. K. Gao & Yu (2000) found the best results for watering cyanobacterial mats at enriched CO_2 concentration, reaching a biomass gain of 31 % within 15 days. Another group cultivated *N. flagelliforme* on cellulose nitrate-acetate membranes placed on solid BG11/BG11$_{N0}$ plates. The membranes were regularly removed and dried to simulate periodical desiccation. The samples did show a similar shape to the natural thalli, especially in combination with low UV-B treatment (Feng et al., 2012). However, the growth rates stayed low in all previous studies and the handling efforts were high. There is obviously a need for establishing an efficient and easy cultivation approach for terrestrial *Nostoc* species.

Chlorophyll fluorescence

Measuring variable chlorophyll fluorescence has become a common application to estimate photosynthetic efficiency and electron transport rate, especially since high-quality and cheap measuring devices are on the market. If a chromophore molecule (such as chlorophyll) gets excited by absorbing a photon, an electron is elevated to a higher level. There are the following primary ways by which the molecule is de-excited and returns to the ground state (Campbell et al., 1998):

Photosynthesis (energy transfer including photochemical reactions)

Photons are absorbed via intrinsic light-harvesting complexes consisting of chlorophylls and carotenoids in eukaryotic photoautotrophs. Cyanobacteria developed small bodies called phycobilisomes as extrinsic light-harvesting complexes, which are located at the periphery of the thylakoid membrane. Phycobilisomes consist of phycobiliproteins such as phycoerythrin, phycocyanin and allophycocyanin. Light harvesting complexes have in common that excited pigments pass their energy onto adjacent pigment molecules (Mirkovic et al., 2017). The energy transfer between the chromophores of a light-harvesting complex happens through resonant energy transfer, which involves quantum coherence (Fassioli et al., 2014). In this way, the energy is transferred to the reaction centers of both photosystems (PSI and PSII) (Mullineaux, 2008).

The reaction centers consist of chlorophyll *a* molecules with a special pair of chlorophyll-a molecules placed at the core (P680 in PSII and P700 in PSI) (Ishikita et al., 2006). In PSII, the electron of the excited P680* gets separated and moves through the electron transport chain (ETC). The electron is accepted by the plastoquinone found at the binding site Q_A of the reaction center. This plastoquinone is tightly fixated on the binding site and is not exchanged. It acts as a single electron recipient and is just temporarily reduced. It passes the received electron onto another plastoquinone bound to site Q_B, which needs to be reduced two times before it can take up two protons from the stroma, forming a reduced quinone QH_2. Consequently, it gets replaced by an oxidized quinone and leaves the reaction center to perform the next step of the ETC (Lambreva et al., 2014).

Heat dissipation

Another way to reach the ground state for a chromophore is to release the energy difference in the form of heat, often referred to as non-photochemical quenching (Murchie & Lawson, 2013).

Fluorescence

Alternatively, the energy difference between the excited and ground states can be emitted as a photon (= fluorescence). This can be measured by a photodetector (Campbell et al., 1998).

To summarize, absorbed light energy is converted to other forms via three major pathways: photochemical reactions (photosynthesis), heat dissipation and chlorophyll fluorescence (Murchie & Lawson, 2013). These three mechanisms stand in competition with each other, summing up to the following energy equation:

$$Absorbed\ photons = photosynthesis + heat\ dissipation + chlorophyll\ fluorescence$$

As a consequence, if the chlorophyll fluorescence is measured, we can derive information about photosynthesis (photochemical quenching) and heat dissipation (nonphotochemical quenching). Because every photon remitted cannot be used for photosynthesis, we can estimate the efficiency of photochemistry. If the chlorophyll fluorescence is measured below 700 nm at room temperature, most of the signal is emitted by the chlorophyll pigments of PSII, as the PSI has a negligible contribution below this threshold. If longer wavelengths are considered (PSI has its emission peak at 730 nm), the contribution of PSI regarding chlorophyll fluorescence is about 30 % in C_3 plants and 50 % in C_4 plants (Genty et al., 1990; Pfündel, 1998). In cyanobacteria, the ratio PSI:PSII ranges from 2:1 up to 5:1 (Luimstra et al., 2019).

Pulse-Amplitude-Modulation (PAM) fluorescence

In the last decades, PAM fluorescence systems have been one of the most important and widely used approaches to measuring chlorophyll fluorescence. These systems use measuring light in µs-range pulses with very low intensity. Applied with low frequency, they do not trigger photochemical reactions, so it is possible to measure the dark fluorescence. The modulated measuring light allows photodetectors to reject fluorescence caused by non-modulated light, such as ambient light (Schreiber, 2004). Due to these possibilities, chlorophyll fluorescence of the PSII can be measured at both light and dark conditions.

Dark-adapted measurements

If the organism is adapted to dark conditions, all reaction centers are oxidized (open = able to accept an electron). Plants exposed only to the weak modulated beam allow measuring the minimal fluorescence (F_0), which does not induce photochemical reactions (so the quinones stay maximally oxidized). As the next step, a short saturating actinic pulse with high intensity is applied to close all photo reaction centers. This means all plastoquinones at Q_A become reduced and cannot take up electrons anymore. Consequently, the energy cannot leave the excited chlorophyll molecules via photochemical reactions and the fluorescence becomes maximal (F_m) (Baker, 2008). The difference between the maximum and minimal fluorescence is called variable fluorescence ($F_v = F_m - F_0$). Furthermore, the maximum quantum yield of PSII (=dark yield) can be calculated as the ratio of the variable and maximum fluorescence (F_v/F_m)(Murchie & Lawson, 2013; Schreiber, 2004). In other literature, it is also referred to as maximum quantum efficiency of the PSII photochemistry (Baker, 2008; Campbell et al., 1998).

Light-adapted measurements

During ambient light exposure, reaction centers are partly closed (Q_A is partly reduced), which leads to increased chlorophyll fluorescence (Schreiber, 2004). Genty et al. (1989) introduced a method to measure the fluorescence parameter ($F_m´$ - F_s)/ $F_m´$. Firstly, the steady-state fluorescence (Fs) is measured at ambient light conditions without inducing further photochemical reactions. As a next step, the sample is exposed to a short saturating pulse to fully reduce Q_A, thus measuring the maximum fluorescence under actinic light ($F_m´$). The ratio ($F_m´$ - F_s)/ $F_m´$ is called effective quantum yield Φ_{PS2} or PSII operating efficiency (Baker, 2008; Schreiber, 2004).

The effective quantum yield has proven to be one of the most robust and valuable fluorescence parameters during light exposure (Baker, 2008). This parameter shows a linear relationship to the linear electron flux and is sensitive to factors that affect the efficiency of open reaction centers, such as photoinhibition and non-photochemical quenching (Genty et al., 1989). When CO_2 assimilation resembles the main sink for ATP and NADPH and thus for electrons of the linear electron flux, Φ_{PS2} proved to be a valuable relative measure of the quantum yield of CO_2 assimilation (Φ_{CO2}). Moreover, interpretations and comparisons using F_v/F_m are more reliable than using the values of F_0 and F_m directly, as F_v/F_m is a relative measure, so differences between samples and measurements such as chlorophyll-content and distance of the probe are levelled out (Baker, 2008).

Interestingly, F_v/F_m seems to be rather constant, around 0.83 for various C_3 plants (not stressed), underlying its importance as maximum efficiency for higher pants (Björkman & Demmig, 1987). However, cyanobacteria show much lower values, mainly in the range of 0.2 - 0.6 (Campbell et al., 1998; Lüttge et al., 1995). There have been several reasons discussed so far. First of all, the fluorescence of the phycobilisomes interferes with the chlorophyll fluorescence. Secondly, the respiratory and the photochemical electron flow overlaps in the thylakoid membrane, reducing commonly used plastoquinones in the dark-adapted state (Milou Schuurmans et al., 2014). Thirdly, the ratio between PSI and PSII is much higher, affecting the non-variable fluorescence, particularly if wavelengths above 700 nm are included in the measurements (Schuurmans et al., 2015).

The aim of this study

We first studied *N. commune* at different locations in the field to get insight into the autecology of this taxon. We measured variable chlorophyll fluorescence and recorded environmental parameters (temperature, available light and relative air humidity) in parallel. Based on the chlorophyll fluorescence, we drew conclusions about the photosynthetic activity and the vitality of the cyanobacteria under different conditions. We also evaluated the time spans after rain events, at which colonies stayed photochemically active. Based on the results of the field survey, we designed cultivation experiments testing different substrates and media to develop an efficient method to grow terrestrial *Nostoc* macroscopic colonies.

We assume that periodical desiccation-rehydration is the key to the successful cultivation of terrestrial *Nostoc*. During air exposure, gas transport is facilitated. Furthermore, when the partly dried colonies are rehydrated, they absorb fresh medium, which ensures that all cells receive new nutrients. In contrast, if *N. commune* is kept hydrated permanently, the swollen gelatinous layer acts as a diffusion barrier, which impedes nutrition supply and gas exchange, especially for the innermost trichomes. As *N. commune* is mainly supplied with rainwater and is diazotrophic, we assume that a low nitrogen concentration resembles the natural situation and is, therefore, preferred by the cyanobacterium.

Two irrigation approaches were developed to test these hypotheses: an artificial rain system (sprinkler) and a platform that periodically submerges the samples (lift). Different watering intervals were tested to observe if periodical desiccation-rehydration positively affects the mass gain of *N. commune.* Moreover, media with different nitrogen concentrations were compared to evaluate the effect of nitrogen on the growth of colonies.

Material & Methods

Field experiments

A portable pulse-modulated chlorophyll fluorometer FMS 2+ (Hansatech Instruments Ltd, Norfolk, United Kingdom) was used to measure the effective quantum yield (light experiment) and the maximum quantum yield (dark experiment). Negative values due to measuring errors were set to zero. The air temperature and relative humidity were tracked in parallel with a HOBO® data logger (1-800-Loggers, ONSET, Bourne, MA, United States). In addition, photosynthetically active radiation (PAR; 400 -700 nm) was measured in lux with a HOBO® pendant logger (UA-002, ONSET). It was converted to the photosynthetic photon flux density (PPFD) [$\mu mol \cdot m^{-2} \cdot s^{-1}$] by multiplying it by 0.0185, which is a factor empirically determined for sunlight taken from Thimijan & Heins (1983). In order to approximate the relative electron transport rate (ETR) the standard formula for plant leaves: $rETR = \Phi PS2 * \mathrm{PPFD}$ was used (Schreiber, 2004; Schreiber et al., 1995).

The field experiments took place in the close vicinity of the WasserCluster Lunz. Around the area of the Lunzer See, two locations with high *Nostoc commune* occurrence were selected: (1) strong incoming irradiance and (2) weak irradiation.

Figure 3 Location of the first daylight and the dark experiment. *Nostoc commune* colonies were found at the concrete wall at the margin to the meadow.

(1) *Nostoc commune* grew on a small concrete wall adjacent to a steep meadow next to the WasserCluster Lunz building (Figure 3). The cyanobacteria were exposed to full sunlight most of the day and only shaded by the building till 09:00. A larger colony was selected for investigation. The Hansatech FMS 2+ was programmed to perform an effective yield measurement (light-adapted measurement routine, phi PSII function) at 15-minute intervals for four days.

A dark experiment was carried out to separate effects caused by irradiation from other environmental conditions: a black box was put over the colonies just before the sun began to rise. The box was removed after dusk to ensure Nostoc could be rehydrated by dew and rain during the night. Every 15 minutes, a measurement of the maximum quantum yield was taken.

(2) A moisty area with high *Nostoc* occurrence was taken as a comparison where *N. commune colonies* were shaded by *Petasites hybridus* (Figure 4). As this plant is an indicator of moist and fertile soils, it shows that this location stands in strong contrast (in terms of humidity, nutrition and exposition) to the previous wall (Ellenberg et al., 2001). Another daylight experiment was performed with the same settings to compare the chlorophyll fluorescence under these different conditions.

Pictures of the sky were taken with a fisheye lens from just above the *Nostoc* colonies. Subsequently, these images were used to calculate the site openness using the Gap Light Analyzer software V2 (Frazer et al., 1999).

Figure 4 Shaded location of *Nostoc commune* growing under the leaves of *Petasites hybridus*.

Culturing experiments

Biological material

Specimens were collected from various locations in the vicinity of the Lunzer See. The cyanobacteria were identified as *Nostoc commune* Vaucher ex Bornet et Flahault 1888 using Komárek (2013). Before beginning the experiment, the cyanobacteria were submerged in deionized water and mechanically cleaned of particles, such as soil, mosses, and other plant materials, under a stereo microscope. Several samples were examined under a microscope to assess the health of the cells, and necrotic portions of the colonies were removed. Following cleaning, *Nostoc* was air-dried at room temperature for two days. The dried *Nostoc* was then cut into small pieces using clean scissors and weighed with an MT5 Microbalance (Mettler Toledo, Columbus, Ohio, USA). The growth experiment utilized fragments with a dry mass ranging from about 0.5 to 2.5 mg.

Culturing Media

Various media were prepared for the growth experiments. Rainwater was collected using a collection tank and filtered through a fine mesh (0.2 µm) before being autoclaved at 121°C for 30 minutes. BG11, a standard medium for cyanobacterial culture, was prepared according to the protocol of the Sammlung von Algenkulturen Göttingen (2013), which is a modified version of Rippka and Herdman (1992) with the micronutrient composition taken from Kuhl and Lorenzen (1964): $NaNHO_3$ [1500 mg/l], $K_2HPO_4{\cdot}3H_2O$ [40 mg/l], $MgSO_4{\cdot}3H_2O$ [75mg/l], $CaCl_2{\cdot}2H_2O$ [36 mg/l], citric acid [6 mg/ml], ferric ammonium citrate [6 mg/ml], EDTA [1 mg/l], Na_2CO_3 [20 mg/l] and micronutrient solution (1ml for 1000 ml medium) (Kuhl & Lorenzen, 1964; Rippka & Herdmooan, 1992; Sammlung von Algenkulturen Göttingen, 2013). Previous studies often used either BG11 or nitrogen-free BG11 for culturing *Nostoc commune* and closely related *N. flagelliforme* (Feng et al., 2012; Guljamow et al., 2017; Qiu & Gao, 2002; Tripathi et al., 1970). To evaluate which medium is the most suitable for culturing *N. commune*, different mixtures of the BG11 medium were tested: BG11 standard (BG11), BG11 diluted 1:10 with Mili-Q water ($BG11_{diluted}$), BG11 with only a tenth of the $NaNHO_3$ concentration ($BG11_{N/10}$) and BG11 without nitrogen ($BG11_{N0}$).

Irrigation setups

Submersed approach

For the submerged setup, 48-well cell culture plates were taken (Cellstar®, Greiner Bio-One GmbH, Kremsmünster, Austria). Wells were filled with the respective medium, and one specimen was placed into each well (Figure 5). The medium was exchanged every five days to provide the cyanobacteria with fresh nutrients and minimize contamination of other organisms.

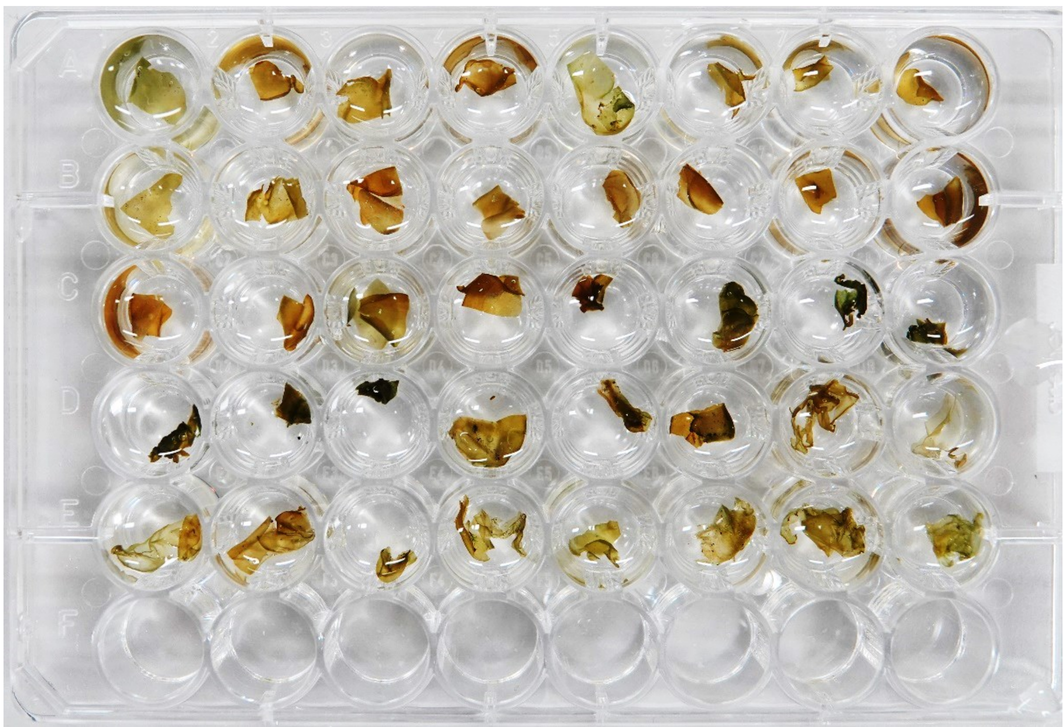

Figure 5 Foto of a permanently submerged culture.

Sprinkler approach

In order to mimic the natural water supply of *Nostoc commune* via rainfall, a sprinkler system (Whisper PowerPump SMALL V.3, Micro Rain Systems, Bad Altenburg, Germany) was implemented (Figure 6). The tank of the sprinkler system was filled with the respective medium. Initially, the samples were submerged in the medium for ten minutes. Afterwards, the samples were placed on a prepared substrate, depending on the experimental design. A time switch was programmed to irrigate the cyanobacteria at regular intervals.

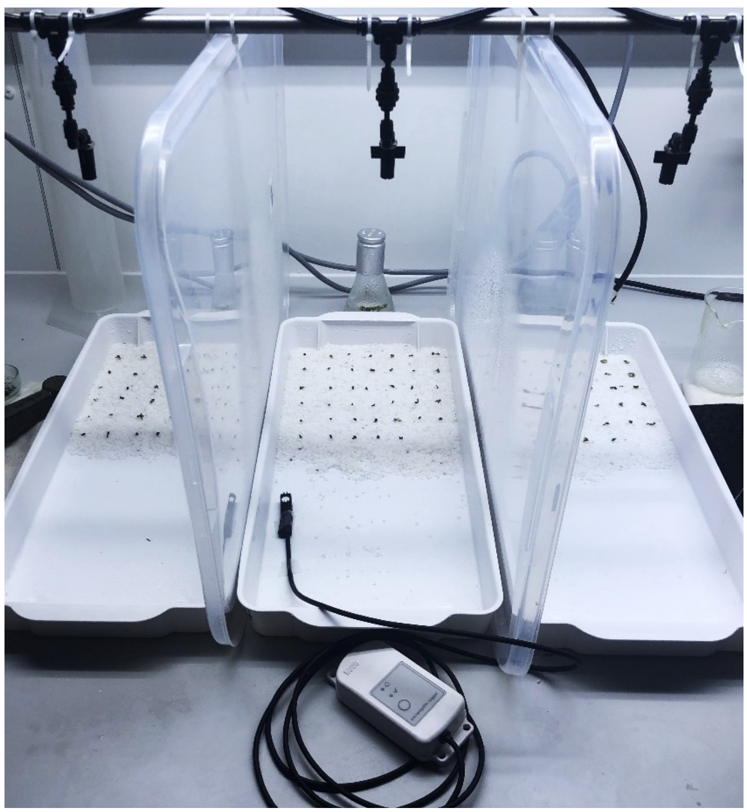

Figure 6 Example of a sprinkler set-up.

Lift approach

In order to ensure uniform hydration of all samples, we developed a new irrigation approach with a lifting platform built with LEGO® Technic building parts (Figure 7). The lift was controlled by a microcontroller (UNO R3, Elegoo, Shenzhen, China). It was programmed to immerse the sample holder into an aquarium (filled with medium) at regular intervals for a predetermined period of time. An ultrasonic detector was included to ensure that the lift travels to the bottom of the aquarium and then returns to its original position. A sample holder was constructed made of silicon chambers with a stainless-steel mesh bottom. This allowed the medium to enter when submerged and let the excess drip off when the stage was lifted out of the liquid (Figure 10). Cyanobacteria were either placed directly on the mesh or on marble chippings, which were placed on the mesh as substrate.

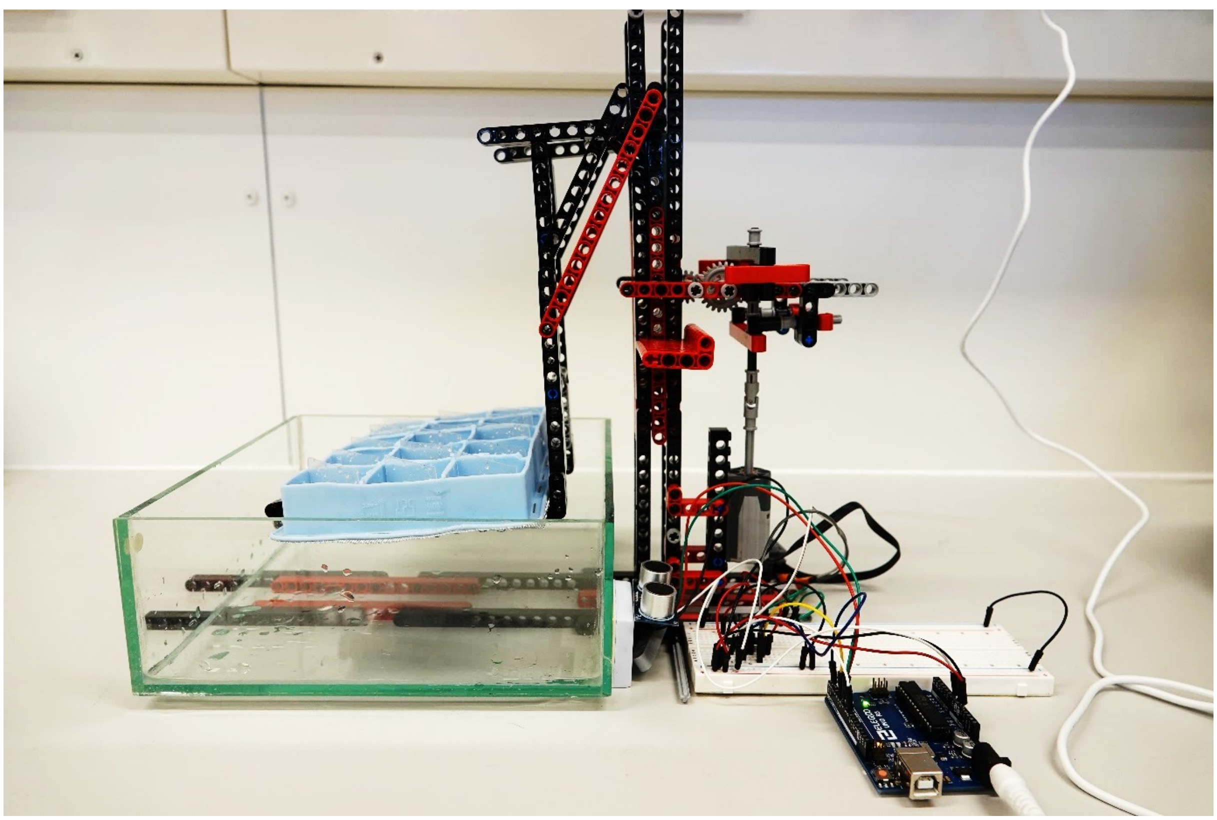

Figure 7 Picture of the constructed programmable lift.

Culturing experiments

Several culturing experiments were conducted to test the hypotheses presented in the introduction and to find the optimum growth conditions for *Nostoc commune* macroscopic colonies. The results of previous experiments were considered and used to design subsequent experiments (Figure 8).

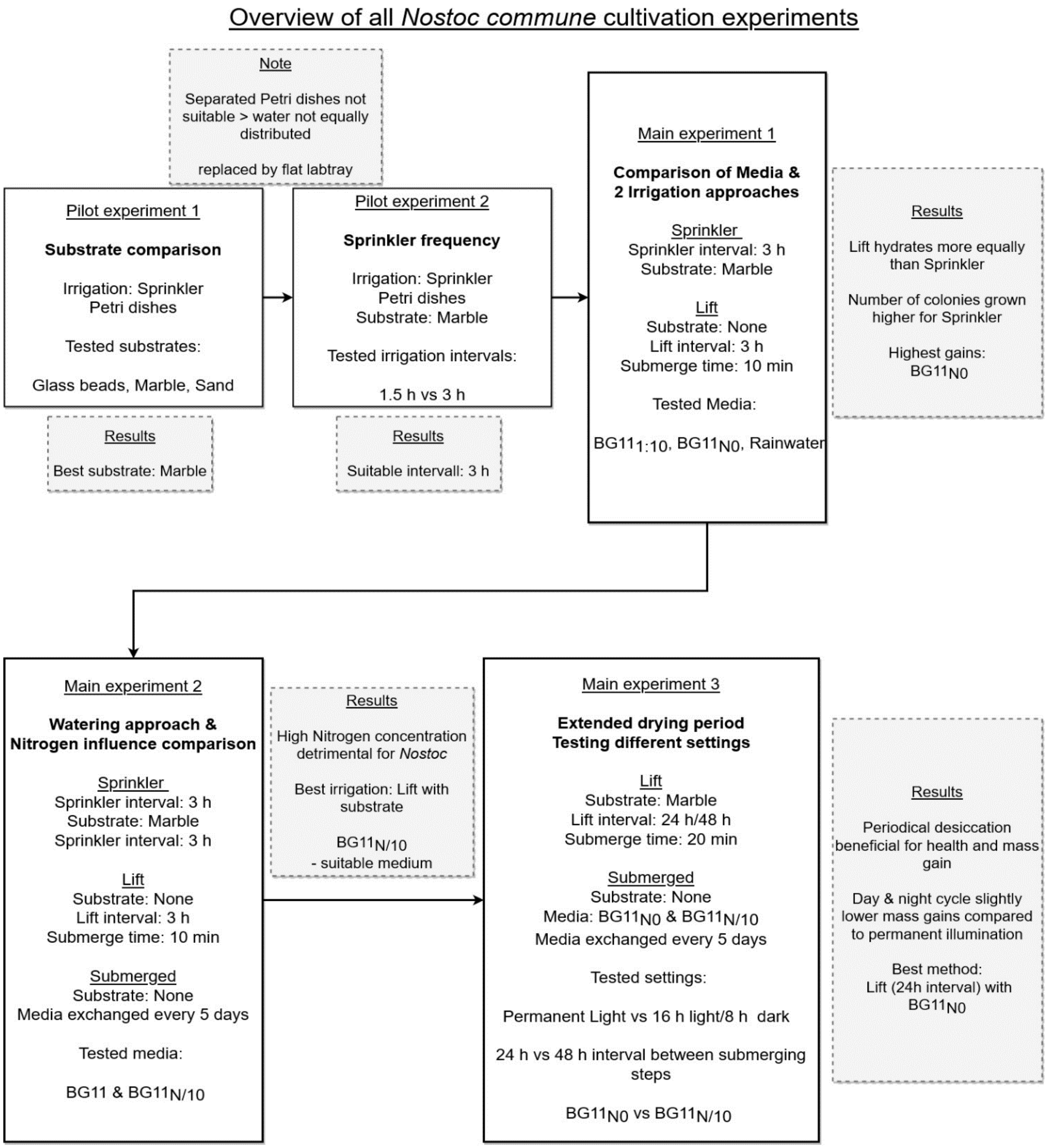

Figure 8 Flow diagram which depicts the order of executed experiments with their testing parameters and most important insights.

Pilot 1 -Substrates

We tested three substrates: fine quartz sand, white marble chippings and white seed beads. Before the experiment, the substrates were washed with Mili-Q water and put into an autoclave at 121°C for 30 minutes. Afterwards, the substrates were dried and filled into little glass Petri dishes, which were put into an aquarium (Figure 9). Ten *Nostoc* colonies were used for every substrate. At the beginning of the experiment, the colonies were submerged in the $BG11_{N0}$ medium. Irrigation was performed with the sprinkler system previously explained. It was activated every three hours, spraying approximately 28 ml of medium over the samples. The experiment was performed at room temperature (on average 23 °C) with a light/dark cycle of 16 h/8 h. The samples were exposed to light with a photon flux density of 35 $\mu mol \cdot m^{-2} \cdot s^{-1}$.

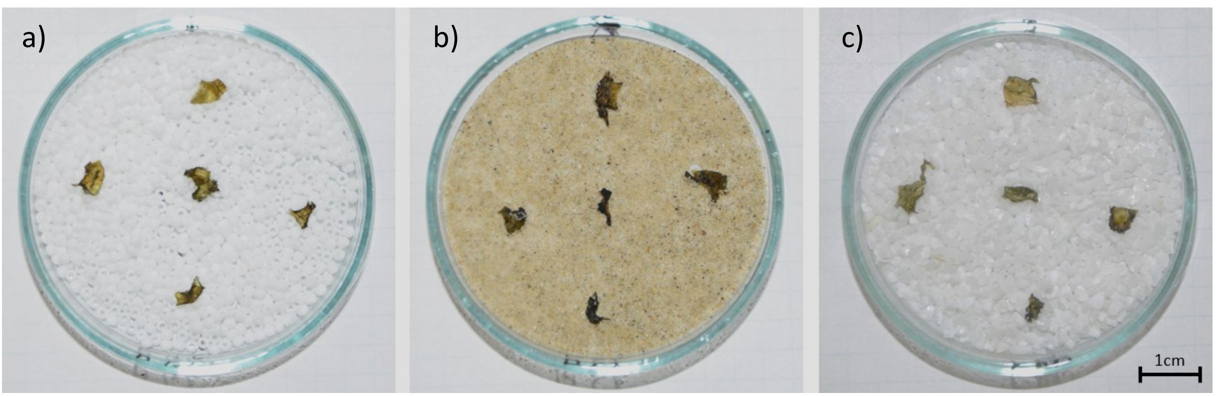

Figure 9 Nostoc commune samples in Petri dishes filled with the three different media: a) glass beads, b) quartz sand, c) marble chippings.

Pilot 2 – Irrigation interval

Based on the results of the first pilot experiment, marble chippings were used for subsequent experiments. The dishes were placed in two separate aquariums, each equipped with a sprinkler system. The experiment tested whether an irrigation interval of 3 hours or 1.5 hours was more beneficial for the vitality of *Nostoc*. For both settings, the amount of medium sprayed per activation was the same (28 ml). The sample size was 10 for each setting and the experiment was conducted at room temperature (average 23 °C) with an average photon flux density of 35 $\mu mol \cdot m^{-2} \cdot s^{-1}$.

Main experiment 1 – Media comparison

In this experiment, three different low-nitrogen media were tested: rainwater, $BG11_{N0}$ and $BG11_{diluted}$. To address the issue of uneven medium distribution between Petri dishes observed in pilot tests, marble chippings were placed in a shallow polypropylene laboratory dish to allow for equal distribution of the medium after spraying (Figure 6). Likewise, the irrigation interval was set to 3 h with 28 ml medium used during each activation.

Furthermore, we also tested the Lift approach, which we developed. The lift was programmed to submerge the sample stage every 3 hours into the aquarium filled with the tested medium for 10 minutes. *Nostoc* specimens were placed on a stainless-steel mesh in silicon chambers, which were divided into two parts by a plastic partition (Figure 10). The same three media were used for the sprinkler experiment: $BG11_{N0}$, $BG11_{diluted}$ and rainwater. The experiment was performed at room temperature (average 23 °C) and a photon flux density of about 35 µmol·m^{-2}·s^{-1}. In addition, pictures were regularly taken of the samples to observe their growth. The sample size was 30 colonies.

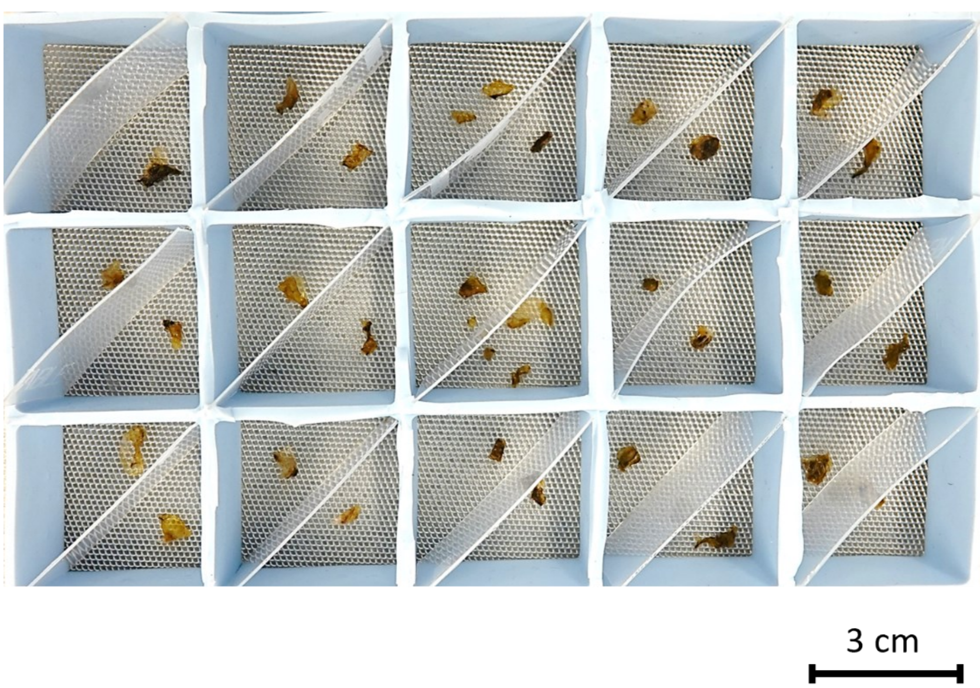

Figure 10 Newly constructed sample chambers for the lift irrigation system.

Main experiment 2 – Watering approach & nitrogen influence

This experiment was performed to directly compare the performance of the different irrigation approaches and simultaneously investigate the influence of nitrogen concentration on the growth of *Nostoc*. Two media were tested: BG11 and $BG11_{N/10}$ (with only 1/10 of the original nitrogen concentration). Each medium was used with every irrigation approach: sprinkler, lift and permanently submerged. This time, the steel mesh in the chambers was covered with marble chippings to make it more comparable to the artificial rain approach and elongate the drying process of the colonies. To prevent colonies and substrate from floating, pieces of a white fly net were placed on the samples with a mesh size of 2.5 mm x 2.5 mm (Figure 11). The experiment was conducted at room temperature (approximately 25 °C) with a photon flux density of around 35 $\mu mol \cdot m^{-2} \cdot s^{-1}$.

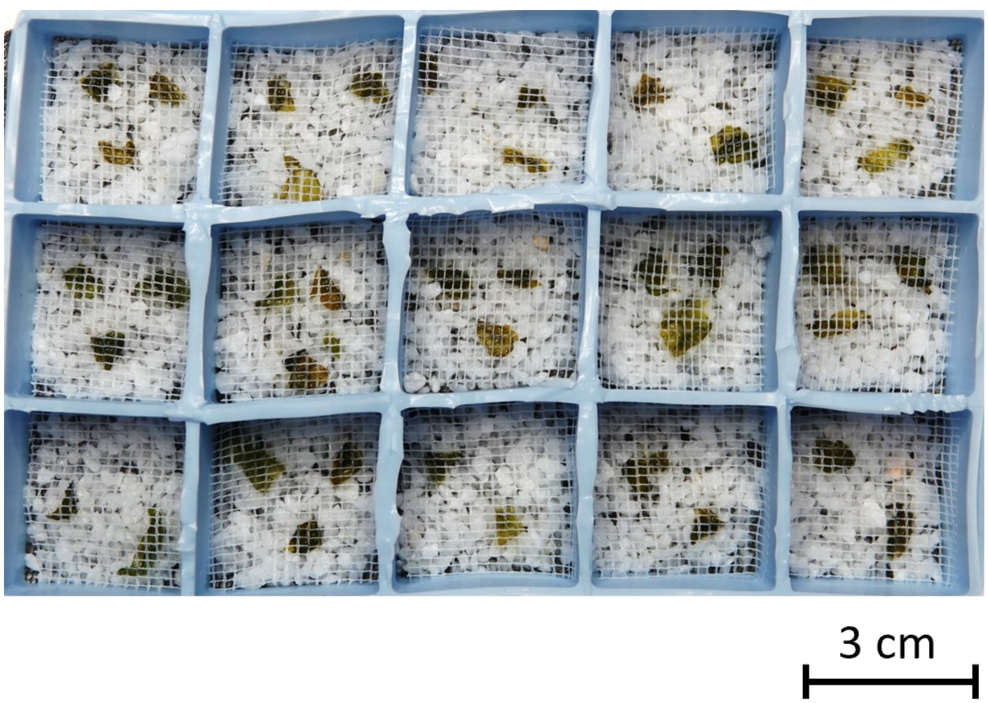

Figure 11 Adaptation of the sample holder. The chambers are filled with substrate. In addition, a fly net is placed into the chambers to keep substrate and specimens on place.

Main experiment 3 – Extended drying period

During the previous experiment, we realized that the colonies stayed fully hydrated during the 3 h drying interval due to the water-retaining capacity of the substrate. Therefore, the times between submerging steps were extended to 24 hours to observe if desiccation and rehydration are beneficial for the growth and health of cultivated *Nostoc.* The immersion time was increased to 20 minutes to ensure the colonies were fully hydrated at the beginning of the extended air phase. We ran this experiment with the $BG11_{N/10}$ medium and the $BG11_{N0}$, which yielded the highest gains in previous experiments. To reduce contamination, the medium in the aquarium was cleaned and replaced with fresh medium after 11 days. In addition, another experiment was performed with 48 h intervals between submersions (medium: $BG11_{N/10}$, substrate: marble). Moreover, two sample sets were permanently submerged in wells of cell culture plates for comparison. One plate was filled with $BG11_{N/10}$ and the other one with $BG11_{N0}$. All samples were continuously illuminated with about 60 $\mu mol \cdot m^{-2} \cdot s^{-1}$ photon flux density.

In addition, an experiment was conducted to determine if a day-night cycle is advantageous for growing *N. commune*. In this case, the samples were illuminated for 16 hours with 60 $\mu mol \cdot m^{-2} \cdot s^{-1}$ photon flux density and then kept for 8 hours in the dark. The submerging step was scheduled to activate when the light turned on and lasted 20 minutes. $BG11_{N/10}$ was used as a medium.

The experiment was performed at room temperature (approximately 25 °C).

Effect of rewetting and desiccation on Φ_{PS2}

In order to assess the effect of rehydration and desiccation on the effective quantum yield, PAM measurements were conducted on a colony that was maintained at a constant temperature (25 °C) and illumination level of 65 µmol·m^{-2}·s^{-1}. For this experiment, the lift irrigation setup was used. A dried *Nostoc commune* sample was placed onto the substrate and the sample holder was programmed to immerse for 20 minutes in $BG11_{N0}$ medium (the colony had been stored dry for four months). After the lift drove out of the liquid, PAM measurements were taken every 15 minutes for 24 hours using the FMS 2+. This procedure was repeated twice more with the same sample immediately afterwards.

Data analysis

The data of the culturing experiments were analyzed with R (R Core Team, 2022) using the development environment RStudio (Posit team, 2023). Only the results with positive mass gain were considered to evaluate the main experiments. This measure was taken to reduce the scattering and the bias that degrading colonies would introduce to the data.

Results

Field experiment

Comparison of the two field study locations

<u>Exposed *Nostoc* colony on a concrete wall</u>

This location had a site openness of 71 % (Figure 12a). It was exposed to the full sun for the whole day except for the early morning, where it was shaded till 09:00 by the building nearby (Figure 12a).

<u>*Nostoc* growing on a moist and shaded spot</u>

The calculated site openness for the spot of the investigated *Nostoc* colony was about 41 % (Figure 12b). Due to the leaves of *Petasites*, the cyanobacteria were shaded most of the time (Figure 4). The soil remained consistently moist throughout the entire observation period.

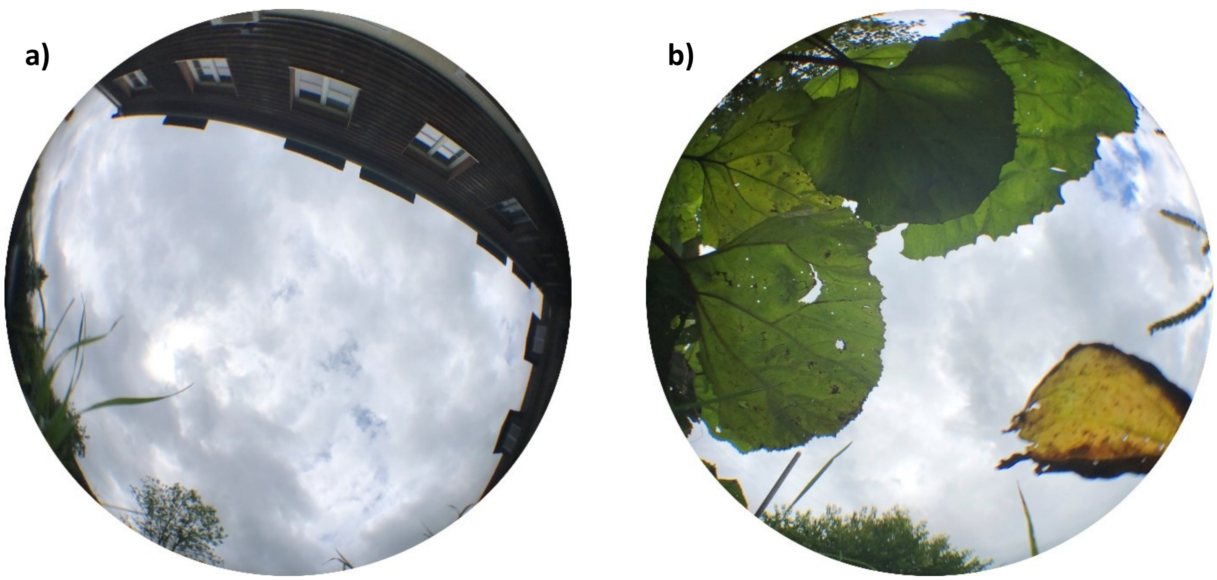

Figure 12 Fish-eye picture of the sky taken from the spots of the investigated colonies.

PAM fluorescence measurements at the sun-exposed location

Daylight experiment

First day (12th of July)

The day started with rainfall, which ceased by 09:00 and gave way to cloudy weather with intermittent sunshine. At the site of the observed *Nostoc* colony, the temperature was slightly above 10 °C in the morning and late evening/night, whereas the daytime peak was around 30°C. The relative humidity was approximately 100% until 09:00, then declined to about 45% in the afternoon. Overall, the Photosynthetic Photon Flux Density (PPFD) reached its maximum at 17:00, as well as the rETR. Throughout the day, the *Nostoc* colonies stayed well-hydrated. The effective quantum yield showed high values in the morning (about 0.55) and in the night hours (about 0.65) (Figure 13, Day 1).

Second day (13th of July)

The second day was sunny throughout. Similar to the first day, temperatures remained relatively low and humidity high during the morning hours. By midday, temperatures had risen to 45°C in the sun, while the humidity dropped to 20%. After 17:00, temperatures began to decrease as relative humidity increased. From 09:00 to 16:00, the PPFD reached the highest levels, the rETR followed this trend and peaked at 11:00. *Nostoc* was hydrated early in the morning. However, by 10:00, it had begun to desiccate and looked relatively dry by 15:00. The quantum yield remained steady at around 0.65 until 06:00 before falling and reaching very low values after 14:00 (Figure 13, Day 2).

Third day (14th of July)

Throughout the day, sunny conditions prevailed. Following sunset, temperatures rapidly increased, reaching values exceeding 50°C on the sunlit wall exposed between 12:00 and 16:00. Concurrently, air humidity decreased to 15%. On this day, the PPFD reached the highest levels, staying intense from 10:00 to 16:00. In contrast to the rETR, which showed the lowest values of all four days. The cyanobacteria remained relatively dry all day, but after 12:00, they were completely desiccated. In the morning, the quantum yield remained low, within the range of 0.2 - 0.3, before falling below 0.1 after 11:00 for the rest of the day (Figure 13, Day 3).

Fourth day (15th of July)

In the early morning, around 04:00, it started to rain until 09:00. For the rest of the day, the weather remained mostly sunny. Despite the rain, morning temperatures were relatively warm compared to other days, exceeding 15°C. By midday, temperatures had risen above 30°C. After the rain stopped, the relative humidity decreased, reaching a minimum of approximately 45% in the early afternoon. On this day, the PPFD fluctuated quite strongly but reached its maximum at 12:00. The *Nostoc* colony, fully desiccated until 04:00, swelled after the onset of rain. By 08:00, it was completely hydrated but subsequently began to dry again, appearing almost desiccated by 17:00. The effective quantum yield increased from 04:00 to 08:00, peaking at 0.45 before decreasing for the remainder of the day (Figure 13, Day 4).

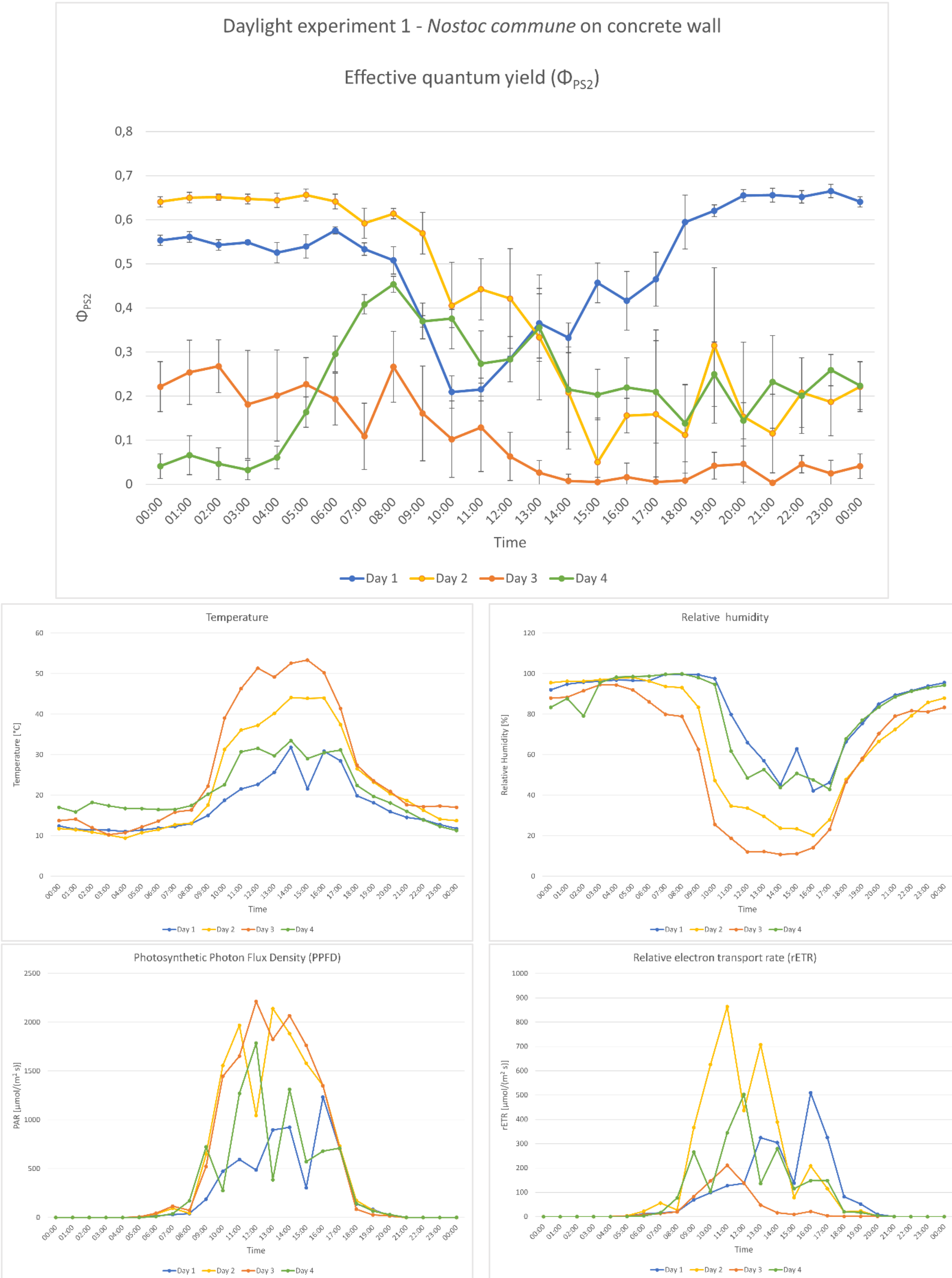

Figure 13 Results of the first daylight experiment (4 consecutive days in July). Measurements were taken on a *Nostoc commune* colony, growing on a concrete wall next to the WasserCluster Lunz building. The following parameters were measured: effective quantum yield (Φ_{PS2} = $(F_m'-F_s)/F_m'$), PAR, temperature and relative humidity. The mean values were calculated using 4 measurements per hour (every 15 minutes). In the graph depicting the maximum quantum yield, the standard deviation, calculated from the 4 measurements taken every hour, was included to assess signal quality.

Dark experiment

In contrast to the daylight experiment, the conditions during the dark experiment (July 17th-19th) were comparable on all three days. The weather was sunny during the day and the night sky was mostly clear. The samples were shielded from sunlight with a black cover. Morning temperatures ranged from 10 to 15°C, rising rapidly after 08:00, with maximum values between 30 °C and 35 °C. After 17:00, air temperatures decreased until midnight. Relative humidity exhibited the opposite pattern, with levels exceeding 85% during the night and early morning. After 08:00, the air humidity decreased rapidly, reaching minimum values from midday until the afternoon. From 17:00 until midnight, the humidity rose again. Throughout the experiment, the *Nostoc* colony remained fully desiccated, with a maximum quantum yield mainly varying between 0 and 0.1 (Figure 14).

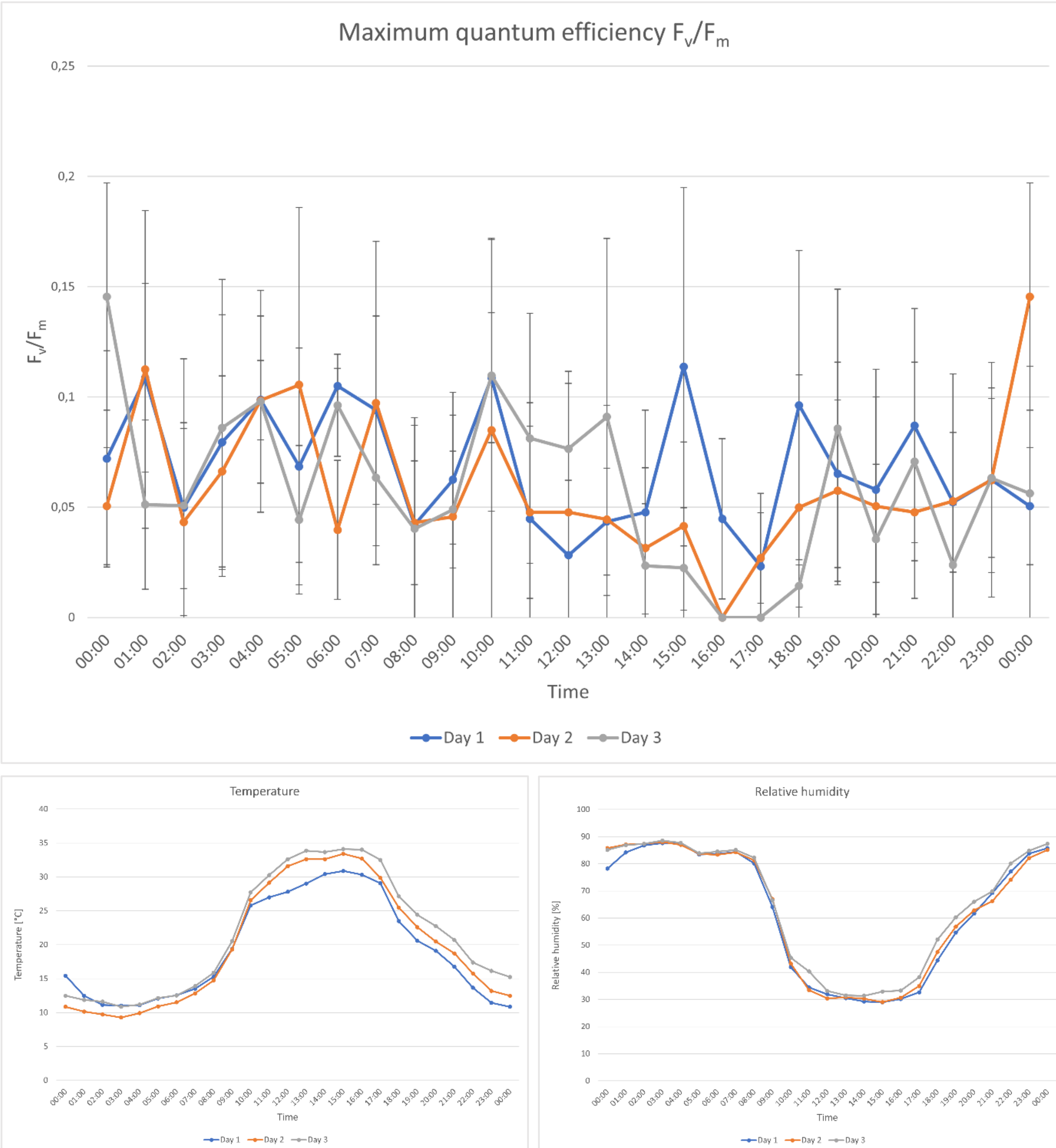

Figure 14 Results of the dark experiment. The measurements were taken on the same colony as the first daylight experiment (colony on a concrete wall). The sample was shielded from the daylight with a black cover. Following parameters were measured: maximum quantum yield $(F_m\text{-}F_0)/F_m$, temperature and relative humidity. The mean values were calculated using 4 measurements per hour (every 15 minutes). In the graph depicting the maximum quantum yield, the standard deviation, calculated from the 4 measurements taken every hour, was included to assess signal quality.

PAM fluorescence measurements at the shaded location

Daylight experiment

Diurnal changes in air temperature and relative humidity were nearly identical on all four days (July 21st-24th). The weather was predominantly sunny, with rain only occurring during the night of day 3 and morning of day 4. In the morning (00:00 - 08:00), the temperature varied from slightly under 15 °C (on the first day) to slightly below 20 °C. After 08:00, the temperatures rose, reaching their maximum between 14:00 and 16:00. Day 2 was the hottest, with a maximum temperature of around 27°C. After 17:00, temperatures decreased until midnight. Overall, relative humidity exhibited less fluctuation compared to the previous location. During the morning and night, the humidity remained around 90%, only dropping to around 80% from 10:00 to 18:00, except on day 2, when it decreased to 70%. PPFD increased from sunrise to 10:00 before decreasing until 12:00. Only on the third day did the radiation continuously rise until 13:00. In the late afternoon, PPFD began to drop until sunset at 21:00. The *Nostoc* colony remained hydrated throughout the observation, showing only slight signs of desiccation in the afternoon of days 2 and 3. During the last two days, the gelatinous mass was fully swollen due to overnight rain. The effective quantum yield was relatively constant, mostly between 0.4 and 0.6. While no significant decrease occurred on the first two days, the yield dropped slightly on the third day around midday. On day 4, it fell more substantially, reaching levels below 0.4 (Figure 15).

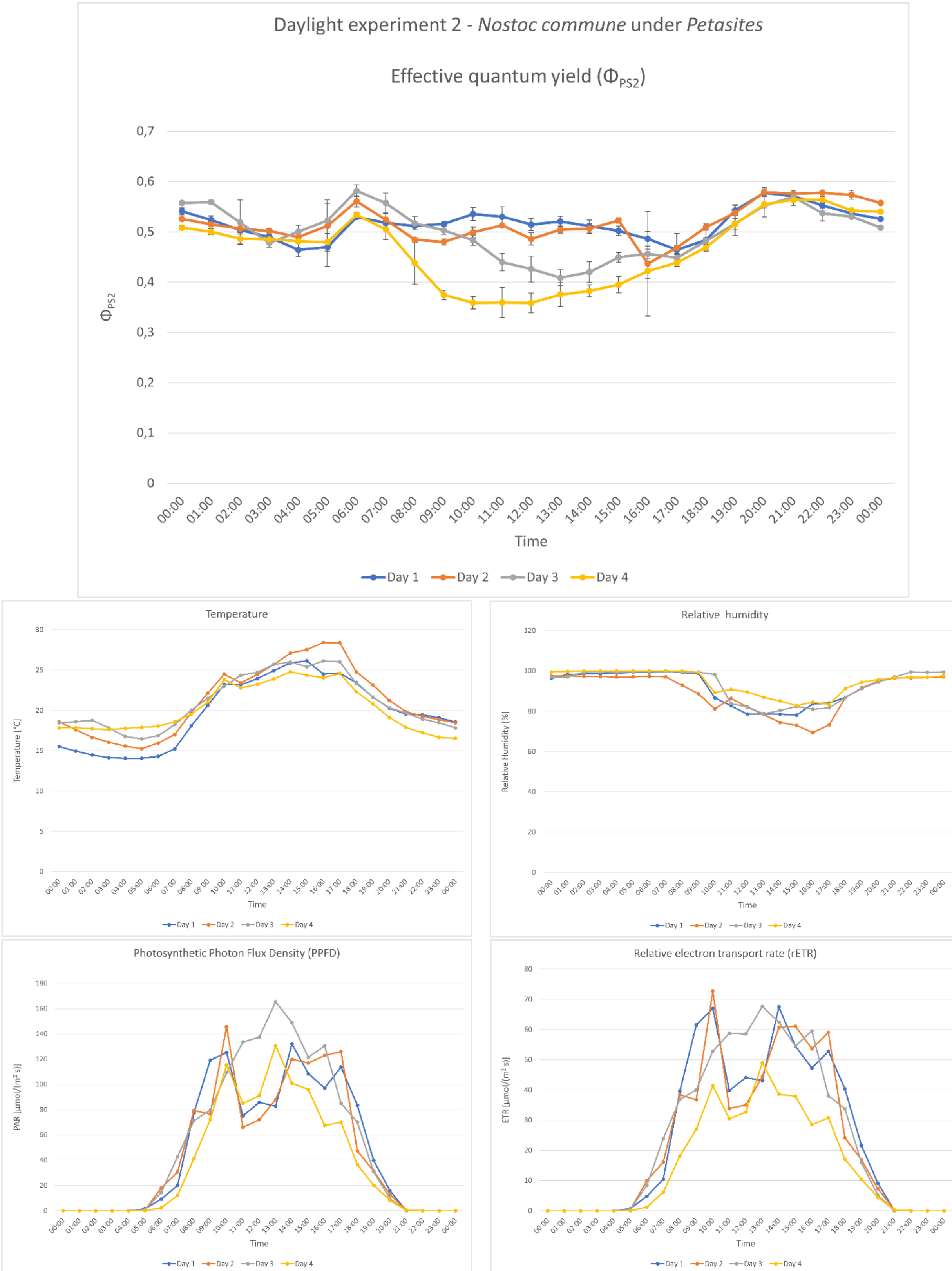

Figure 15 Results of the second daylight experiment (4 consecutive days in July). Measurements were taken on a *Nostoc commune* colony found in a moist area growing under *Petasites hybridus*. Following parameters were measured: effective quantum yield (Φ_{PS2} = (F_m'-F_s)/F_m'), PAR, temperature and relative humidity. The mean values were calculated using 4 measurements per hour (every 15 minutes). In the graph depicting the maximum quantum yield, the standard deviation, calculated from the 4 measurements taken every hour, was included to assess signal quality.

Correlation between effective quantum yield and other parameters

Looking at the combined data from both daylight experiments, correlations occur between the effective quantum yield and temperature/humidity/PAR. Regarding temperature and relative humidity, the Pearson coefficient indicates a negative correlation with the quantum yield ($-0.45 > r_{Pearson} > -0.4$). On the contrary, the analysis shows a positive correlation of Φ_{PS2} with the relative humidity ($r_{Pearson} = 0.58$). In all three cases, the t-tests revealed significant differences ($p < 0.05$, Figure 16 a, b & c). the correlations were also calculated just for the time that colonies were hydrated. This measure was taken as it seemed that the measurements on the desiccated colony did not contain valuable information about the influence of environmental parameters but only introduced a broader scattering of data points. In this case, the Pearson coefficient is under 0.5 for the relative humidity. At the same time, the negative correlation with PAR is more pronounced ($r_{Pearson} < -0.5$). Again, the t-test showed a significant correlation for all three environment parameters (Figure 16 d, e & f).

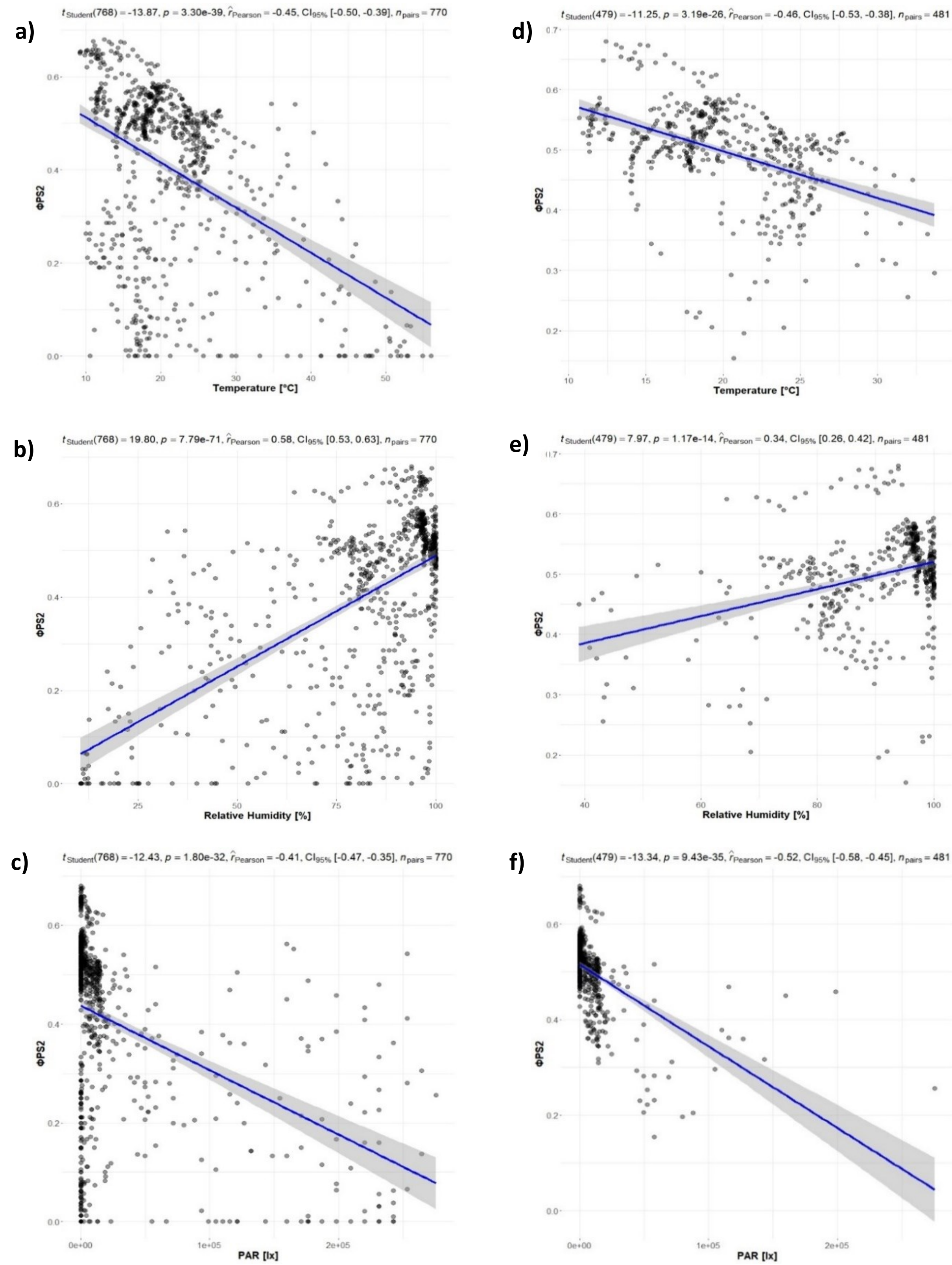

Figure 16 Scatter plots showing the correlation between the effective quantum yield (Φ_{PS2}) and different parameters: a) temperature, b) relative humidity, c) photosynthetically active radiation (PAR). The results of the calculated t-tests and the Pearson correlation coefficient are written in the headline. The plots were created using the R function ggstatsplot (Patil, 2021).

Culturing experiments

Pilot experiments

Overall, colonies grown on the marble chippings showed a higher mean mass gain than those cultured on glass beads, although not significantly (Figure 17 a). Furthermore, the gelatinous mass could be easier removed from the marble chippings surface than from the glass beads. The results from the sand substrate had to be discarded due to the inability to completely remove sand grains from the samples, resulting in a distortion of the mass measurements as they became integrated into the gelatinous matrix.

In the second pilot experiment, the mass gain did not show a significant difference between the two irrigation intervals (Figure 17 b). Some Petri dishes in the 1.5 h interval had been flooded and the excess medium had to be removed manually. In the case of the 3 h interval, no such floodings occurred.

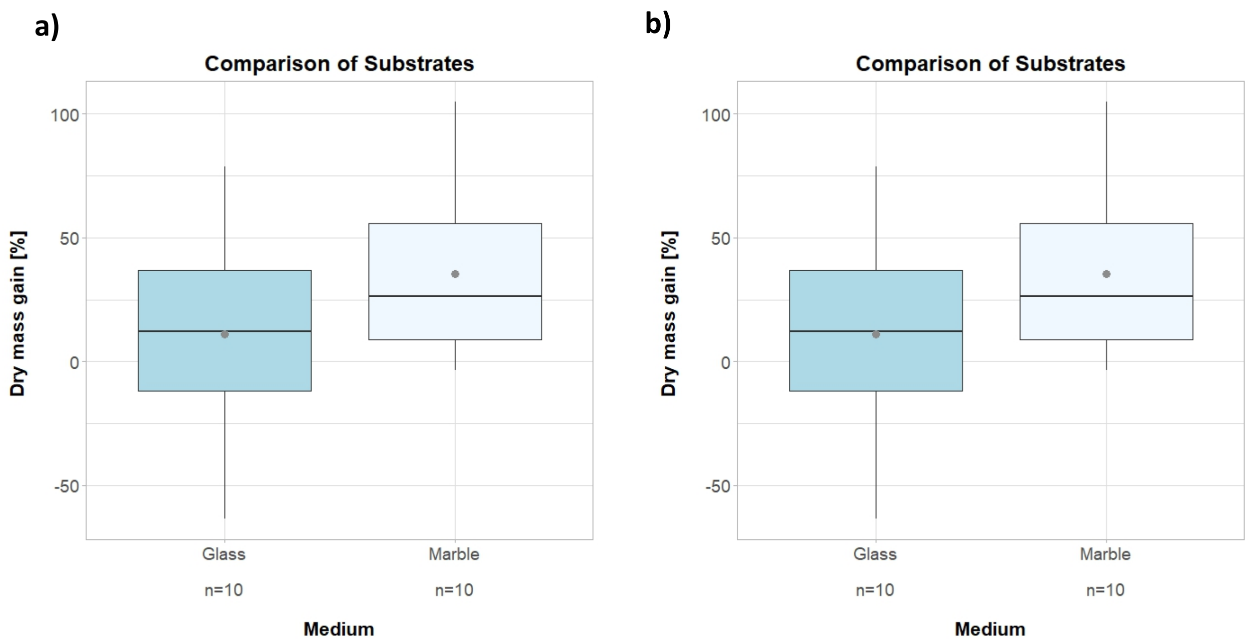

Figure 17 Results of the two pilot experiments depicted as boxplots. The grey point shows the mean value of the dry mass gain in each sample set. Samples were kept at room temperature and illuminated for 16 h followed by 8 h in the dark. Runtime: 21 days.

Main experiment 1 – Comparison of media and irrigation approaches

Several colonies had a lower mass at the end of the experiment compared to initial values. These colonies had all a yellowish color and a slimy consistency, both signs of degradation. In the pilot experiments, such samples were included in the analysis, which led to high deviations. In the main experiment series, these colonies were excluded, which is why the effective sample size shown in the graphs differs from the original sample size (n = 40).

For both irrigation set-ups, the dry mass gains of the *Nostoc* with $BG11_{N0}$ treatment were approximately within the same range (Figure 18, Table 1). In the case of using BG11 diluted with Milli-Q water, the sprinkler system performed significantly better than the samples irrigated with the lift approach, where only two samples survived. On average, samples treated with rainwater gained slightly more biomass in the lift set-up, but the number of degraded samples was also higher than in the artificial rain treatment (Figure 18). However, the difference was not significant (Table 1).

Table 1 Results of the conducted Mann-Whitney U tests to evaluate the significance of the difference between irrigation approaches. P-values below 0.05 show a significance for the 5 % threshold.

Mann-Whitney U test

	p-value	**U-parameter**
$BG11_{N0}$: Lift vs. Sprinkler	0.7865	115
Rainwater: Lift vs. Sprinkler	0.1449	222
$BG11_{diluted}$: Lift vs. Sprinkler	0.004301	0

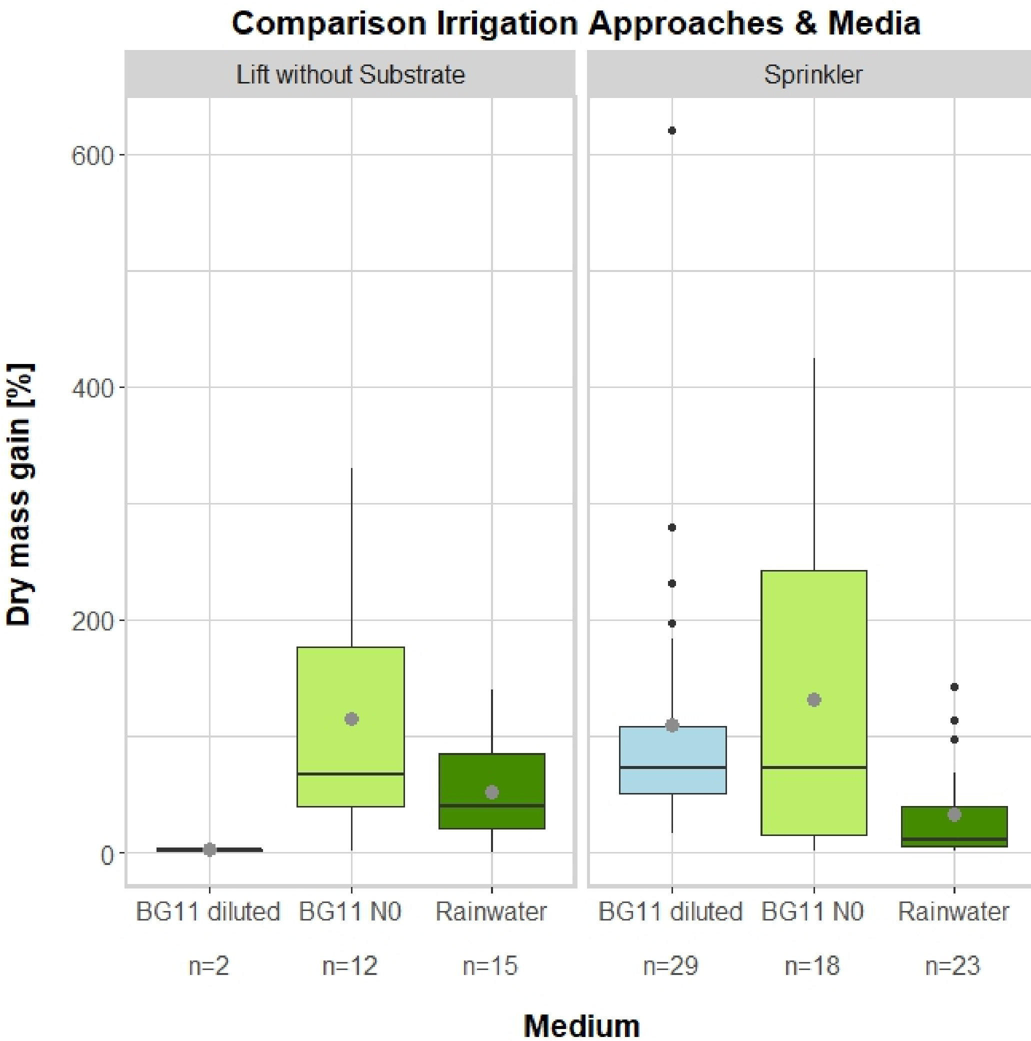

Figure 18 Results of main experiment 1 depicted as boxplots. 3 different media were tested: BG11 N0 (without nitrogen), rainwater (filtered) and BG11 diluted (1:10 with MiliQ water). The sample size was 30 colonies each. Specimens which did not grow but did degrade have been excluded from the analysis to reduce the deviation between data points. Number of samples used for calculations is written below every plot (n). Mean mass gains are indicated as grey points in the graph. Colors of the boxplots indicate which medium was used. The irrigation approach used is written in the headline. Samples were kept at room temperature and were permanently illuminated. Runtime: 21 days.

Main experiment 2 – Influence of nitrogen concentration & irrigation method on growth

In all three irrigation regimes, the samples with $BG11_{N0}$ showed a higher mass gain than the standard BG11 medium (Figure 20), with significant differences for permanently submerged culture (Table 2; $p < 0.05$). The highest measured dry mass gains were found in the lift set-up (Figure 20). In the BG11 sprinkler treatment, most colonies were degraded/dying at the end of the 21-day culturing period. Nearly all colonies treated with BG11 had a pale yellowish color at the end of the experiment. At halftime, several still made a healthy appearance. In contrast, most of the samples with $BG11_{N0}$ treatment showed a dark green, healthy color after 21 days. However, the contamination with other algae and cyanobacteria is more strongly expressed in the $BG11_{N0}$ treatment (Figure 19).

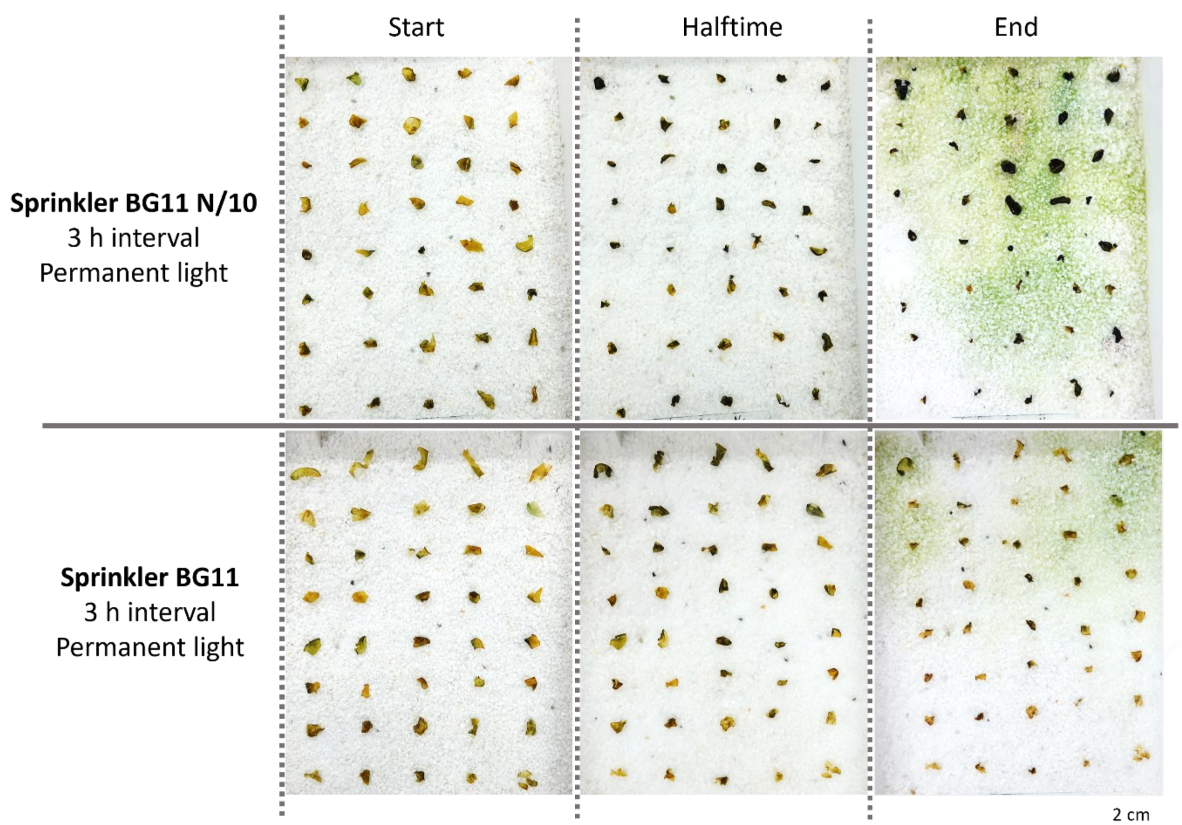

Figure 19 Pictures taken from the sprinkler sample sets in at three different time points of the experiment: start, halftime and end.

Table 2 Results of the conducted Mann-Whitney U tests to evaluate the significance of the difference between BG11 and $BG11_{N/10}$ treatment regarding dry mass gain. P-values below 0.05 show a significance for the 5 % threshold.

Mann-Whitney U test

	p-value	**U-parameter**
$BG11_{N0}$: Lift vs. Sprinkler	0.0158	104
Rainwater: Lift vs. Sprinkler	0.08715	107
$BG11_{diluted}$: Lift vs. Sprinkler	0.0004	141

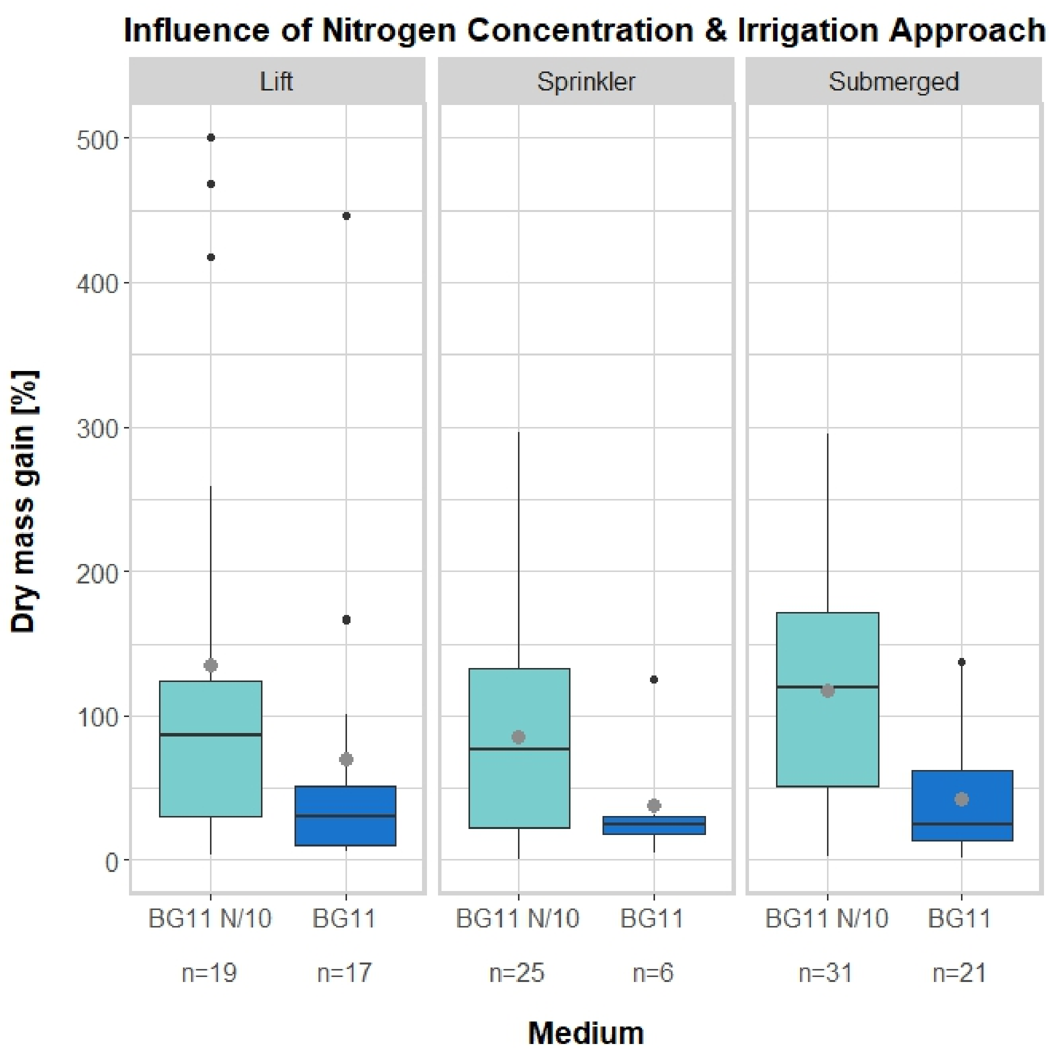

Figure 20 Results of main experiment 2 depicted as boxplots. The irrigation interval was 3 hours for the lift and sprinkler systems. The sample size was 40 colonies each. Specimens which did not grow but did degrade have been excluded from the analysis to reduce the deviation between data points. Number of used samples for calculations is written below every plot (n). Mean mass gains are indicated as grey points in the graph. Colors of the boxplots indicate which medium was used: BG11 and BG11 N/10 (tenth of normal nitrogen concentration). The irrigation approach used is written in the headline. Samples were kept at room temperature and were permanently illuminated. Runtime: 21 days.

Main experiment 3 – Extended drying periods

All in all, colonies with an air exposure period of 24 h showed the highest relative dry mass gains of all experiments (Figure 21). Doubling the period to 48 h did not enhance growth. The colonies showed a significantly lower dry mass gain than the samples with a 24-hour interval ($p < 0.05$ in Table 3). Although the colonies were clearly smaller at the end of the experiment, only one colony degraded, whereas all other samples demonstrated a healthy green color and firm texture (Figure 22). Introducing a night phase did not reduce the biomass production significantly, though it decreased the photosynthetically usable time by about 30 % ($p > 0.05$ in Table 3). Only six colonies did degrade and most of the others showed healthy consistency and green color (Figure 21, Figure 22).

The differences between the BG11 medium without nitrogen and a reduced nitrogen concentration were not significant ($p > 0.05$ in Table 3). Nevertheless, more samples degraded in the $BG11_{N/10}$ treatment (Figure 22). The developed lift approach delivered, on average, a 5 times significantly higher dry mass gain compared to the permanently submerged culture (Figure 21, Table 3).

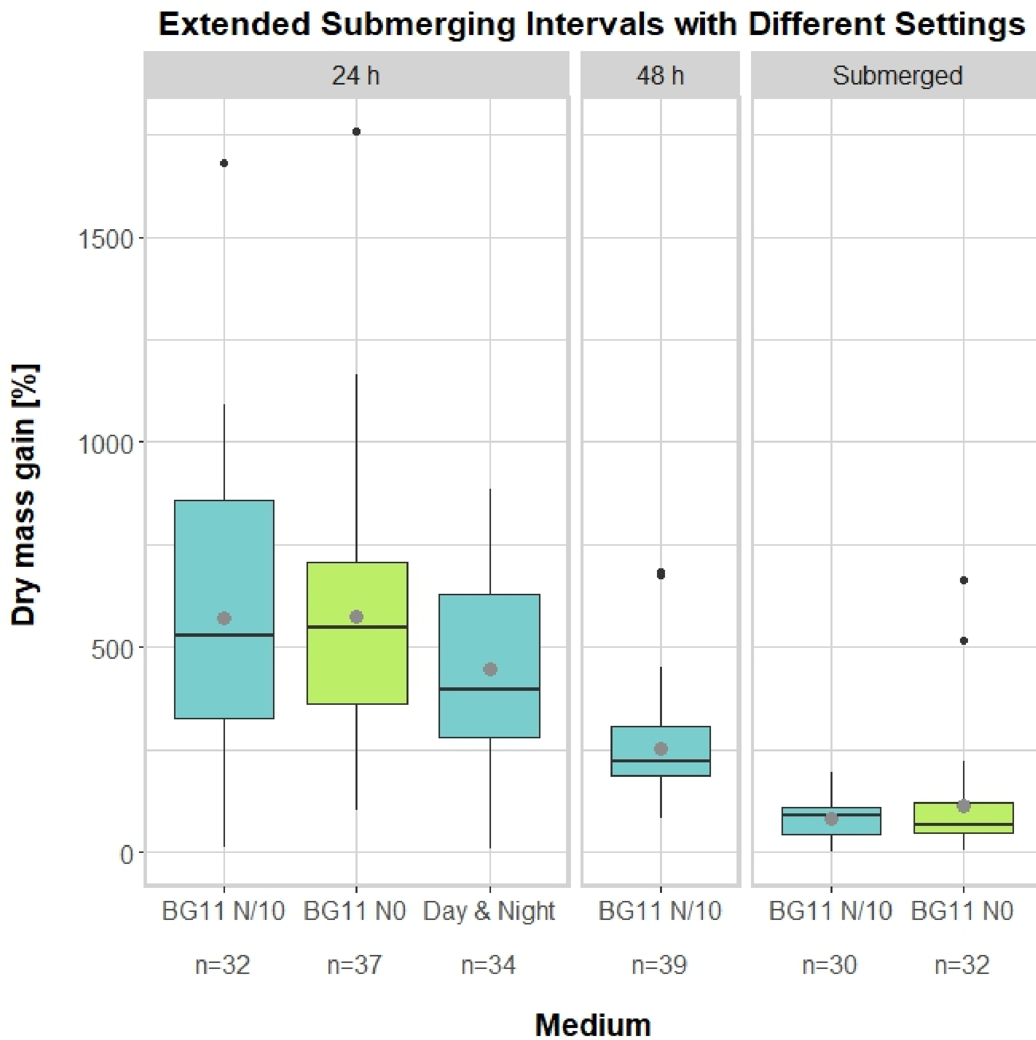

Figure 21 Results of main experiment 3 with extended submerging intervals depicted as boxplots. The sample size was 40 colonies each. Specimens which did not grow but did degrade have been excluded from the analysis to reduce the deviation between data points. Number of used samples for calculations is written below every plot (n). Mean mass gains are indicated as grey points in the graph. Colors of the boxplots indicate which medium was used: BG11 N0 (without nitrogen) and BG11 N0 (tenth of normal nitrogen concentration). Day & night (medium used: BG11 N/10) indicates samples which were exposed to a cycle of 16 h light and 8 h dark. All other samples were permanently illuminated. Interval between submerging steps is written in the headline. Runtime: 21 days.

Table 3 Results of the conducted Mann-Whitney U tests to evaluate the significance of the differences in dry mass gain between treatment pairs. P-values below 0.05 show a significance for the 5 % threshold.

Mann-Whitney U test

Comparison	**p-value**	**U-parameter**
Lift vs. Submerged (BG11$_{N0}$)	0.1.644e-12	1112
Lift vs. Submerged (BG11$_{N/10}$)	5.692e-12	910
BG11$_{N0}$ vs. BG11$_{N/10}$ (Lift)	0.9857	594
BG11$_{N0}$ vs. BG11$_{N/10}$ (Submerged)	0.9387	486
24 h vs. 48 h (Lift, BG11$_{N/10}$)	2.124e-05	980
Permanent light vs. 16 ***h light/8 h dark***	0.1689	652

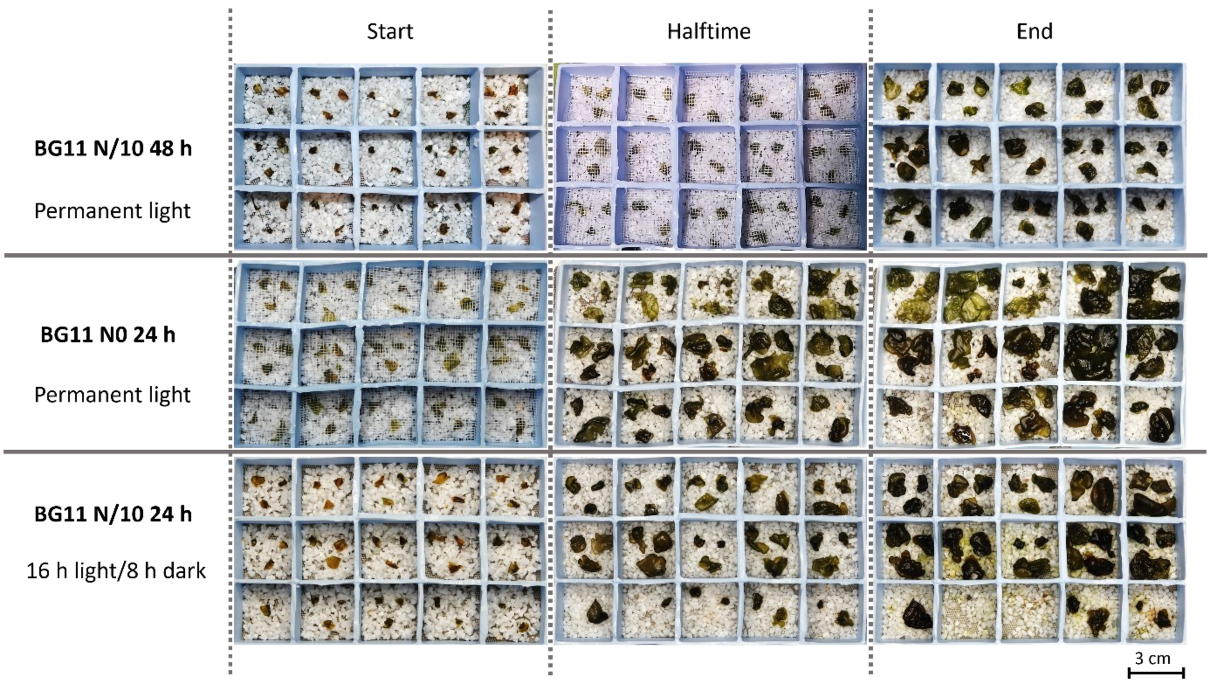

Figure 22 Pictures of selected sample sets showing the condition of colonies at the start, halftime and at the end. Pictures were taken directly after the 20 min submerging phase to depict colonies fully hydrated. During the experiment the colonies were covered with quadratic pieces of a fly net as shown on the second picture of the first row and the first picture of the second row. This measure was taken to keep the samples in place and prevent them from floating up.

Experiment to evaluate the effective quantum yield dependence on colony hydration

A *Nostoc* colony, which had been stored dry for four months, was rehydrated by immersing the sample holder in $BG11_{N0}$ medium. After 20 minutes, it was lifted out of the liquid and PAM fluorescence measurements were stated. At the beginning the effective quantum yield of about 0 was measured. In the next 9 hours, Φ_{PS2} increased from 0 to 0.4 (Figure 23 a). 14 hours after the initial rehydration, the signal started to decrease rapidly. At this time, the colony appeared partly desiccated. Three hours later, the quantum yield reached values below 0.1, fluctuating at these levels for the rest of the time.

At the end of the 24 hours, the sample was again immersed for 20 minutes into the medium. This time, the specimen recovered more quickly and showed an effective quantum yield of about 0.3 after being 20 minutes submerged. The yield increased within the first hour over 0.4. For 14 hours, the Φ_{PS2} signal stayed around this value. After 15:00, the yield decreased rapidly and reached 0 within 2 hours (Figure 23 b).

With each repeated rehydration, the fluorescence signal recovered more rapidly. After the third rehydration, the sample showed a Φ_{PS2} of about 0.4 immediately after the immersion period. It increased within 1.5 hours above 0.5. After 18 hours, the signal started to decrease, ceasing after 24 hours (Figure 23 c).

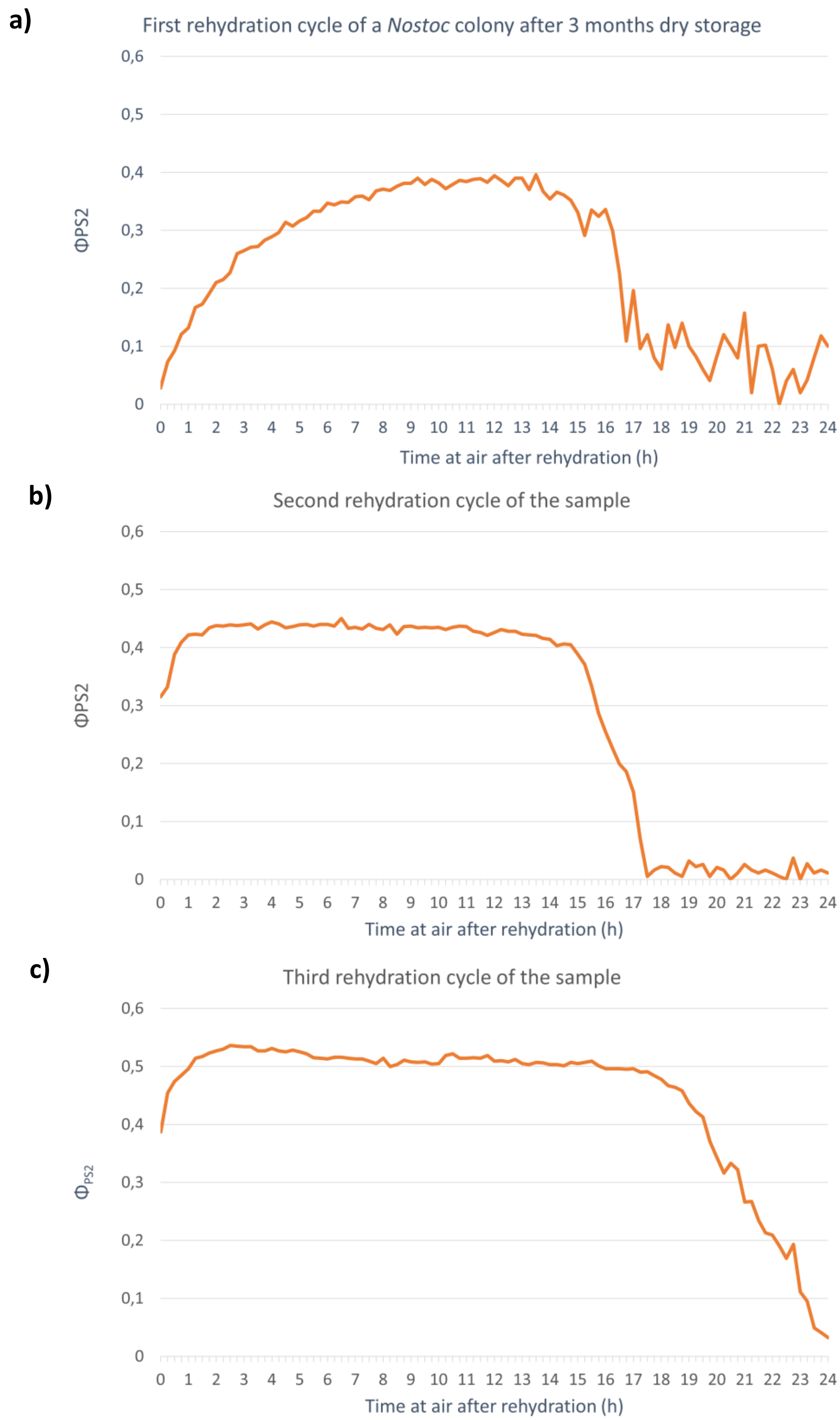

Figure 23 PAM fluorescence measurements of a *Nostoc commune* colony to show the effect of desiccation on the effective quantum yield (Φ_{PS2}). The sample was rehydrated after being stored dry for 4 months after collection. The measurements were performed at permanent illumination [65 µmol·m^{-2}·s^{-1}] and at room temperature (24 °C). Depicted are three consecutive experiments on the same colony. Before each measurement series started, the specimen was submerged at the beginning into BG11$_{N0}$ medium for 20 minutes. Three rehydration cycles were conducted with the same sample. Each measurement series was run for 24 H: a) initial rehydration, b) second rehydration, c) third rehydration.

Discussion

Field survey

Effective quantum yield of sun-exposed *Nostoc* colonies

Nostoc colonies growing on the concrete wall receive direct sunlight most of the day. Only in the morning, the cyanobacteria are shaded. This building next to the location is the only factor that delimits the site openness, which is considerably higher (around 70 %) than the shaded location (Figure 12). The weather conditions and the hydration of the colonies varied significantly during the four consecutive days of the experiment.

Hydrated colony

Day 1 of the measurement series shows the change in the effective quantum yield of a hydrated colony over the course of a day with moderate sunny conditions (Figure 13). The highest tracked Φ_{PS2} values were about 0.65. Compared with plants, which show effective yields of 0.83 in a relaxed, non-stressed state, it may seem low (Björkman & Demmig, 1987). However, the comparison to other cyanobacteria reveals that such values are rather high for cyanobacteria as they mostly show values around 0.2-0.6 depending on species and environmental conditions (Campbell et al., 1998; Lüttge et al., 1995). Therefore, it can be assumed that the *N. commune* samples with an effective yield above 0.5 are well-hydrated and unstressed.

Lüttge et al. (1995) reported that the effective quantum yields, as well as the maximum quantum yields, decrease around noon, recovering in the evening in terrestrial cyanobacterial mats, which supports the findings of this study. Furthermore, a similar course of Φ_{PS2} (decrease after dawn and following recovery in the afternoon/evening) was reported in different plant species and coastal phytoplankton mainly dominated by diatoms (Adams & Demmig-Adams, 2004; Hymus et al., 1999; Lima Neto et al., 2015; Sun et al., 2022).

Previous studies explained this decrease by non-photochemical quenching (NPQ) of the fluorescence via heat dissipation, which is a crucial way to reduce photodamage caused by excessive energy in the reaction centers (Adams & Demmig-Adams, 2004; Demmig-Adams, 1990; Demmig-Adams & Adams, 1990; Lima Neto et al., 2015).

In higher plants, the xanthophyll cycle plays a vital role in de-excitation via heat dissipation (Adams & Demmig-Adams, 2004; Demmig-Adams & Adams, 1990). If light exposure is high and exceeds the maximal usable amount of ATP synthase, the protons accumulate in the thylakoid lumen, which leads to acidification. If the pH falls below a certain threshold, violaxanthin de-epoxidase converts violaxanthin into zeaxanthin. Zeaxanthin increases the level of heat dissipation. At low light conditions, the process is reversed and zeaxanthin is reconverted into violaxanthin (Demmig-Adams et al., 2020).

However, cyanobacteria cannot use the xanthophyll cycle to quickly and reversibly change the zeaxanthin content depending on the actual demand as they lack violaxanthin (Demmig-Adams, 1990; Demmig-Adams et al., 1990). Nevertheless, zeaxanthin can be found in several cyanobacteria, such as *Nostoc* (Schagerl & Müller, 2006; Takaichi et al., 2009). It was shown that cultures exposed to higher irradiances showed increased content of carotenoids such as zeaxanthin, myxoxanthophyll and β-carotene, which could be a long-term adaptation to high light intensities (Schagerl & Müller, 2006).

Despite these slow adaptations, a blue-light-induced NPQ was found in cyanobacteria (El Bissati et al., 2000). A few years later, Wilson et al. (2006) discovered that the orange carotenoid protein (OCP) plays a major role in this phycobilisomes-associated mechanism. This water-soluble protein containing a ketocarotenoid (3'-hydroxyechinenone) has an inactivated (orange) and an activated (red) state. In low light conditions and in the dark, OCP is detached from the light-harvesting phycobilisomes (inactive). If exposed to high blue-green light, it gets activated and binds to the phycobilisomes. In its activated form, it non-photochemically quenches the excessive energy via heat dissipation and protects the reaction center from photodamage. When the light conditions get low again, the fluorescence recovery protein (FRP) mediates the inactivation of OCP (Gorbunov et al., 2011; Muzzopappa & Kirilovsky, 2020; Pagels et al., 2021). In addition, OCP proved to be an efficient singlet oxygen quencher, which helps to reduce the damage caused by reactive oxygens species caused by excess energy (Muzzopappa & Kirilovsky, 2020).

Especially in terrestrial cyanobacteria such as *Nostoc commune,* tolerating highly sun-exposed places, photoprotective mechanisms are essential. Therefore, it is likely that the observed decrease in the effective quantum yield during Day 1 is caused mainly by NPQ mediated by OCP (Figure 13).

Transition from hydrated to desiccated state

On the second day, the effective yield did not show an increase in the afternoon/evening but dropped to a lower level, which cannot be explained by NPQ (Figure 13). A possible explanation could be that the colonies started to dry, which caused the colonies to reduce photosynthesis. The loss of water would also explain the decrease of F_m' as the maximal fluorescence is limited by the electron donation from the H_2O splitting, which is catalyzed by the oxygen-evolving complex of the PSII (McEvoy et al., 2005; Schreiber et al., 1995). As a consequence, if no water is available (drought stress), more and more photo reaction centers will be inactivated as the core (P680 pairs) stays oxidized and cannot be reduced again by electrons received from the water splitting. Therefore, the chlorophyll cannot be excited anymore and the F_m' signal will cease.

The lack of water availability could explain why the effective quantum yield decreased on day 2 in the afternoon to such a low level and stayed there with no significant sign of recovery after sunset (Figure 13). In the afternoon on the consecutive day (Day 3) the Φ_{PS2} signal diminished completely. It seems as if the *Nostoc* colony was desiccated, which suppressed photochemistry. This is also supported by the calculated rETR (Figure 13), which is a commonly used parameter in cyanobacterial studies (Celis-Plá et al., 2021; Santos-Merino et al., 2021).

One could argue that the decrease during bright days is caused by photoinhibition induced by excess light. Photoinhibition describes the irreversible failure of photochemical activity, which cannot be recovered without replacing damaged proteins through the PSII repair cycle (Tyystjärvi, 2013). Due to the excessive energy, reactive oxygen species (ROS), especially singlet oxygens, are produced mainly through the excited triplet state of chlorophylls (Ballottari et al., 2013; Lingvay et al., 2020). Subsequently, the ROS likely damages the D1 and D2 proteins of the PSII, which leads to inactivated reaction centers (Kale et al., 2017). As the efficiency of PSII increased again from 0.05 to 0.45 within 4 hours after it started raining (Figure 13), desiccation was likely the cause for the long-term reduction of the quantum yield. Satoh et al. (2002) studied the recovery time of the maximum quantum yield after rewetting and found a 50 % recovery after 1 hour under laboratory conditions. Other studies observed a similar behavior of the quantum yield when they simulated drought stress with a high sorbitol concentration in the surrounding medium (Fukuda et al., 2008; Hirai et al., 2004). If *Nostoc* was dehydrated, it exhibited almost no Φ_{PS2} signal. In addition, they suggested a mechanism in *Nostoc commune*, which inhibits the photochemical activity when sensing a certain drying threshold to protect the photosystems from damage of excessive light energy (Hirai et al., 2004). These observations are congruent with other studies showing that carbon fixation keeps stable until a water content of 40 % but ceases rapidly when the water content drops below 30 % (Kvíderová et al., 2011; Novis et al., 2007b). All these findings are supported by our PAM fluorescence measurements on the rehydrated colony in the laboratory settings (Figure 23). *N. commune* showed a fast recovery on rewetting, especially if the desiccation period was relatively short (Figure 23 b & c). When it was rewetted for the first time after four months, the recovery took longer (about 9 hours, Figure 23 a). However, at that time, the effective yield could not reach its full potential and needed repeated cycles of rehydration. It was observed that if the water loss reached a certain level, the effective quantum yield decreased rapidly (Figure 23). To sum up, it is likely that the rapid reduction in the quantum yield occurs due to protective mechanisms activated by sensing water loss.

Dark experiment

We performed a dark experiment immediately after the PAM fluorescence measurements under ambient light conditions on the same colony. The main reason was to exclude the light-induced NPQ effects and study the dependence of the maximum quantum yield on temperature and humidity only. Over the whole period, the investigated colonies stayed dry as it did not rain. The quantum yield fluctuated mainly between 0.05 and 0.10. However, these values are most likely caused by signal noise, as indicated by the large standard deviations (Figure 14). Effectively, *Nostoc commune* showed no photochemical activity in the desiccated state, which is congruent to the observations in the studies previously mentioned, where dehydrated *Nostoc* showed almost no quantum yield (Hirai et al., 2004; Satoh et al., 2002). *N. commune* colonies need soaking and cannot be rehydrated just by water vapor like aerophytic algae (Mollenhauer et al., 1999). Dew proves insufficient to activate the PSII, which was previously also reported for *N. flagelliforme* (H. Huang et al., 2005). H. Huang et al. (2005) showed that only the PSI activity recovered if just small water amounts are supplied to the colonies. All in all, because of the dry state of the cyanobacteria, the dark experiment could not deliver any information about the dependence of the quantum yield on temperature and humidity. Nevertheless, we conclude from our results that desiccated *N. commune* cannot be sufficiently rehydrated by dew and stays photochemical inactive without rain.

Effective quantum yield of shaded *Nostoc* colonies

Diurnal changes of air temperature and humidity were less pronounced compared to the sun-exposed site and the light supply never exceeded 170 µmol·m^{-2}·s^{-1} (Figure 15). However, Φ_{PS2} still decreased after sunset and recovered in the late afternoon and evening, showing a similar habit as the sun-exposed colony but to a much lesser extent (compare Figure 13, Figure 15). Interestingly, a slight dip in Φ_{PS2} occurs in the early morning (from 01:00 to 03:00) on all four days, which is followed by a peak at 06:00. A possible explanation is that the plastoquinone pool is not fully oxidized in cyanobacteria during a dark-adapted state, which reduces the measured quantum yield. This is caused by the intertwined electron flow in the thylakoid membranes of photosynthesis and respiration (Matthijs et al., 1984). Both pathways share the same plastoquinone pool, which leads to part of the quinones being reduced during nighttime (Milou Schuurmans et al., 2014; Schuurmans et al., 2015). Furthermore, it was observed that cyanobacteria show a lower maximal fluorescence in the dark-adapted state compared to low-intensity light (Schuurmans et al., 2015; Wilson et al., 2006). It was explained by state transition between two states. In state 1, light-harvesting phycobilisomes deliver mainly the electrons to PSII, whereas in state 2, more energy is directed to the PSI. Dark-adapted cells are suggested to be in state 2 and shift to state 1 when illuminated (Mullineaux & Allen, 1990; Oxborough & Baker, 1997). This would explain the increase of Φ_{PS2} under low light conditions in the early morning (from 04:00 to 06:00, Figure 15). However, the underlying mechanisms of the state transition and the cause of the difference in fluorescence quenching between the states are still discussed (Farhan Bhatti et al., 2020).

The dependence of Φ_{PS2} on selected environmental parameters

To evaluate key environmental parameters affecting the effective quantum yield, correlations were calculated and graphically represented as scatter plots (Figure 9). If all days of PAM fluorescence measurements under ambient light are included, relative humidity shows the highest correlation coefficient in absolute terms. Furthermore, the humidity is the only one showing a positive correlation. Generally, the points are widely scattered over the whole graph, showing no clear linear correlation (Figure 9 a, b & c). If only the time frame when the *Nostoc* colonies were in a hydrated state is considered, the distribution of measuring points along the trend line becomes narrower (Figure 9 d, e & f). Interestingly, the Pearson coefficient decreased significantly regarding the correlation between humidity and effective yield (Figure 9 d). This indicates that the photochemical activity primarily depends on the hydration status, which is congruent to the conclusions drawn in the previous sections (compare *Transition from hydrated to desiccated state*): only if the water supply is sufficient, other parameters come into play. Notably, the illumination shows a stronger negative correlation than before (Figure 9 f). This can be explained by NPQ mechanisms, which are initiated in high light conditions and reduce the effective quantum yield. Despite the ability of *N. commune* to tolerate high light intensities due to protective mechanisms, the optimal assimilation condition seems to be reached under moderate illumination.

However, one must be careful in the interpretation of bivariate correlations, as all three parameters show high dependency on each other. If the light gets more intense, the temperature rises, the relative humidity decreases and the colonies begin to desiccate (especially for the *Nostoc* exposed to full sunlight). In order to truly evaluate the influence of each parameter, one would have to decouple temperature, humidity, PAR and the water saturation of the organism in laboratory experiments.

Laboratory Section

Evaluating the suitability of three different substrates

Marble chippings turned out to be the most suitable substrate with two main advantages: harvesting is easy and the contrast of the white stones to the brownish-greenish *Nostoc* is high, which facilitates biomass estimations via digital imaging. In contrast, the fine sand grains were nearly impossible to remove from the mucilage of the colonies, which affected the measured mass enormously. The contrast was also high in the glass beads, but the colonies adhered much more to the glass surface. Peeling the whole colony without losing material off the beads was much more challenging. Moreover, the colonies had a slightly higher mass increase growing on marble compared to glass beads (Figure 17 a). In addition, it appears that marble is a suitable substrate due to its chemical properties, as this taxon is primarily found on carbonate substrates (Dodds et al., 1995; Potts M, 2000).

Choosing the best irrigation interval

To study the effect of periodical desiccation-rehydration we had to find suitable irrigation intervals. The second pilot experiment showed that using 1.5-hour intervals for the sprinkler system, the cyanobacteria stayed hydrated all the time. In the 3-hour interval, the colonies could partly desiccate and efficiently rehydrate. At longer intervals, the samples dried out too much and water uptake was reduced (observed in preliminary hydration experiments, not further discussed in this work). Considering these results and the fact that both irrigation regimes performed comparably in times of mass gain (Figure 17 b), we decided to operate the sprinkler system in 3-hour intervals for the main experiments.

Introducing a newly developed irrigation method and testing different media

One of the problems of putting the colonies in separate Petri dishes was the unequal distribution of medium by the sprinkler system. Some Petri dishes were completely dry, while others were wet or even flooded (in the case of the 1.5 h interval irrigation). To counteract this problem, a plastic laboratory tray was filled with substrate for the artificial rain method. In this way, the liquid can distribute in the whole tray after the spraying process.

The uneven distribution of the medium prompted the development of a new irrigation method. For this purpose, a lift made of LEGO® Technic was constructed, capable of carrying a sample holder. Controlled by a microcontroller, the motor of the lift was programmed to periodically immerse the sample holder into the medium every 3 hours for a duration of 10 minutes. The 3-hour interval was chosen to compare it to the sprinkler approach used in this experiment. This method resulted in uniform rewets of *Nostoc*.

The data of main experiment 1 shows that rainwater and $BG11_{N0}$ treatments differ not significantly between both irrigation approaches regarding dry mass gain (Table 1, Figure 18). At the same time, the difference in the $BG11_{diluted}$ treatment is quite substantial. Only two of the colonies survived in the lift treatment ($BG11_{diluted}$), while the rest turned pale yellowish and degraded.

In general, more colonies tend to degrade in lift experiments when compared to the sprinkler irrigation approach. It is possible that the rapid drying of colonies on the steel mesh causes stress to the organisms or that the colony is damaged when pressed against the mesh during desiccation. In addition, it was noted that when the sample holder is submerged, dry *Nostoc* tends to float on the surface of the water due to tension, which prevents optimal rehydration of the colony. Based on these observations, the following changes were made to the lift set-up for the next two main experiments: Marble chippings were filled into the chambers, completely covering the mesh and preventing the colonies from coming into direct contact with it. In addition, a white fly net was placed in each chamber, keeping the colonies in place while allowing sufficient light to pass through. These measures ensured that all colonies were perfectly rehydrated and delayed the desiccation.

Evaluating the influence of nitrogen concentration on the growth of *Nostoc commune*

Main experiment 2 revealed that colonies treated with standard BG11 show a smaller relative mass gain compared to those treated with $BG11_{N/10}$ using the same irrigation approach (Figure 20). It needs to be mentioned that the sprinkler irrigation with BG11 resulted in most samples dying off. This can be seen in Figure 19, where almost all *Nostoc* specimens show a pale-yellowish color, indicating degradation. In comparison, most of the samples supplied with $BG11_{N0}$

experiments were dark green and had a firm texture. We clearly found that *Nostoc commune* is sensitive against high nitrogen concentrations. Otero & Vincenzini (2003) demonstrated that diazotrophic cultivation promoted EPS production. This could partly explain the higher biomass gain observed in the $BG11_{N0}$ treated samples as the EPS builds the matrix of the *N. commune* colonies (Figure 20).

Interestingly, the results of a previous study, in which *N. commune* was cultivated in liquid culture, showed a positive effect of nitrogen on the growth rate. However, the samples were not cultured as macroscopic colonies but as free-living cells isolated from a biocrust (Roncero-Ramos, Román, et al., 2019). A possible explanation could be that culturing single cells preferred other conditions compared to macroscopic colonies or various strains have different preferences. Nevertheless, it cannot be excluded that it was misclassified as it did not appear in the typical macroscopic colonies but within a cyanobacterial biocrust. The isolated cells were characterized by morphology and an analyzed DNA sequence showed 99 % similarity to a reference sample (Roncero-Ramos, Muñoz-Martín, et al., 2019). Moreover, their cultures have not been screened at the end of the cultivation experiment, which makes it possible that other cyanobacteria were grown.

In addition, Cui et al. (2017) stated that *N. flagelliforme* trichomes in $BG11_{N0}$ under static conditions showed a threefold lower growth compared to the ones kept in BG11. But, they did not define how they measured the growth nor showed the underlying data for this statement. However, they also reported that EPS production was lowest in the BG11 medium. Nevertheless, there could be a difference in culturing macroscopic colonies or free floating single trichomes/microcolonies. Also, the preference for nitrogen-free medium is species-specific for *N. commune* as nitrogen was reported to promote biomass gain in liquid cultivation of *N. linckia* (Touloupakis et al., 2023).

Is periodical desiccation-rehydration beneficial for culturing terrestrial *Nostoc*?

Filling the lift sample chambers with substrate caused the samples to be permanently hydrated during the three hours at air between the submerging steps. Therefore, in main experiment 3, the drying period was extended to 24 h to test the hypothesis whether periodical desiccation and rewetting are beneficial for culturing terrestrial *Nostoc*. This interval allowed the colonies to dry significantly, which is also reflected in the reduction of the effective quantum yield after 24 hours (Figure 23). It turned out that the lifting platform with a 24-hour interval had the highest relative mass gains among all experiments conducted (Figure 21). For both media tested ($BG11_{N/10}$ and $BG11_{N0}$), an average relative gain in mass of over 500 % was observed after 21 days of culturing. Some specimens even showed dry mass gains above 1500 %. In comparison, the permanently submerged cultures gained about 100 % of their initial mass in the same period, which is significantly lower ($p < 0.05$, Table 3). The results clearly show how much more efficient the newly developed lift irrigation is, resulting in 5 times higher gains than aquacultures after three weeks. We conclude that periodical desiccation-rehydration is beneficial for growing terrestrial *Nostoc.* This is congruent with former studies underlying the importance of periodical drying, particularly in cultivating the closely related species *N. flagelliforme* (Feng et al., 2012). K. Gao & Ye (2003) suggested that the desiccation prevents bacterial degradation of colonies, which would explain why so many samples degraded more in the 3-hour interval experiment than when the period was extended to 24 hours (Figure 20, Figure 21). Moreover, a partially dried-out colony may represent the most effective stage regarding photochemical activity due to its smaller gelatinous matrix, thus reducing the diffusion layer for CO_2 (Kvíderová et al., 2011).

Moreover, the results of the main experiment 3 show that low nitrogen concentration has no beneficial effect over diazotrophic cultivation ($p >> 0.05$, Table 3). The only difference was in the increased number of degraded colonies. It appears as if atmospheric nitrogen is sufficient to supply *Nostoc commune;* we therefore suggest nitrogen-free BG11 as basal culture medium for growing macro-colonies.

Further extension of the drying period

Doubling the air period to 48 hours significantly reduced the biomass yield ($p < 0.05$, Table 3), which can be explained by the fact that after 24 hours, the colonies were already desiccated. As the field experiments showed, the effective quantum yield decreases rapidly after a certain water loss (Figure 13). In addition, the Φ_{PS2} signal ceased completely after 24 h in the experiment shown in Figure 23. This indicates the stop of CO_2 assimilation, which is mandatory for photoautotrophic growth. In other words, only about 24 of the 48 hours were conducive to photosynthesis, which is effectively half of the time. This agrees well with the observed mass gains. Colonies grew by an average of 250% in the 48-hour experiment, which is half as much as in the 24-hour experiment (Figure 21). However, only a single specimen did degrade. All others looked at the end very healthy regarding firm consistency and color (Figure 22). This could be an indicator that a certain desiccation periods could be essential for the long-term health of a colony and maybe even necessary for permanent culturing. This must be tested in culturing experiments on a much longer time scale. Nevertheless, also the colonies of the 24-hour $BG11_{N0}$ treatment had also very firm textures and healthy green colors and only three samples degraded (Figure 22). This marks the potential of this culturing method for fast growth and healthy colonies.

Do dark phases support the growth of *Nostoc*?

We also tested if a day and night cycle (16 h light/8 h night) is beneficial for the growth of *Nostoc commune* as it resembles the natural condition and was used in previous studies (Møller et al., 2014). Despite reducing the photochemical active time by 33 %, the samples cultured with dark phases showed, on average, only a 100 % lower relative dry mass gain compared to permanent illumination (Figure 21). However, the differences were statistically not significant ($p > 0.05$, Table 3).

Møller et al. (2014) used the same 16 h light/8 h dark cycle but cultured the *Nostoc commune* colonies floating on the surface of the water. They found the best results at 25 °C with a doubling time of about 13 days. Assuming the growth rate would not change, in 26 days, the mass gain would be 400 %. In comparison, our newly developed lift approach delivered an average mass gain of over 400 % within just 21 days, using the same light cycle (Figure 21).

Possible improvements and use cases for other terrestrial *Nostoc*

The developed cultivation approach showed high dry mass gains in a period of three weeks. However, experiments should be conducted to observe the viability and growth of colonies on a long-term time scale. In addition, several parameters such as light intensity, air humidity and micronutrient composition could be tested to further improve cultivation conditions. Moreover, an enriched CO_2 supply could be beneficial for growing *N. commune*, as it has already been shown for *N. flagelliforme* (K. Gao & Yu, 2000).

Previous studies found that periodical desiccations are essential for optimizing the growth of *N. flagelliforme* (K. Gao & Ye, 2003; Scherer & Zhong, 1991). The developed irrigation lift is obviously suitable for the efficient cultivation of macroscopic colonies. It is a milestone for large-scale cultivation to meet the demand for edible cyanobacterium in China, which would greatly relieve the natural populations. Due to the adaptation of *N. flagelliforme* to different climatic environments compared to *N. commune,* different parameters such as illumination and immersing interval surely must be adapted for optimal cultivation.

Conclusion

Nostoc commune can tolerate a huge range of environmental conditions, growing in full sun exposition on a concrete wall as well as in shaded spots on moist soil. The photochemical activity of *Nostoc* showed furthermost a strong dependency on the hydration status of the colonies. Only if the water supply is high enough, other environment parameters influence photosynthesis. However, dew cannot sufficiently rehydrate the colonies to reactivate the PSII system. *N. commune* needs to be soaked with water, to rapidly recover the effective quantum yield. If the samples are desiccated for a longer period, it takes more time to fully recover the photochemical potential.

Although *N. commune* can tolerate high light intensities and temperature, it seems as if it finds optimal growth conditions under moderate light intensities and temperatures around 25 °C. Nevertheless, more experiments must be performed to evaluate the detailed role of various environmental parameters (such as humidity, temperature and light).

Periodical desiccation-rehydration had a strong beneficial effect on the cultivation of *N. commune* regarding growth and health. Significantly higher mass gains were detected for a 24-hour drying interval compared to shorter intervals and permanently submerged cultures. In addition, we demonstrated that for the experimental settings used, the water loss of *Nostoc* colonies after 24 hours caused the photochemical activity to cease. Therefore, doubling the drying time resulted in approximately half the mass gain reported for the 24-hour interval.

Our results clearly indicate that a high inorganic nitrogen supply is detrimental to the growth and health of *N. commune*. $BG11_{N0}$ seems to be the best choice for cultivation. The findings suggest that nitrogen acts as a stress factor on *N. commune*, and is promoting competitors, which are co-cultivated in raw samples.

In addition, using a dark/light cycle instead of permanent illumination did not stimulate the growth of the colonies. The average dry mass yields tended to be smaller. It could have a positive effect on the vitality of the colonies and may be included in future approaches to save energy.

To sum up, the highest mass gains were reported for the newly developed lift irrigation (with marble chippings as substrate), immersing the samples into an aquarium filled with $BG11_{N0}$ medium every 24 h for 20 min at approximately 25 °C room temperature. Exchanging the medium at least every ten days and cleaning the aquarium to reduce contamination by other algal organisms is recommended. If axenic *N. commune* is used, the potential contamination by other organisms could be further reduced or completely excluded. On average, the colonies gained over 500 % of their initial dry mass after 21 days and appeared very healthy with an intense dark green color and firm texture.

However, further experiments must be conducted to optimize the additional parameters, such as the atmospheric CO_2 concentration and optimal light conditions. Moreover, future studies could test if the dry mass gain is mainly due to increased EPS production, due to cell division or a balanced combination of both.

The developed method can likely be adapted for the specific needs of other terrestrial *Nostoc* species, such as *N. flagelliforme* and *N. sphaeroides*. As these *Nostoc* species have plenty of potential applications in the food industry, cosmetics, and medicine, their successful cultivation will become of great interest. In this study, an efficient cultivation method was developed for *N. commune* macroscopic colonies, resulting in one of the fastest mass gains reported so far. This work could be an important step for farming terrestrial *Nostoc* on a large scale.

References

Adams, W. W., & Demmig-Adams, B. (2004). Chlorophyll Fluorescence as a Tool to Monitor Plant Response to the Environment. In G. C. Papageorgiou & Govindjee (Eds.), *Chlorophyll a Fluorescence. Advances in Photosynthesis and Respiration* (Vol. 19, pp. 583–604). Springer. https://doi.org/10.1007/978-1-4020-3218-9_22

Baker, N. R. (2008). Chlorophyll fluorescence: a probe of photosynthesis in vivo. *Annual Review of Plant Biology*, *59*, 89–113. https://doi.org/10.1146/ANNUREV.ARPLANT.59.032607.092759

Ballottari, M., Mozzo, M., Girardon, J., Hienerwadel, R., & Bassi, R. (2013). Chlorophyll triplet quenching and photoprotection in the higher plant monomeric antenna protein Lhcb5. *Journal of Physical Chemistry B*, *117*(38), 11337–11348. https://doi.org/10.1021/JP402977Y

Bergman, B., Johansson, C., & Söderbäck, E. (1992). The *Nostoc-Gunnera* symbiosis. *The New Phytologist*, *122*(3), 379–400. https://doi.org/10.1111/J.1469-8137.1992.TB00067.X

Björkman, O., & Demmig, B. (1987). Photon yield of O2 evolution and chlorophyll fluorescence characteristics at 77 K among vascular plants of diverse origins. *Planta*, *170*(4), 489–504. https://doi.org/10.1007/BF00402983

Cameron, R. E. (1962). Species of *Nostoc* Vaucher Occurring in the Sonoran Desert in Arizona. *Transactions of the American Microscopical Society*, *81*(4), 379. https://doi.org/10.2307/3223790

Campbell, D., Hurry, V., Clarke, A. K., Gustafsson, P., & Öquist, G. (1998). Chlorophyll fluorescence analysis of cyanobacterial photosynthesis and acclimation. *Microbiology and Molecular Biology Reviews : MMBR*, *62*(3), 667–683. https://doi.org/10.1128/MMBR.62.3.667-683.1998

Celis-Plá, P. S. M., Rearte, T. A., Neori, A., Masojídek, J., Bonomi-Barufi, J., Álvarez-Gómez, F., Ranglová, K., Carmo da Silva, J., Abdala, R., Gómez, C., Caporgno, M., Torzillo, G., Silva Benavides, A. M., Ralph, P. J., Fávero Massocato, T., Atzmüller, R., Vega, J., Chávez, P., & Figueroa, F. L. (2021). A new approach for cultivating the cyanobacterium *Nostoc calcicola* (MACC-612) to produce biomass and bioactive compounds using a thin-layer raceway pond. *Algal Research*, *59*, 102421. https://doi.org/10.1016/J.ALGAL.2021.102421

Cui, L., Xu, H., Zhu, Z., & Gao, X. (2017). The effects of the exopolysaccharide and growth rate on the morphogenesis of the terrestrial filamentous cyanobacterium *Nostoc flagelliforme*. *Biology Open*, *6*(9), 1329–1335. https://doi.org/10.1242/bio.026955

Davey, M. C. (1989). The effects of freezing and desiccation on photosynthesis and survival of terrestrial Antarctic algae and cyanobacteria. *Polar Biology*, *10*(1), 29–36. https://doi.org/10.1007/BF00238287/METRICS

De Philippis, R., Margheri, M. C., & Vincenzini, M. (1996). Fermentation in symbiotic and free-living Cyanobacteria. *Algological Studies/Archiv Für Hydrobiologie, Supplement Volumes*, *83*, 459–468. https://doi.org/10.1127/ALGOL_STUD/83/1996/459

Demmig-Adams, B. (1990). Carotenoids and photoprotection in plants: A role for the xanthophyll zeaxanthin. *Biochimica et Biophysica Acta (BBA) - Bioenergetics*, *1020*(1), 1–24. https://doi.org/10.1016/0005-2728(90)90088-L

Demmig-Adams, B., & Adams, W. W. (1990). The carotenoid zeaxanthin and "high-energy-state quenching" of chlorophyll fluorescence. *Photosynthesis Research*, *25*(3), 187–197. https://doi.org/10.1007/BF00033160/METRICS

Demmig-Adams, B., Adams, W. W., Czygan, F. C., Schreiber, U., & Lange, O. L. (1990). Differences in the capacity for radiationless energy dissipation in the photochemical apparatus of green and blue-green algal lichens associated with differences in carotenoid composition. *Planta*, *180*(4), 582–589. https://doi.org/10.1007/BF02411457/METRICS

Demmig-Adams, B., Stewart, J. J., Adams, W. W., López-Pozo, M., & Polutchko, S. K. (2020). Zeaxanthin, a Molecule for Photoprotection in Many Different Environments. *Molecules 2020, Vol. 25, Page 5825*, *25*(24), 5825. https://doi.org/10.3390/MOLECULES25245825

Dodds, W. K., Gudder, D. A., & Mollenhauer, D. (1995). Review - The ecology of *Nostoc*. *Journal of Phycology*, *31*, 2–18. https://doi.org/10.1111/j.0022-3646.1995.00002.x

Dvořák, P., Hašler, P., & Poulíčková, A. (2020). New insights into the genomic evolution of cyanobacteria using herbarium exsiccatae. *European Journal of Phycology*, *55*(1), 30–38. https://doi.org/10.1080/09670262.2019.1638523

El Bissati, K., Delphin, E., Murata, N., Etienne, A. L., & Kirilovsky, D. (2000). Photosystem II fluorescence quenching in the cyanobacterium *Synechocystis* PCC 6803: involvement of two different mechanisms. *Biochimica et Biophysica Acta (BBA) - Bioenergetics*, *1457*(3), 229–242. https://doi.org/10.1016/S0005-2728(00)00104-3

Ellenberg, H., Weber, H. E., Düll, R., Wirth, V., & Werner, W. (2001). *Zeigerwerte von Pflanzen in Mitteleuropa* (3., durchges. Aufl.). Verlag Erich Goltze.

Farhan Bhatti, A., Choubeh, R. R., Kirilovsky, D., Wientjes, E., & Van Amerongen, H. (2020). *State transitions in cyanobacteria studied with picosecond fluorescence at room temperature*. https://doi.org/10.1016/j.bbabio.2020.148255

Fassioli, F., Dinshaw, R., Arpin, P. C., & Scholes, G. D. (2014). Photosynthetic light harvesting: excitons and coherence. *Journal of The Royal Society Interface*, *11*(92). https://doi.org/10.1098/RSIF.2013.0901

Feng, Y. N., Zhang, Z. C., Feng, J. L., & Qiu, B. S. (2012). Effects of UV-B radiation and periodic desiccation on the morphogenesis of the edible terrestrial cyanobacterium *Nostoc flagelliforme*. *Applied and Environmental Microbiology*, *78*(19), 7075–7081. https://doi.org/10.1128/AEM.01427-12

Fidor, A., Grabski, M., Gawor, J., Gromadka, R., Egrzyn, G. W., & Mazur-Marzec, H. (2020). *Nostoc edaphicum* CCNP1411 from the Baltic Sea-A New Producer of yclopeptides. *Marine Drugs*, *18*(9). https://doi.org/10.3390/MD18090442

Frazer, G., Canham, C., & Lertzman, K. (1999). Gap light analyzer (GLA): Imaging software to extract canopy structure and gap light transmission indices from true-colour sheye photographs, users manual and program documentation. *Burnaby: Simon Fraser University*. https://www.sfu.ca/rem/forestry/downloads/gap-light-analyzer.html

Fukuda, S. Y., Yamakawa, R., Hirai, M., Kashino, Y., Koike, H., & Satoh, K. (2008). Mechanisms to Avoid Photoinhibition in a Desiccation-Tolerant Cyanobacterium, *Nostoc commune*. *Plant and Cell Physiology*, *49*(3), 488–492. https://doi.org/10.1093/PCP/PCN018

Gao, K. (1998). Chinese studies on the edible blue-green alga, *Nostoc flagelliforme*: A review. *Journal of Applied Phycology*, *10*, 37–49. https://doi.org/10.1023/A:1008014424247

Gao, K., Qiu, B., Xia, J., & Yu, A. (1998). Light dependency of the photosynthetic recovery of *Nostoc flagelliforme*. *Journal of Applied Phycology*, *10*, 51–53. https://doi.org/10.1023/A:1008011531325

Gao, K., & Ye, C. (2003). Culture of the terrestrial cyanobacterium, *Nostoc flagelliforme* (Cyanophyceae), under aquatic conditions. *Journal of Phycology*, *39*(3), 617–623. https://doi.org/10.1046/j.1529-8817.2003.02013.x

Gao, K., & Yu, A. (2000). Influence of CO2, light and watering on growth of *Nostoc flagelliforme* mats. *Journal of Applied Phycology*, *12*, 185–189. https://doi.org/10.1023/A:1008123203409

Gao, X., Ai, Y., & Qiu, B.-S. (2012). Drought adaptation of a terrestrial macroscopic cyanobacterium, *Nostoc flagelliforme*, in arid areas: A review. *African Journal of Microbiology Research*, *6*(28). https://doi.org/10.5897/AJMR12.894

Gao, X., Liu, K., & Qiu, B. S. (2011). An investigation on the genetic background of *Nostoc flagelliforme* by similarity analysis of its partial genomic DNA and phylogenetic comparison of deduced related species. *Acta Physiologiae Plantarum*, *33*(4), 1301–1318. https://doi.org/10.1007/s11738-010-0662-z

Gao, X., Xu, H., Ye, S., & Liang, W. (2016). A proposal on the restoration of *Nostoc flagelliforme* for sustainable improvement in the ecology of arid steppes in China. *Environments - MDPI*, *3*(2), 1–6. https://doi.org/10.3390/environments3020014

Gao, X., Yang, Y. W., Cui, L. J., Zhou, D. B., & Qiu, B. S. (2015). Preparation of desiccation-resistant aquatic-living *Nostoc flagelliforme* (Cyanophyceae) for potential ecological application. *Microbial Biotechnology*, *8*(6), 1006–1012. https://doi.org/10.1111/1751-7915.12279

Genty, B., Briantais, J. M., & Baker, N. R. (1989). The relationship between the quantum yield of photosynthetic electron transport and quenching of chlorophyll fluorescence. *Biochimica et Biophysica Acta (BBA) - General Subjects*, *990*(1), 87–92. https://doi.org/10.1016/S0304-4165(89)80016-9

Genty, B., Wonders, J., & Baker, N. R. (1990). Non-photochemical quenching of Fo in leaves is emission wavelength dependent: consequences for quenching analysis and its interpretation. *Photosynthesis Research*, *26*(2), 133–139. https://doi.org/10.1007/BF00047085/METRICS

Gorbunov, M. Y., Kuzminov, F. I., Fadeev, V. V., Kim, J. D., & Falkowski, P. G. (2011). A kinetic model of non-photochemical quenching in cyanobacteria. *Biochimica et Biophysica Acta (BBA) - Bioenergetics*, *1807*(12), 1591–1599. https://doi.org/10.1016/J.BBABIO.2011.08.009

Guevara, R., Armesto, J. J., & Caru, M. (2002). Genetic diversity of *Nostoc* microsymbionts from *Gunnera tinctoria* revealed by PCR-STRR fingerprinting. *Microbial Ecology*, *44*(2), 127–136. https://doi.org/10.1007/S00248-002-1019-Y

Guljamow, A., Kreische, M., Ishida, K., Liaimer, A., Altermark, B., Bähr, L., Hertweck, C., Ehwald, R., & Dittmann, E. (2017). High-density cultivation of terrestrial *Nostoc* strains leads to reprogramming of secondary metabolome. *Applied and Environmental Microbiology*, *83*(23). https://doi.org/10.1128/AEM.01510-17

Guo, S., Shan, S., Jin, X., Lei, Z., Li, Z., Zhao, L., An, Q., & Zhang, W. (2015). Water stress proteins from *Nostoc commune* Vauch. Exhibit anti-colon cancer activities in vitro and in vivo. *Journal of Agricultural and Food Chemistry*, *63*(1), 150–159. https://doi.org/10.1021/jf503208p

Han, D., Deng, Z., Lu, F., & Hu, Z. (2013). Biology and Biotechnology of Edible *Nostoc*. *Handbook of Microalgal Culture: Applied Phycology and Biotechnology: Second Edition*, 433–444. https://doi.org/10.1002/9781118567166.CH23

Hill, D. R., Hladuns, S. L., Scherero, S., & Pottssn, M. (1994). Water stress proteins of *Nostoc commune* (Cyanobacteria) are secreted with UV-A/B-absorbing pigments and associate with 1,4-beta-D-xylanxylanohydrolase activity. *The Journal of Biological Chemistry*, *269*(10), 7726–7734. https://doi.org/10.1016/S0021-9258(17)37347-7

Hill, D. R., Peat, A., & Potts, M. (1994). Biochemistry and structure of the glycan secreted by desiccation-tolerant *Nostoc commune* (Cyanobacteria). *Protoplasma*, *182*(3–4), 126–148. https://doi.org/10.1007/BF01403474/METRICS

Hirai, M., Yamakawa, R., Nishio, J., Yamaji, T., Kashino, Y., Koike, H., & Satoh, K. (2004). Deactivation of photosynthetic activities is triggered by loss of a small amount of water in a desiccation-tolerant cyanobacterium, *Nostoc commune*. *Plant & Cell Physiology*, *45*(7), 872–878. https://doi.org/10.1093/PCP/PCH094

Hori, K., Ishibashi, G., & Okita, T. (1994). Hypocholesterolemic effect of blue-green alga, ishikurage (*Nostoc commune*) in rats fed atherogenic diet. *Plant Foods for Human Nutrition (Dordrecht, Netherlands)*, *45*(1). https://doi.org/10.1007/BF01091230

Hu, C., Gao, K., & Whitton, B. A. (2012). Semi-arid regions and deserts. *Ecology of Cyanobacteria II: Their Diversity in Space and Time*, *9789400738553*, 345–369. https://doi.org/10.1007/978-94-007-3855-3_12

Huang, H., Bai, K. Z., Zhong, Z. P., Li, L. B., & Kuang, T. Y. (2005). Energy transfer from phycobilisomes to photosystems of *Nostoc flagelliforme* Born. et Flah. During the rewetting course and its physiological significance. *Journal of Integrative Plant Biology*, *47*(6), 703–708. https://doi.org/10.1111/j.1744-7909.2005.00105.x

Huang, Z., Liu, Y., Paulsen, B. S., & Klaveness, D. (1998). Studies on polysaccharides from three edible species of *Nostoc* (Cyanobacteria) with different colony morphologies: Comparison of monosaccharide compositions and viscosities of polysaccharides from field colonies and suspension cultures. *Journal of Phycology*, *34*(6), 962–968. https://doi.org/10.1046/j.1529-8817.1998.340962.x

Huo, D., Li, H., Cai, F., Guo, X., Qiao, Z., Wang, W., Yu, G., & Li, R. (2021). Genome evolution of filamentous cyanobacterium *Nostoc* species: From facultative symbiosis to free living. *Microorganisms*, *9*(10). https://doi.org/10.3390/MICROORGANISMS9102015/S1

Hymus, G. J., Ellsworth, D. S., Baker, N. R., & Long, S. P. (1999). *Does Free-Air Carbon Dioxide Enrichment Affect Photochemical Energy Use by Evergreen Trees in Different Seasons? A Chlorophyll Fluorescence Study of Mature Loblolly Pine 1*. https://doi.org/10.1104/pp.120.4.1183

Inoue-Sakamoto, K., Tanji, Y., Yamaba, M., Natsume, T., Masaura, T., Asano, T., Nishiuchi, T., & Sakamoto, T. (2018). Characterization of extracellular matrix components from the desiccation-tolerant cyanobacterium *Nostoc commune*. *Journal of General and Applied Microbiology*, *64*(1), 15–25. https://doi.org/10.2323/jgam.2017.03.001

Ishikita, H., Saenger, W., Biesiadka, J., Loll, B., & Knapp, E. W. (2006). How photosynthetic reaction centers control oxidation power in chlorophyll pairs P680, P700, and P870. *Proceedings of the National Academy of Sciences of the United States of America*, *103*(26), 9855–9860. https://doi.org/doi.org/10.1073/pnas.0601446103

Itoh, T., Tsuchida, A., Muramatsu, Y., Ninomiya, M., Ando, M., Tsukamasa, Y., & Koketsu, M. (2014). Antimicrobial and anti-inflammatory properties of Nostocionone isolated from *Nostoc commune* Vauch and its derivatives against Propionibacterium acnes. *Anaerobe*, *27*, 56–63. https://doi.org/10.1016/j.anaerobe.2014.03.006

Jaki, B., Orjala, J., & Sticher, O. (1999). A novel extracellular diterpenoid with antibacterial activity from the cyanobacterium *Nostoc commune*. *Journal of Natural Products*, *62*(3), 502–503. https://doi.org/10.1021/np980444x

Jänchen, J., Feyh, N., Szewzyk, U., & De Vera, J. P. P. (2016). Provision of water by halite deliquescence for *Nostoc commune* biofilms under Mars relevant surface conditions. *International Journal of Astrobiology*, *15*(2), 107–118. https://doi.org/10.1017/S147355041500018X

Jia, S., Ding, Z., Tan, N., Wang, N., Han, P., & Yuan, N. (2012). Heterotrophic fed-batch cultures of *Nostoc flagelliforme* and production of extracellular polysaccharides. *Advanced Materials Research*, *518–523*, 5468–5471. https://doi.org/10.4028/WWW.SCIENTIFIC.NET/AMR.518-523.5468

Kale, R., Hebert, A. E., Frankel, L. K., Sallans, L., Bricker, T. M., & Pospíšil, P. (2017). Amino acid oxidation of the D1 and D2 proteins by oxygen radicals during photoinhibition of Photosystem II. *Proceedings of the National Academy of Sciences of the United States of America*, *114*(11), 2988–2993. https://doi.org/10.1073/pnas.1618922114

Kanekiyo, K., Hayashi, K., Takenaka, H., Lee, J.-B., & Hayashi, T. (2007). Anti-herpes Simplex Virus Target of an Acidic Polysaccharide, Nostoflan, from the Edible Blue-Green Alga *Nostoc flagelliforme*. *Biol. Pharm. Bull*, *30*(8), 1573–1575. https://doi.org/10.1248/bpb.30.1573

Katoh, H., Furukawa, J., Tomita-Yokotani, K., & Nishi, Y. (2012). Isolation and purification of an axenic diazotrophic drought-tolerant cyanobacterium, *Nostoc commune*, from natural cyanobacterial crusts and its utilization for field research on soils polluted with radioisotopes. *Biochimica et Biophysica Acta - Bioenergetics*, *1817*(8), 1499–1505. https://doi.org/10.1016/j.bbabio.2012.02.039

Khoja, T. M., & Whitton, B. A. (1975). Heterotrophic growth of filamentous blue-green algae. *British Phycological Journal*, *10*(2), 139–148. https://doi.org/10.1080/00071617500650131

Kluge, M., Mollenhauer, D., Wolf, E., & Schüßler, A. (2002). The *Nostoc-Geosiphon* Endocytobiosis. *Cyanobacteria in Symbiosis*, 19–30. https://doi.org/10.1007/0-306-48005-0_3

Komárek, J. (2013). Cyanoprokaryota. Part 3: Heterocytous Genera. In *Freshwater Flora of Central Europe. eds: Büdel B, Gärtner G,Krienitz L, Schagerl M : Vol. 19/3*. Springer Spektrum.

Kuhl, A., & Lorenzen, H. (1964). Chapter 10 Handling and Culturing of *Chlorella*. In D. M. Prescott (Ed.), *Methods in Cell Biology* (Vol. 1, pp. 159–187). Academic Press. https://doi.org/https://doi.org/10.1016/S0091-679X(08)62092-0

Kvíderová, J., Elster, J., & Šimek, M. (2011). In situ response of *Nostoc commune* s.l. colonies to desiccation in Central Svalbard, Norwegian High Arctic. *Fottea*, *11*(1), 87–97. https://doi.org/10.5507/fot.2011.009

Lambreva, M. D., Russo, D., Polticelli, F., Scognamiglio, V., Antonacci, A., Zobnina, V., Campi, G., & Rea, G. (2014). Structure/Function/Dynamics of Photosystem II Plastoquinone Binding Sites. *Current Protein & Peptide Science*, *15*(4), 285. https://doi.org/10.2174/1389203715666140327104802

Li, H., Liu, S., Liu, Y., Li, W., Niu, A., Ren, P., Liu, Y., Jiang, C., Inam, M., & Guan, L. (2021). Effects of in vitro digestion and fermentation of *Nostoc commune* Vauch. polysaccharides on properties and gut microbiota. *Carbohydrate Polymers*, *281*(1). https://doi.org/10.1016/j.carbpol.2021.119055

Li, H., Xu, J., Liu, Y., Ai, S., Qin, F., Li, Z., Zhang, H., & Huang, Z. (2011). Antioxidant and moisture-retention activities of the polysaccharide from *Nostoc commune*. *Carbohydrate Polymers*, *83*(4), 1821–1827. https://doi.org/10.1016/j.carbpol.2010.10.046

Li, Z., & Guo, M. (2018). Healthy efficacy of *Nostoc commune* Vaucher. *Oncotarget*, *9*(18), 14669–14679. https://doi.org/10.18632/oncotarget.23620

Liang, Y., Shu, X., & Wang, W. (2022). Biochemical composition, heavy metal content and their geographic variations of the form species *Nostoc commune* across China. *Food Science and Technology*, *42*, e20022. https://doi.org/10.1590/FST.20022

Lima Neto, M. C., De Oliveira Martins, M., Ferreira-Silva, S. L., & Silveira, J. A. G. (2015). *Jatropha curcas* and *Ricinus communis* display contrasting photosynthetic mechanisms in response to environmental conditions. *Scientia Agricola*, *72*(3), 260–269. https://doi.org/10.1590/0103-9016-2014-0325

Lingvay, M., Akhtar, P., Sebők-Nagy, K., Páli, T., & Lambrev, P. H. (2020). Photobleaching of Chlorophyll in Light-Harvesting Complex II Increases in Lipid Environment. *Frontiers in Plant Science*, *11*, 547650. https://doi.org/10.3389/FPLS.2020.00849

Lipman, C. B. (1941). The Successful Revival of *Nostoc commune* from a Herbarium Specimen Eighty- Seven Years Old. *Bulletin of the Torrey Botanical Club*, *68*(9), 664. https://doi.org/10.2307/2481755

Luimstra, V. M., Merijn Schuurmans, · J, Carolina, ·, De Carvalho, F. M., Matthijs, H. C. P., Klaas, ·, Hellingwerf, J., & Huisman, J. (2019). Exploring the low photosynthetic efficiency of cyanobacteria in blue light using a mutant lacking phycobilisomes. *Photosynthesis Research*, *141*, 291–301. https://doi.org/10.1007/s11120-019-00630-z

Lüttge, U., Büdel, B., Ball, E., Strube, F., & Weber, P. (1995). Photosynthesis of terrestrial cyanobacteria under light and desiccation stress as expressed by chlorophyll fluorescence and gas exchange. *Journal of Experimental Botany*, *46*(3), 309–319. https://doi.org/10.1093/JXB/46.3.309

Margheri, M. C., & Allotta, G. (1993). Homoacetic fermentation in the cyanobacterium *Nostoc* sp. strain Cc from *Cycas circinalis*. *FEMS Microbiology Letters*, *111*, 378–1097. https://doi.org/10.1111/j.1574-6968.1993.tb06388.x

Matthijs, H. C. P., Ludérus, E. M. E., Löffler, H. J. M., Scholts, M. J. C., & Kraayenhof, R. (1984). Energy metabolism in the cyanobacterium *Plectonema boryanum*. Participation of the thylakoid photosynthetic electron transfer chain in the dark respiration of NADPH and NADH. *Biochimica et Biophysica Acta (BBA) - Bioenergetics*, *766*(1), 29–37. https://doi.org/10.1016/0005-2728(84)90213-5

McEvoy, J. P., Gascon, J. A., Batista, V. S., & Brudvig, G. W. (2005). The mechanism of photosynthetic water splitting. *Photochemical & Photobiological Sciences: Official Journal of the European Photochemistry Association and the European Society for Photobiology*, *4*(12), 940–949. https://doi.org/10.1039/B506755C

Meeks, J. C., & Elhai, J. (2002). Regulation of Cellular Differentiation in Filamentous Cyanobacteria in Free-Living and Plant-Associated Symbiotic Growth States. *Microbiology and Molecular Biology Reviews*, *66*(1), 94–121. https://doi.org/10.1128/MMBR.66.1.94-121.2002

Meeks, J. C., Joseph, C. M., & Haselkorn, R. (1988). Organization of the nif genes in cyanobacteria in symbiotic association with *Azolla* and . *Archives of Microbiology*, *150*(1), 61–71. https://doi.org/10.1007/BF00409719

Milou Schuurmans, R., Merijn Schuurmans, J., Bekker, M., Kromkamp, J. C., Matthijs, H. C. P., & Hellingwerf, K. J. (2014). The redox potential of the plastoquinone pool of the cyanobacterium *Synechocystis* species strain PCC 6803 is under strict homeostatic control. *Plant Physiology*, *165*(1), 463–475. https://doi.org/10.1104/PP.114.237313

Mirkovic, T., Ostroumov, E. E., Anna, J. M., Van Grondelle, R., Govindjee, & Scholes, G. D. (2017). Light absorption and energy transfer in the antenna complexes of photosynthetic organisms. *Chemical Reviews*, *117*(2), 249–293. https://doi.org/10.1021/ACS.CHEMREV.6B00002

Mollenhauer, D., Bengtsson, R., & Lindstrøm, E. A. (1999). Macroscopic cyanobacteria of the genus *Nostoc*: A neglected and endangered constituent of european inland aquatic biodiversity. *European Journal of Phycology*, *34*(4), 349–360. https://doi.org/10.1080/09670269910001736412

Møller, C. L., Vangsøe, M. T., & Sand-Jensen, K. (2014). Comparative growth and metabolism of gelatinous colonies of three cyanobacteria, *Nostoc commune*, *Nostoc pruniforme* and *Nostoc zetterstedtii*, at different temperatures. *Freshwater Biology*, *59*(10), 2183–2193. https://doi.org/10.1111/FWB.12421

Mullineaux, C. W. (2008). Phycobilisome-reaction centre interaction in cyanobacteria. *Photosynthesis Research*, *95*(2–3), 175–182. https://doi.org/10.1007/S11120-007-9249-Y

Mullineaux, C. W., & Allen, J. F. (1990). State 1-State 2 transitions in the cyanobacterium *Synechococcus* 6301 are controlled by the redox state of electron carriers between Photosystems I and II. *Photosynthesis Research*, *23*(3), 297–311. https://doi.org/10.1007/BF00034860/METRICS

Murchie, E. H., & Lawson, T. (2013). Chlorophyll fluorescence analysis: a guide to good practice and understanding some new applications. *Journal of Experimental Botany*, *64*(13), 3983–3998. https://doi.org/10.1093/jxb/ert208

Muzzopappa, F., & Kirilovsky, D. (2020). Changing Color for Photoprotection: The Orange Carotenoid Protein. *Trends in Plant Science*, *25*(1), 92–104. https://doi.org/10.1016/j.tplants.2019.09.013

Novis, P. M., Whitehead, D., Gregorich, E. G., Hunt, J. E., Sparrow, A. D., Hopkins, D. W., Elberling, B., & Greenfield, L. G. (2007a). Annual carbon fixation in terrestrial populations of *Nostoc commune* (Cyanobacteria) from an Antarctic dry valley is driven by temperature regime. *Global Change Biology*, *13*(6), 1224–1237. https://doi.org/10.1111/j.1365-2486.2007.01354.x

Novis, P. M., Whitehead, D., Gregorich, E. G., Hunt, J. E., Sparrow, A. D., Hopkins, D. W., Elberling, B., & Greenfield, L. G. (2007b). Annual carbon fixation in terrestrial populations of *Nostoc commune* (Cyanobacteria) from an Antarctic dry valley is driven by temperature regime. *Global Change Biology*, *13*(6), 1224–1237. https://doi.org/10.1111/j.1365-2486.2007.01354.x

Nowruzi, B., Haghighat, S., Fahimi, H., & Mohammadi, E. (2018). *Nostoc* cyanobacteria species: a new and rich source of novel bioactive compounds with pharmaceutical potential. In *Journal of Pharmaceutical Health Services Research* (Vol. 9, Issue 1, pp. 5–12). Blackwell Publishing Ltd. https://doi.org/10.1111/jphs.12202

Otero, A., & Vincenzini, M. (2003). Extracellular polysaccharide synthesis by *Nostoc* strains as affected by N source and light intensity. *Journal of Biotechnology*, *102*(2), 143–152. https://doi.org/10.1016/S0168-1656(03)00022-1

Oxborough, K., & Baker, N. R. (1997). Resolving chlorophyll a fluorescence images of photosynthetic efficiency into photochemical and non-photochemical components-calculation of qP and Fv 0 /Fm 0 without measuring Fo 0. In *Photosynthesis Research* (Vol. 54). Kluwer Academic Publishers. https://doi.org/10.1023/A:1005936823310

Pagels, F., Vasconcelos, V., & Guedes, A. C. (2021). Carotenoids from Cyanobacteria: Biotechnological Potential and Optimization Strategies. *Biomolecules*, *11*(5). https://doi.org/10.3390/BIOM11050735

Paracelsus. (1566). *Das Buch Meteororum*. Bryckman.

Patil, I. (2021). Visualizations with statistical details: The “ggstatsplot” approach. *Journal of Open Source Software*, *6*(61), 3167. https://doi.org/10.21105/JOSS.03167

Pfündel, E. (1998). Estimating the contribution of Photosystem I to total leaf chlorophyll fluorescence. *Photosynthesis Research*, *56*(2), 185–195. https://doi.org/10.1023/A:1006032804606

Posit team. (2023). RStudio: Integrated Development for R. In *RStudio, Inc., Boston, MA* (1.4.1106; p. http://www.posit.co/). Posit Software, PBC. http://www.rstudio.com/

Potts, M. (1997). Etymology of the Genus Name *Nostoc* (Cyanobacteria). *International Journal of Systematic Bacteriology*, 584. https://doi.org/10.1099/00207713-47-2-584

Potts M. (2000). *Nostoc*. In Whitton BA & Potts M (Eds.), *The Ecology of Cyanobacteria: Their Diversity in Time and Space* (pp. 465–504). Kluwer Academic Publishers. https://doi.org/10.1007/0-306-46855-7

Pui-Hay But, P., Cheng, L., Kwan Chan, P., Tai-Wai Lau, D., & Wing-Hin But, J. (2002). *Nostoc flagelliforme* and faked items retailed in Hong Kong. *Journal of Applied Phycology*, *24*, 143–145. https://doi.org/10.1023/A:1019518329032

Qiu, B., & Gao, K. (2002). Daily production and photosynthetic characteristics of *Nostoc flagelliforme* grown under ambient and elevated CO 2 conditions. *Journal of Applied Phycology*, *14*, 77–83. https://doi.org/10.1023/A:1019434414245

R Core Team. (2022). *R: A Language and Environment for Statistical Computing* (4.2.2). R Foundation for Statistical Computing, Vienna, Austria. https://www.R-project.org/

Rikkinen, J. (2013). Molecular studies on cyanobacterial diversity in lichen symbioses. *MycoKeys 6: 3-32*, *6*, 3–32. https://doi.org/10.3897/MYCOKEYS.6.3869

Rippka, R., & Herdman, M. (1992). Pasteur Culture Collection of Cyanobacterial Strains in Axenic Culture. Catalogue & Taxonomic Handbook. In *Catalogue of strains* (Vol. 1, p. 103). Institut Pasteur.

Rodgers, G. A., & Stewart, W. D. P. (1977). The cyanophyte-hepatic symbiosis I. Morphology and physiology. *New Phytologist*, *78*(2), 441–458. https://doi.org/10.1111/J.1469-8137.1977.TB04851.X

Rodriguez, S., Torres, F. G., & López, D. (2017). Preparation and characterization of polysaccharide films from the cyanobacteria *Nostoc commune*. *Polymers from Renewable Resources*, *8*(4), 133–150. https://doi.org/10.1177/204124791700800401

Román, J. R., Roncero-Ramos, B., Chamizo, S., Rodríguez-Caballero, E., & Cantón, Y. (2018). Restoring soil functions by means of cyanobacteria inoculation: Importance of soil conditions and species selection. *Land Degradation and Development*, *29*(9), 3184–3193. https://doi.org/10.1002/ldr.3064

Roncero-Ramos, B., Muñoz-Martín, M. Á., Chamizo, S., Fernández-Valbuena, L., Mendoza, D., Perona, E., Cantón, Y., & Mateo, P. (2019). Polyphasic evaluation of key cyanobacteria in biocrusts from the most arid region in Europe. *PeerJ*, *7:e6169*. https://doi.org/10.7717/peerj.6169

Roncero-Ramos, B., Román, J. R., Gómez-Serrano, C., Cantón, Y., & Acién, F. G. (2019). Production of a biocrust-cyanobacteria strain (*Nostoc commune*) for large-scale restoration of dryland soils. *Journal of Applied Phycology*, *31*(4), 2217–2230. https://doi.org/10.1007/s10811-019-1749-6

Sakamoto, T., Hashimoto, A., Yamaba, M., Wada, N., Yoshida, T., Inoue-Sakamoto, K., Nishiuchi, T., & Matsugo, S. (2019). Four chemotypes of the terrestrial cyanobacterium *Nostoc commune* characterized by differences in the mycosporine-like amino acids. *Phycological Research*, *67*(1), 3–11. https://doi.org/10.1111/PRE.12333

Sammlung von Algenkulturen Göttingen. (2013). Medium Recipe Vers. 05.2013. In *Sammlung von Algenkulturen Göttingen*. Elsevier/Academic Press. http://sagdb.uni-goettingen.de/culture_media/20%20BG11%20Medium.pdf

Sand-Jensen, K. (2014). Ecophysiology of gelatinous *Nostoc* colonies: unprecedented slow growth and survival in resource-poor and harsh environments. *Annals of Botany*, *114*(1), 17–33. https://doi.org/10.1093/AOB/MCU085

Sand-Jensen, K., & Jespersen, T. S. (2012). Tolerance of the widespread cyanobacterium *Nostoc commune* to extreme temperature variations (-269 to 105°C), pH and salt stress. *Oecologia*, *169*(2), 331–339. https://doi.org/10.1007/s00442-011-2200-0

Santos-Merino, M., Torrado, A., Davis, G. A., Rottig, A., Bibby, T. S., Kramer, D. M., & Ducat, D. C. (2021). Improved photosynthetic capacity and photosystem I oxidation via heterologous metabolism engineering in cyanobacteria. *Proceedings of the National Academy of Sciences of the United States of America*, *118*(11), 2021523118. https://doi.org/10.1073/pnas.2021523118

Satoh, K., Hirai, M., Nishio, J., Yamaji, T., Kashino, Y., & Koike, H. (2002). Recovery of photosynthetic systems during rewetting is quite rapid in a terrestrial cyanobacterium, *Nostoc commune*. *Plant & Cell Physiology*, *43*(2), 170–176. https://doi.org/10.1093/PCP/PCF020

Schagerl, M., & Müller, B. (2006). Acclimation of chlorophyll a and carotenoid levels to different irradiances in four freshwater cyanobacteria. *Journal of Plant Physiology*, *163*(7), 709–716. https://doi.org/10.1016/J.JPLPH.2005.09.015

Scherer, S., & Zhong, Z. P. (1991). Desiccation independence of terrestrial *Nostoc commune* ecotypes (cyanobacteria). *Microbial Ecology*, *22*(1), 271–283. https://doi.org/10.1007/BF02540229

Schreiber, U. (2004). Pulse-Amplitude-Modulation (PAM) Fluorometry and Saturation Pulse Method: An Overview. In G. C. Papageorgiou & Govindjee (Eds.), *Chlorophyll a Fluorescence. Advances in Photosynthesis and Respiration* (Vol. 19, pp. 280–312). Springer. https://doi.org/10.1007/978-1-4020-3218-9_11

Schreiber, U., Bilger, W., & Neubauer, C. (1995). Chlorophyll Fluorescence as a Nonintrusive Indicator for Rapid Assessment of In Vivo Photosynthesis. *Ecophysiology of Photosynthesis*, 49–70. https://doi.org/10.1007/978-3-642-79354-7_3

Schüßler, A., & Kluge, M. (2001). *Geosiphon* pyriforme, an Endocytosymbiosis Between Fungus and Cyanobacteria, and its Meaning as a Model System for Arbuscular Mycorrhizal Research. In B. Hock (Ed.), *Fungal Associations. The Mycota* (Vol. 9, pp. 151–161). Springer Berlin Heidelberg. https://doi.org/10.1007/978-3-662-07334-6_9

Schüßler, A., Martin, H., Cohen, D., Fitz, M., & Wipf, D. (2007). Arbuscular Mycorrhiza: Studies on the *Geosiphon* Symbiosis Lead to the Characterization of the First Glomeromycotan Sugar Transporter. *Plant Signaling & Behavior*, *2*(5), 431. https://doi.org/10.4161/PSB.2.5.4465

Schüßler, A., & Wolf, E. (2005). *Geosiphon pyriformis*—a Glomeromycotan Soil Fungus Forming Endosymbiosis with Cyanobacteria. In S. Declerck, J. Fortin, & D. Strullu (Eds.), *In Vitro Culture of Mycorrhizas. Soil Biology* (Vol. 4, pp. 271–289). Springer, Berlin, Heidelberg. https://doi.org/10.1007/3-540-27331-X_15

Schuurmans, R. M., Van Alphen, P., Merijn Schuurmans, J., Matthijs, H. C. P., & Hellingwerf, K. J. (2015). Comparison of the Photosynthetic Yield of Cyanobacteria and Green Algae: Different Methods Give Different Answers. PLoS ONE 10(9): e0139061. https://doi.org/10.1371/journal.pone.0139061

Shirkey, B., McMaster, N. J., Smith, S. C., Wright, D. J., Rodriguez, H., Jaruga, P., Birincioglu, M., Helm, R. F., & Potts, M. (2003). Genomic DNA of *Nostoc commune* (Cyanobacteria) becomes covalently modified during long-term (decades) desiccation but is protected from oxidative damage and degradation. *Nucleic Acids Research*, *31*(12), 2995–3005. https://doi.org/10.1093/nar/gkg404

Stal, L. J., & Moezelaar, R. (1997). Fermentation in cyanobacteria. *FEMS Microbiology Reviews*, *21*(2), 179–211. https://doi.org/10.1016/S0168-6445(97)00056-9

Sun, J. Z., Wang, T., Huang, R., Yi, X., Zhang, D., Beardall, J., Hutchins, D. A., Liu, X., Wang, X., Deng, Z., Li, G., Gao, G., & Gao, K. (2022). Enhancement of diatom growth and phytoplankton productivity with reduced O2 availability is moderated by rising CO2. *Communications Biology 2022 5:1*, *5*(1), 1–12. https://doi.org/10.1038/s42003-022-03006-7

Takaichi, S., Maoka, T., & Mochimaru, M. (2009). Unique carotenoids in the terrestrial cyanobacterium *Nostoc commune* NIES-24: 2-hydroxymyxol 2′-fucoside, nostoxanthin and canthaxanthin. *Current Microbiology*, *59*(4), 413–419. https://doi.org/10.1007/S00284-009-9453-4

Takenaka, H., Yamaguchi, Y., Sakaki, S., Watarai, K., Tanaka, N., Hori, M., Seki, H., Tsuchida, M., Yamada, A., Nishimori, T., & Morinaga, T. (1998). Safety evaluation of *Nostoc flagelliforme* (Nostocales, Cyanophyceae) as a potential food. *Food and Chemical Toxicology : An International Journal Published for the British Industrial Biological Research Association*, *36*(12), 1073–1077. https://doi.org/10.1016/S0278-6915(98)00089-1

Tamaru, Y., Takani, Y., Yoshida, T., & Sakamoto, T. (2005). Crucial role of extracellular polysaccharides in desiccation and freezing tolerance in the terrestrial cyanobacterium *Nostoc commune*. *Applied and Environmental Microbiology*, *71*(11), 7327–7333. https://doi.org/10.1128/AEM.71.11.7327-7333.2005

Thimijan, R. W., & Heins, R. D. (1983). Photometric, Radiometric, and Quantum Light Units of Measure: A Review of Procedures for Interconversion. *HortScience*, *18*(6), 818–822. https://doi.org/10.21273/HORTSCI.18.6.818

Tikhonova, I., Kuzmin, A., Deeva, D., Sorokovikova, E., Potapov, S., Lomakina, A., & Belykh, O. (2017). Cyanobacteria *Nostoc punctiforme* from Abyssal Benthos of Lake Baikal: Unique Ecology and Metabolic Potential. *Indian Journal of Microbiology*, *57*(4), 422–426. https://doi.org/10.1007/s12088-017-0673-1

Torres-Maza, A., Yupanqui-Bacilio, C., Castro, V., Aguirre, E., Villanueva, E., & Rodríguez, G. (2020). Comparison of the hydrocolloids *Nostoc commune* and *Nostoc sphaericum*: Drying, spectroscopy, rheology and application in nectar. *Scientia Agropecuaria*, *11*(4), 583–589. https://doi.org/10.17268/SCI.AGROPECU.2020.04.14

Touloupakis, E., Zittelli, G. C., Benavides, A. M. S., & Torzillo, G. (2023). Growth and photosynthetic performance of *Nostoc linckia* (formerly *N. calcicola*) cells grown in BG11 and BG110 media. *Photochemical and Photobiological Sciences*, *22*(4), 795–807. https://doi.org/10.1007/S43630-022-00353-6

Tripathi, R., Dhuldhaj Umesh P., & Singh, S. (1970). Short Communication: Effects of temperature on growth, pigment composition and protein content of an Antarctic Cyanobacterium *Nostoc commune*. *Nusantara Bioscience*, *4*(3). https://doi.org/10.13057/nusbiosci/n040308

Tseng:, C. C., Yeh, H. Y., Liao, Z. H., Hung, S. W., Chen, B., Lee, P. T., Nan, F. H., Shih, W. L., Chang, C. C., & Lee, M. C. (2021). An in vitro study shows the potential of *Nostoc commune* (Cyanobacteria) polysaccharides extract for wound-healing and anti-allergic use in the cosmetics industry. *Journal of Functional Foods*, *87*, 104754. https://doi.org/10.1016/J.JFF.2021.104754

Tyystjärvi, E. (2013). Photoinhibition of Photosystem II. *International Review of Cell and Molecular Biology*, *300*, 243–303. https://doi.org/10.1016/B978-0-12-405210-9.00007-2

Wilson, A., Ajlani, G., Verbavatz, J. M., Vass, I., Kerfeld, C. A., & Kirilovsky, D. (2006). A soluble carotenoid protein involved in phycobilisome-related energy dissipation in cyanobacteria. *The Plant Cell*, *18*(4), 992–1007. https://doi.org/10.1105/TPC.105.040121

Yang, Y., Park, Y., Cassada, D. A., Snow, D. D., Rogers, D. G., & Lee, J. (2011). In vitro and in vivo safety assessment of edible blue-green algae, *Nostoc commune* var. *sphaeroides* Kützing and *Spirulina platensis*. *Food and Chemical Toxicology*, *49*(7), 1560–1564. https://doi.org/10.1016/j.fct.2011.03.052

Ye, T., Wang, B., Li, C., Bian, P., Chen, L., & Wang, G. (2021). Exposure of cyanobacterium *Nostoc* sp. to the Mars-like stratosphere environment. *Journal of Photochemistry and Photobiology B: Biology*, *224*, 112307. https://doi.org/10.1016/J.JPHOTOBIOL.2021.112307

Yu, H., Jia, S., & Dai, Y. (2009). Growth characteristics of the cyanobacterium *Nostoc flagelliforme* in photoautotrophic, mixotrophic and heterotrophic cultivation. *Journal of Applied Phycology*, *21*(1), 127–133. https://doi.org/10.1007/s10811-008-9341-5

Yu, H., Jia, S., & Dai, Y. (2010). Accumulation of exopolysaccharides in liquid suspension culture of *Nostoc flagelliforme* cells. *Applied Biochemistry and Biotechnology*, *160*(2), 552–560. https://doi.org/10.1007/s12010-008-8428-4

Appendix

Tables with the raw data of all experiments:

Appendix 1 Raw data of the PAM fluorescence measurements (ambient light) of *Nostoc commune* at the sun-exposed location **1/2**

Date	Time	Fs	Fm'	ΦPS2	PAR [lx]	Temperature [°C]	Relative Humidity [%]
12.07.2022	00:00	125	282,5	0,56	0,00	12,38	91,95
12.07.2022	00:15	129	283	0,54	0,00	12,46	92,13
12.07.2022	00:30	129	283	0,54	0,00	12,39	92,19
12.07.2022	00:45	123	285	0,57	0,00	12,46	92,03
12.07.2022	01:00	122	287	0,58	0,00	11,89	93,25
12.07.2022	01:15	122	282	0,57	0,00	11,40	95,15
12.07.2022	01:30	124	276	0,55	0,00	11,51	95,62
12.07.2022	01:45	128	285	0,55	0,00	11,73	95,43
12.07.2022	02:00	124	281	0,56	0,00	11,54	95,43
12.07.2022	02:15	130	281	0,54	0,00	11,56	95,87
12.07.2022	02:30	130	278	0,53	0,00	11,32	95,60
12.07.2022	02:45	127	278	0,54	0,00	11,43	96,46
12.07.2022	03:00	122	271	0,55	0,00	11,54	96,09
12.07.2022	03:15	131	286	0,54	0,00	11,41	96,35
12.07.2022	03:30	132	293	0,55	0,00	11,40	96,43
12.07.2022	03:45	131	293	0,55	0,00	11,26	96,06
12.07.2022	04:00	131	293	0,55	0,00	10,68	96,33
12.07.2022	04:15	135	286	0,53	0,00	10,94	97,47
12.07.2022	04:30	134	281	0,52	0,00	11,25	97,06
12.07.2022	04:45	145	288	0,50	0,00	11,34	96,69
12.07.2022	05:00	140	286	0,51	30,81	11,30	96,87
12.07.2022	05:15	137	288	0,52	133,50	11,39	97,08
12.07.2022	05:30	142	320	0,56	236,14	11,48	96,68
12.07.2022	05:45	146	337	0,57	431,26	11,56	96,25
12.07.2022	06:00	149	344	0,57	1232,15	11,74	95,88
12.07.2022	06:15	148	347	0,57	862,46	11,87	95,65
12.07.2022	06:30	149	352	0,58	985,71	12,00	95,64
12.07.2022	06:45	147	355	0,59	1149,97	12,01	98,99
12.07.2022	07:00	225	478	0,53	1807,11	11,96	99,63
12.07.2022	07:15	259	556	0,53	1026,77	12,27	99,66
12.07.2022	07:30	267	596	0,55	646,88	12,33	99,69
12.07.2022	07:45	286	593	0,52	2957,07	12,62	99,72
12.07.2022	08:00	287	594	0,52	2135,68	12,75	99,66
12.07.2022	08:15	285	600	0,53	1724,98	12,81	99,62
12.07.2022	08:30	282	598	0,53	1807,11	12,84	99,76
12.07.2022	08:45	312	580	0,46	3121,38	13,67	99,90
12.07.2022	09:00	303	506	0,40	12485,53	14,38	98,94
12.07.2022	09:15	311	526	0,41	5914,20	14,49	99,74
12.07.2022	09:30	317	483	0,34	10514,12	15,34	99,58
12.07.2022	09:45	317	472	0,33	11828,39	15,95	99,67
12.07.2022	10:00	306	398	0,23	27599,52	17,65	99,18
12.07.2022	10:15	295	379	0,22	24971,02	18,23	98,10
12.07.2022	10:30	301	391	0,23	22342,51	18,49	98,00
12.07.2022	10:45	275	325	0,15	27599,52	20,69	95,16
12.07.2022	11:00	262	330	0,21	23656,74	19,29	91,94
12.07.2022	11:15	238	296	0,20	38113,64	21,33	90,49
12.07.2022	11:30	209	263	0,21	42056,47	23,92	68,54
12.07.2022	11:45	189	253	0,25	24971,02	21,68	68,47
12.07.2022	12:00	186	263	0,29	21028,24	20,51	71,30
12.07.2022	12:15	173	241	0,28	23656,74	22,83	66,69
12.07.2022	12:30	162	225	0,28	32856,58	22,05	64,89
12.07.2022	12:45	162	226	0,28	27599,52	25,35	61,25
12.07.2022	13:00	151	203	0,26	131426,42	31,95	43,16
12.07.2022	13:15	163	254	0,36	21028,24	25,19	57,79
12.07.2022	13:30	157	270	0,42	16428,31	22,71	64,19
12.07.2022	13:45	147	257	0,43	24971,02	22,82	63,02
12.07.2022	14:00	166	241	0,31	34170,86	31,18	48,33
12.07.2022	14:15	135	211	0,36	60456,15	33,24	42,02
12.07.2022	14:30	140	199	0,30	49942,03	33,67	43,36
12.07.2022	14:45	111	174	0,36	55199,09	29,27	47,06
12.07.2022	15:00	119	195	0,39	23656,74	22,52	59,20
12.07.2022	15:15	112	215	0,48	12485,53	21,67	64,83
12.07.2022	15:30	116	227	0,49	11828,39	20,40	63,22
12.07.2022	15:45	119	224	0,47	17742,54	21,86	64,39
12.07.2022	16:00	129	189	0,32	68341,72	30,33	43,82
12.07.2022	16:15	97	179	0,46	94627,01	31,05	41,53
12.07.2022	16:30	94	171	0,45	76227,33	32,28	39,00
12.07.2022	16:45	93	166	0,44	27599,52	29,85	44,55
12.07.2022	17:00	97	156	0,38	52570,59	31,48	40,82
12.07.2022	17:15	85	160	0,47	55199,09	29,86	42,93
12.07.2022	17:30	80	159	0,50	17085,45	27,03	48,87
12.07.2022	17:45	76	157	0,52	27599,52	25,52	52,59
12.07.2022	18:00	81	163	0,50	12485,53	22,07	60,01
12.07.2022	18:15	66	176	0,63	6242,77	19,56	64,36
12.07.2022	18:30	67	180	0,63	3121,38	18,67	69,51
12.07.2022	18:45	65	172	0,62	8214,13	19,22	71,66
12.07.2022	19:00	71	180	0,61	5914,20	18,67	74,24
12.07.2022	19:15	70	181	0,61	4107,09	18,39	73,43
12.07.2022	19:30	66	177	0,63	5585,63	18,12	76,15
12.07.2022	19:45	70	192	0,64	2546,38	17,38	77,98
12.07.2022	20:00	69	194	0,64	1478,54	16,84	82,37
12.07.2022	20:15	68	199	0,66	944,64	16,23	83,99
12.07.2022	20:30	70	197	0,65	482,58	15,60	86,69
12.07.2022	20:45	66	202	0,67	343,97	15,13	87,12
12.07.2022	21:00	69	195	0,65	87,28	14,58	88,55
12.07.2022	21:15	67	198	0,66	0,00	14,27	89,83
12.07.2022	21:30	66	203	0,68	0,00	14,61	89,34
12.07.2022	21:45	71	197	0,64	0,00	14,69	90,07
12.07.2022	22:00	70	192	0,64	0,00	14,48	90,42
12.07.2022	22:15	69	198	0,65	0,00	14,11	91,47
12.07.2022	22:30	70	200	0,65	0,00	13,88	92,13
12.07.2022	22:45	67	203	0,67	0,00	13,42	92,57
12.07.2022	23:00	67	206	0,68	0,00	13,07	93,93
12.07.2022	23:15	71	206	0,66	0,00	13,38	93,07
12.07.2022	23:30	66	206	0,68	0,00	12,41	93,93
12.07.2022	23:45	72	205	0,65	0,00	12,23	94,57

Date	Time	Fs	Fm'	ΦPS2	PAR [lx]	Temperature [°C]	Relative Humidity [%]
13.07.2022	00:00	72	210	0,66	0,00	11,67	94,05
13.07.2022	00:15	76	210	0,64	0,00	11,57	95,80
13.07.2022	00:30	74	205	0,64	0,00	11,96	96,09
13.07.2022	00:45	79	213	0,63	0,00	11,91	96,34
13.07.2022	01:00	74	210	0,65	0,00	11,96	96,02
13.07.2022	01:15	76	214	0,65	0,00	11,56	96,10
13.07.2022	01:30	71	213	0,67	0,00	11,20	96,03
13.07.2022	01:45	76	211	0,64	0,00	11,30	97,06
13.07.2022	02:00	75	213	0,65	0,00	11,23	96,71
13.07.2022	02:15	75	210	0,64	0,00	11,50	96,72
13.07.2022	02:30	75	219	0,66	0,00	10,86	95,83
13.07.2022	02:45	75	218	0,66	0,00	10,08	95,98
13.07.2022	03:00	74	213	0,65	0,00	10,01	97,25
13.07.2022	03:15	77	209	0,63	0,00	10,67	97,48
13.07.2022	03:30	73	213	0,66	0,00	10,17	96,42
13.07.2022	03:45	75	212	0,65	0,00	9,84	96,71
13.07.2022	04:00	74	213	0,65	0,00	9,21	96,75
13.07.2022	04:15	74	214	0,65	0,00	9,25	97,40
13.07.2022	04:30	75	214	0,65	0,00	9,18	97,67
13.07.2022	04:45	79	208	0,62	0,00	10,08	98,89
13.07.2022	05:00	77	218	0,65	30,81	10,59	97,81
13.07.2022	05:15	81	230	0,65	138,60	10,83	97,43
13.07.2022	05:30	82	236	0,65	302,91	10,70	98,39
13.07.2022	05:45	78	241	0,68	739,27	10,96	99,04
13.07.2022	06:00	83	243	0,66	1314,28	11,30	96,71
13.07.2022	06:15	86	246	0,65	1724,98	11,36	96,13
13.07.2022	06:30	89	246	0,64	2299,98	11,49	96,45
13.07.2022	06:45	94	247	0,62	2217,81	11,89	95,97
13.07.2022	07:00	100	241	0,59	4435,66	12,59	93,99
13.07.2022	07:15	104	231	0,55	9199,84	13,11	92,21
13.07.2022	07:30	92	231	0,60	3942,78	12,82	93,61
13.07.2022	07:45	87	236	0,63	2957,07	12,30	94,98
13.07.2022	08:00	89	238	0,63	2382,11	12,46	94,67
13.07.2022	08:15	88	228	0,61	2217,81	12,87	94,50
13.07.2022	08:30	88	230	0,62	2464,24	13,34	92,39
13.07.2022	08:45	92	229	0,60	2628,51	13,92	91,03
13.07.2022	09:00	89	226	0,61	2957,07	14,76	89,98
13.07.2022	09:15	89	225	0,60	3449,95	15,69	88,24
13.07.2022	09:30	99	200	0,51	57827,60	18,61	81,73
13.07.2022	09:45	88	201	0,56	76227,33	21,32	73,82
13.07.2022	10:00	87	194	0,55	78855,83	22,77	73,38
13.07.2022	10:15	71	110	0,36	84112,89	32,17	43,41
13.07.2022	10:30	57	87	0,35	84112,89	34,74	37,36
13.07.2022	10:45	51	81	0,37	89369,95	35,57	35,05
13.07.2022	11:00	40	65	0,39	94627,01	35,92	34,90
13.07.2022	11:15	39	66	0,41	105141,13	36,91	33,93
13.07.2022	11:30	34	60	0,43	105141,13	36,87	33,18
13.07.2022	11:45	27	59	0,54	120912,31	34,71	36,83
13.07.2022	12:00	30	47	0,36	115655,25	37,79	32,73
13.07.2022	12:15	22	43	0,49	84112,89	35,66	36,60
13.07.2022	12:30	17	37	0,54	15771,18	37,90	32,43
13.07.2022	12:45	24	34	0,29	10514,12	37,71	32,76
13.07.2022	13:00	23	32	0,28	120912,31	39,00	30,92
13.07.2022	13:15	20	34	0,41	120912,31	42,02	28,14
13.07.2022	13:30	21	25	0,16	110398,19	39,37	30,53
13.07.2022	13:45	13	25	0,48	110398,19	40,38	28,69
13.07.2022	14:00	14	21	0,33	110398,19	43,57	25,67
13.07.2022	14:15	17	18	0,06	110398,19	44,63	23,45
13.07.2022	14:30	17	20	0,15	81484,39	44,05	22,58
13.07.2022	14:45	12	17	0,29	105141,13	44,19	23,12
13.07.2022	15:00	12	15	0,00	94627,01	43,84	25,18
13.07.2022	15:15	17	16	0,00	57827,60	41,33	24,69
13.07.2022	15:30	17	17	0,00	99884,07	44,45	23,69
13.07.2022	15:45	16	14	0,00	89369,95	46,05	20,16
13.07.2022	16:00	11	14	0,21	81484,39	45,59	18,42
13.07.2022	16:15	13	15	0,13	76227,33	45,11	19,22
13.07.2022	16:30	13	15	0,13	70970,27	41,62	23,07
13.07.2022	16:45	12	14	0,14	63084,66	43,76	20,22
13.07.2022	17:00	13	13	0,00	57827,60	41,36	25,27
13.07.2022	17:15	13	13	0,00	52570,59	38,63	24,87
13.07.2022	17:30	9	12	0,25	34170,86	39,03	23,82
13.07.2022	17:45	8	13	0,39	13799,76	30,64	37,80
13.07.2022	18:00	10	10	0,00	11171,26	27,61	44,32
13.07.2022	18:15	10	11	0,09	9199,84	26,81	46,23
13.07.2022	18:30	8	11	0,27	8871,27	26,19	47,97
13.07.2022	18:45	11	12	0,08	8871,27	25,70	52,37
13.07.2022	19:00	10	13	0,23	6242,77	24,68	53,89
13.07.2022	19:15	6	12	0,50	4107,09	23,54	56,17
13.07.2022	19:30	7	12	0,42	3449,95	22,66	58,54
13.07.2022	19:45	8	9	0,11	2464,24	21,96	61,24
13.07.2022	20:00	6	10	0,40	1478,54	21,22	64,64
13.07.2022	20:15	22	23	0,04	1108,90	20,63	65,37
13.07.2022	20:30	21	24	0,13	549,30	20,03	67,55
13.07.2022	20:45	21	22	0,05	236,14	19,65	68,77
13.07.2022	21:00	16	16	0,00	61,62	19,40	70,06
13.07.2022	21:15	17	20	0,15	0,00	19,10	70,54
13.07.2022	21:30	15	19	0,21	0,00	18,32	73,93
13.07.2022	21:45	18	20	0,10	0,00	18,08	75,37
13.07.2022	22:00	17	19	0,11	0,00	17,28	76,64
13.07.2022	22:15	15	20	0,25	0,00	17,19	77,51
13.07.2022	22:30	15	21	0,29	0,00	15,97	79,50
13.07.2022	22:45	17	21	0,19	0,00	14,68	83,42
13.07.2022	23:00	18	20	0,10	0,00	14,10	85,18
13.07.2022	23:15	15	21	0,29	0,00	13,67	86,71
13.07.2022	23:30	17	21	0,19	0,00	14,25	85,60
13.07.2022	23:45	17	20,5	0,17	0,00	14,45	85,77

Appendix 2 Data of the PAM fluorescence measurements (ambient light) of *Nostoc commune* at the sun-exposed location **2/2**

Date	Time	Fs	Fm'	ΦPS2	PAR [lx]	Temperature [°C]	Relative Humidity [%]
14.07.2022	00:00	17	20	0,15	0,00	15,00	85,85
14.07.2022	00:15	16	21	0,24	0,00	14,80	86,28
14.07.2022	00:30	15	21	0,29	0,00	12,71	88,21
14.07.2022	00:45	15	19	0,21	0,00	12,41	91,65
14.07.2022	01:00	15	22	0,32	0,00	14,27	89,93
14.07.2022	01:15	17	23	0,26	0,00	14,82	87,11
14.07.2022	01:30	17	20	0,15	0,00	14,35	86,98
14.07.2022	01:45	15	21	0,29	0,00	13,04	89,56
14.07.2022	02:00	14	20	0,30	0,00	13,31	90,64
14.07.2022	02:15	14	21	0,33	0,00	12,70	90,02
14.07.2022	02:30	16	21	0,24	0,00	11,28	92,23
14.07.2022	02:45	16	20	0,20	0,00	10,65	93,47
14.07.2022	03:00	17	17	0,00	0,00	10,54	93,93
14.07.2022	03:15	15	19	0,21	0,00	10,16	94,21
14.07.2022	03:30	14	19	0,26	0,00	10,00	95,41
14.07.2022	03:45	15	20	0,25	0,00	10,36	94,70
14.07.2022	04:00	15	21	0,29	0,00	10,24	94,49
14.07.2022	04:15	14	19	0,26	0,00	10,51	94,97
14.07.2022	04:30	17	18	0,06	0,00	11,11	94,13
14.07.2022	04:45	16	20	0,20	0,00	11,24	94,10
14.07.2022	05:00	17	21	0,19	20,56	11,82	93,37
14.07.2022	05:15	13	19	0,32	354,23	12,33	91,44
14.07.2022	05:30	15	19	0,21	395,29	12,29	91,29
14.07.2022	05:45	17	21	0,19	739,27	12,37	92,11
14.07.2022	06:00	16	20	0,20	1478,54	13,04	88,70
14.07.2022	06:15	16	18	0,11	2217,81	13,40	86,94
14.07.2022	06:30	15	20	0,25	2299,98	13,54	85,72
14.07.2022	06:45	15	19	0,21	3449,95	14,53	83,04
14.07.2022	07:00	17	20	0,15	4928,49	15,15	81,81
14.07.2022	07:15	15	18	0,17	5585,63	15,57	80,74
14.07.2022	07:30	16	16	0,00	3449,95	15,65	80,72
14.07.2022	07:45	15	17	0,12	11171,26	17,09	76,58
14.07.2022	08:00	15	24	0,38	3942,78	15,68	81,17
14.07.2022	08:15	16	22	0,27	4107,09	16,06	79,24
14.07.2022	08:30	17	21	0,19	3942,78	16,66	79,53
14.07.2022	08:45	17	22	0,23	3942,78	17,11	75,78
14.07.2022	09:00	17	22	0,23	3942,78	17,92	73,98
14.07.2022	09:15	19	24	0,21	3942,78	19,28	69,98
14.07.2022	09:30	19	24	0,21	49942,03	21,83	63,16
14.07.2022	09:45	26	25	0,00	55199,09	30,01	43,54
14.07.2022	10:00	23	23	0,00	84112,89	36,85	27,64
14.07.2022	10:15	21	24	0,13	44684,98	35,63	30,77
14.07.2022	10:30	23	29	0,21	89369,95	42,41	20,57
14.07.2022	10:45	24	26	0,08	94627,01	41,42	23,36
14.07.2022	11:00	23	26	0,12	89369,95	43,14	22,36
14.07.2022	11:15	21	25	0,16	105141,13	48,57	17,51
14.07.2022	11:30	24	24	0,00	105141,13	47,68	17,88
14.07.2022	11:45	19	25	0,24	57827,60	45,98	17,19
14.07.2022	12:00	22	25,5	0,14	126169,36	50,70	12,69
14.07.2022	12:15	25	26	0,04	115655,25	50,54	12,51
14.07.2022	12:30	99	106	0,07	120912,31	52,81	11,35
14.07.2022	12:45	96	97	0,01	115655,25	51,48	11,64
14.07.2022	13:00	97	95	0,00	84112,89	47,34	12,44
14.07.2022	13:15	89	95	0,06	115655,25	50,03	12,15
14.07.2022	13:30	91	92	0,01	84112,89	48,82	12,48
14.07.2022	13:45	93	96	0,03	110398,19	50,55	11,70
14.07.2022	14:00	93	96	0,03	110398,19	52,46	11,10
14.07.2022	14:15	95	94	0,00	115655,25	52,81	10,52
14.07.2022	14:30	95	94	0,00	110398,19	52,06	10,85
14.07.2022	14:45	98	95	0,00	110398,19	52,95	10,63
14.07.2022	15:00	93	95	0,02	105141,13	51,91	11,25
14.07.2022	15:15	94	91	0,00	84112,89	50,66	12,04
14.07.2022	15:30	93	92	0,00	76227,33	56,03	10,51
14.07.2022	15:45	94	94	0,00	115655,25	54,92	10,79
14.07.2022	16:00	88	94	0,06	94627,01	53,34	11,95
14.07.2022	16:15	92	88	0,00	81484,39	51,65	12,68
14.07.2022	16:30	95	89	0,00	47313,53	47,93	15,72
14.07.2022	16:45	91	86	0,00	68341,72	48,18	16,21
14.07.2022	17:00	88	90	0,02	44684,98	44,19	19,61
14.07.2022	17:15	88	87	0,00	49942,03	44,57	19,91
14.07.2022	17:30	92	85	0,00	31542,35	43,77	19,05
14.07.2022	17:45	87	87	0,00	26285,29	33,17	33,61
14.07.2022	18:00	90	88	0,00	6242,77	29,44	39,76
14.07.2022	18:15	91	88	0,00	6242,77	27,92	44,74
14.07.2022	18:30	86	89	0,03	3121,38	26,52	48,85
14.07.2022	18:45	86	85	0,00	2957,07	25,64	52,64
14.07.2022	19:00	85	86	0,01	1971,41	24,67	54,77
14.07.2022	19:15	90	92	0,02	1642,85	23,82	56,90
14.07.2022	19:30	84	91	0,08	1273,21	23,10	59,18
14.07.2022	19:45	83	88	0,06	985,71	22,59	62,12
14.07.2022	20:00	86	88	0,02	1149,97	22,13	65,44
14.07.2022	20:15	87	86	0,00	1067,84	21,26	69,64
14.07.2022	20:30	80	87	0,08	1232,15	20,81	71,54
14.07.2022	20:45	79	86	0,08	657,14	19,57	75,21
14.07.2022	21:00	84	83	0,00	128,35	18,31	77,93
14.07.2022	21:15	80	81	0,01	0,00	17,94	78,29
14.07.2022	21:30	83	73	0,00	0,00	17,82	78,25
14.07.2022	21:45	82	81	0,00	0,00	16,54	81,72
14.07.2022	22:00	79	81	0,03	0,00	16,76	82,58
14.07.2022	22:15	78	81	0,04	0,00	16,74	82,41
14.07.2022	22:30	78	84	0,07	0,00	16,58	84,25
14.07.2022	22:45	78	82	0,05	0,00	18,55	77,58
14.07.2022	23:00	78	81	0,04	0,00	18,14	78,48
14.07.2022	23:15	81	81	0,00	0,00	16,60	83,43
14.07.2022	23:30	85	80	0,00	0,00	16,84	82,92
14.07.2022	23:45	77	82	0,06	0,00	17,81	79,96

Date	Time	Fs	Fm'	ΦPS2	PAR [lx]	Temperature [°C]	Relative Humidity [%]
15.07.2022	00:00	74	80	0,08	0,00	17,35	81,91
15.07.2022	00:15	75	79	0,05	0,00	17,75	81,69
15.07.2022	00:30	76	78	0,03	0,00	17,07	83,14
15.07.2022	00:45	82	83	0,01	0,00	15,90	86,77
15.07.2022	01:00	77	83	0,07	0,00	16,14	86,21
15.07.2022	01:15	77	82	0,06	0,00	15,48	87,94
15.07.2022	01:30	80	81	0,01	0,00	15,32	90,28
15.07.2022	01:45	74	84	0,12	0,00	16,64	86,51
15.07.2022	02:00	80	80	0,00	0,00	18,42	77,55
15.07.2022	02:15	77	80	0,04	0,00	18,39	78,77
15.07.2022	02:30	76	81	0,06	0,00	17,71	81,58
15.07.2022	02:45	75	82	0,09	0,00	18,50	78,79
15.07.2022	03:00	75	80	0,06	0,00	17,91	90,18
15.07.2022	03:15	250	253	0,01	0,00	17,18	96,73
15.07.2022	03:30	176	182	0,03	0,00	17,31	97,33
15.07.2022	03:45	220	225	0,02	0,00	17,22	97,86
15.07.2022	04:00	309	319	0,03	0,00	16,78	98,10
15.07.2022	04:15	337	354	0,05	0,00	16,85	98,30
15.07.2022	04:30	676	732	0,08	0,00	16,66	98,39
15.07.2022	04:45	691	757	0,09	0,00	16,67	98,51
15.07.2022	05:00	632	727	0,13	0,00	16,78	98,61
15.07.2022	05:15	638	749	0,15	0,00	16,78	98,48
15.07.2022	05:30	643	769	0,16	46,22	16,68	98,42
15.07.2022	05:45	561	711	0,21	20,56	16,57	98,96
15.07.2022	06:00	562	749	0,25	87,28	16,61	98,86
15.07.2022	06:15	563	778	0,28	446,66	16,45	98,69
15.07.2022	06:30	543	793	0,32	456,92	16,38	98,88
15.07.2022	06:45	540	819	0,34	1314,28	16,46	98,91
15.07.2022	07:00	519	844	0,39	1314,28	16,45	99,37
15.07.2022	07:15	515	852	0,40	821,40	16,31	99,53
15.07.2022	07:30	521	892	0,42	2957,07	16,33	99,93
15.07.2022	07:45	523	925	0,44	3449,95	16,90	100,00
15.07.2022	08:00	522	939	0,44	3449,95	16,58	99,97
15.07.2022	08:15	515	963	0,47	7885,56	16,97	100,00
15.07.2022	08:30	517	979	0,47	11828,39	17,86	100,00
15.07.2022	08:45	258	455	0,43	13799,76	18,45	99,87
15.07.2022	09:00	262	404	0,35	23656,74	19,99	98,31
15.07.2022	09:15	253	409	0,38	22342,51	19,69	98,04
15.07.2022	09:30	246	391	0,37	81484,39	20,85	97,56
15.07.2022	09:45	242	388	0,38	28913,80	20,60	98,24
15.07.2022	10:00	252	424	0,41	8542,70	23,04	94,71
15.07.2022	10:15	279	436	0,36	13142,62	24,90	93,49
15.07.2022	10:30	242	385	0,37	26285,29	21,98	94,57
15.07.2022	10:45	288	454	0,37	11828,39	20,71	96,12
15.07.2022	11:00	231	375	0,38	44684,98	22,26	91,67
15.07.2022	11:15	240	318	0,25	19713,96	29,87	72,15
15.07.2022	11:30	229	301	0,24	99884,07	35,29	41,19
15.07.2022	11:45	195	252	0,23	110398,19	35,55	42,15
15.07.2022	12:00	162	208	0,22	105141,13	35,16	42,73
15.07.2022	12:15	107	146	0,27	110398,19	33,53	46,01
15.07.2022	12:30	77	111	0,31	126169,36	30,10	50,56
15.07.2022	12:45	62	94	0,34	44684,98	27,51	54,76
15.07.2022	13:00	58	108	0,46	10514,12	27,47	59,31
15.07.2022	13:15	51	71	0,28	19713,96	32,37	45,20
15.07.2022	13:30	49	74	0,34	17742,54	26,73	57,98
15.07.2022	13:45	47	71	0,34	35485,14	32,43	48,46
15.07.2022	14:00	40	48	0,17	94627,01	33,53	43,79
15.07.2022	14:15	29	43	0,33	34170,86	33,76	44,69
15.07.2022	14:30	33	37	0,11	99884,07	38,47	34,52
15.07.2022	14:45	23	31	0,26	55199,09	28,22	52,15
15.07.2022	15:00	26	30	0,13	23656,74	26,57	56,17
15.07.2022	15:15	23	29	0,21	15771,18	29,94	49,45
15.07.2022	15:30	20	25	0,20	60456,15	31,38	45,76
15.07.2022	15:45	16	22	0,27	23656,74	28,32	51,67
15.07.2022	16:00	17	24	0,29	18399,68	26,46	55,81
15.07.2022	16:15	19	22	0,14	21028,24	27,32	57,36
15.07.2022	16:30	20	25	0,20	34170,86	33,88	39,09
15.07.2022	16:45	18	24	0,25	73598,78	34,40	38,24
15.07.2022	17:00	18	21	0,14	63084,66	31,66	42,04
15.07.2022	17:15	12	19	0,37	15771,18	31,44	43,57
15.07.2022	17:30	17	19	0,11	49942,03	33,86	37,52
15.07.2022	17:45	14	18	0,22	24971,02	27,70	48,66
15.07.2022	18:00	24	27	0,11	9856,98	24,03	61,89
15.07.2022	18:15	25	27	0,07	5092,75	22,26	67,99
15.07.2022	18:30	27	30	0,10	8871,27	21,78	69,54
15.07.2022	18:45	22	30	0,27	7885,56	21,63	72,08
15.07.2022	19:00	24	29	0,17	3614,21	20,34	74,12
15.07.2022	19:15	23	29	0,21	4599,92	20,35	76,20
15.07.2022	19:30	20	28	0,29	2217,81	19,27	78,33
15.07.2022	19:45	16	24	0,33	3942,78	18,94	79,87
15.07.2022	20:00	22	24	0,08	2628,51	18,72	81,76
15.07.2022	20:15	20	24	0,17	2217,81	18,31	82,83
15.07.2022	20:30	21	25	0,16	1191,03	17,72	84,44
15.07.2022	20:45	20	24	0,17	528,79	17,65	84,71
15.07.2022	21:00	19	26	0,27	174,56	17,13	86,87
15.07.2022	21:15	23	25	0,08	20,56	16,40	87,51
15.07.2022	21:30	19	28	0,32	0,00	15,75	89,68
15.07.2022	21:45	20	27	0,26	0,00	14,84	90,03
15.07.2022	22:00	25	27	0,07	0,00	14,26	90,49
15.07.2022	22:15	20	27	0,26	0,00	14,13	91,54
15.07.2022	22:30	19	25	0,24	0,00	13,78	91,52
15.07.2022	22:45	20	26	0,23	0,00	13,43	91,93
15.07.2022	23:00	18	26	0,31	0,00	12,90	92,07
15.07.2022	23:15	19	25	0,24	0,00	12,17	92,50
15.07.2022	23:30	17	23	0,26	0,00	12,19	94,13
15.07.2022	23:45	17	22	0,23	0,00	11,93	93,47
16.07.2022	00:00	17	21	0,19	0,00	11,71	93,01

Appendix 3 Data of the PAM measurements (dark experiment) of *Nostoc commune* at the sun-exposed location **1/2**

Date	Time	Fo	Fm	Fv	Fv/Fm	Temperature [°C]	Relative Humidity [%]
17.07.2022	00:00	49	55	6	0,11	15,88	75,94
17.07.2022	00:15	47	56	9	0,16	15,94	76,89
17.07.2022	00:30	49	55	6	0,11	15,36	78,91
17.07.2022	00:45	51	54	3	0,06	14,57	81,07
17.07.2022	01:00	51	54	3	0,06	13,42	82,45
17.07.2022	01:15	48	56	8	0,14	12,79	84,26
17.07.2022	01:30	50	49	0	0,00	12,02	84,39
17.07.2022	01:45	51	51	0	0,00	11,70	85,57
17.07.2022	02:00	52	48	0	0,00	11,37	85,97
17.07.2022	02:15	49	53	4	0,08	11,24	86,33
17.07.2022	02:30	47	54	7	0,13	10,98	86,72
17.07.2022	02:45	47	53	6	0,11	10,91	88,00
17.07.2022	03:00	49	54	5	0,09	11,22	87,70
17.07.2022	03:15	50	54	4	0,07	11,26	87,37
17.07.2022	03:30	50	54	4	0,07	11,05	87,35
17.07.2022	03:45	44	52	8	0,15	10,50	87,91
17.07.2022	04:00	51	54	3	0,06	10,85	88,74
17.07.2022	04:15	49	54	5	0,09	10,74	87,64
17.07.2022	04:30	49	56	7	0,13	10,83	88,80
17.07.2022	04:45	51	51	0	0,00	11,98	85,08
17.07.2022	05:00	49	55	6	0,11	12,16	83,15
17.07.2022	05:15	49	54	5	0,09	12,04	83,20
17.07.2022	05:30	49	55	6	0,11	11,98	83,34
17.07.2022	05:45	49	55	6	0,11	12,09	84,01
17.07.2022	06:00	47	54	7	0,13	12,32	83,12
17.07.2022	06:15	50	53	3	0,06	12,40	83,81
17.07.2022	06:30	46	53	7	0,13	12,62	84,05
17.07.2022	06:45	50	53	3	0,06	12,88	83,59
17.07.2022	07:00	48	54	6	0,11	12,92	84,34
17.07.2022	07:15	51	53	2	0,04	13,23	86,07
17.07.2022	07:30	53	53	0	0,00	13,69	84,60
17.07.2022	07:45	52	53	1	0,02	14,21	82,45
17.07.2022	08:00	51	53	2	0,04	14,54	82,15
17.07.2022	08:15	50	52	2	0,04	15,01	81,43
17.07.2022	08:30	47	51	4	0,08	15,51	79,13
17.07.2022	08:45	47	52	5	0,10	16,09	77,94
17.07.2022	09:00	46	50	4	0,08	16,67	73,93
17.07.2022	09:15	46	54	8	0,15	17,61	71,01
17.07.2022	09:30	47	53	6	0,11	20,35	59,65
17.07.2022	09:45	48	53	5	0,09	22,95	51,63
17.07.2022	10:00	51	50	0	0,00	24,75	48,16
17.07.2022	10:15	48	52	4	0,08	25,90	43,47
17.07.2022	10:30	44	49	5	0,10	26,38	38,39
17.07.2022	10:45	46	44	0	0,00	26,15	37,52
17.07.2022	11:00	42	44	2	0,05	26,78	36,57
17.07.2022	11:15	45	45	0	0,00	27,27	35,03
17.07.2022	11:30	44	44	0	0,00	27,01	33,15
17.07.2022	11:45	41	44	3	0,07	26,90	32,93
17.07.2022	12:00	44	45	1	0,02	27,63	31,79
17.07.2022	12:15	43	46	3	0,07	27,66	31,58
17.07.2022	12:30	44	47	3	0,06	27,86	32,16
17.07.2022	12:45	43	44	1	0,02	28,09	31,99
17.07.2022	13:00	44	44	0	0,00	28,11	30,60
17.07.2022	13:15	43	46	3	0,07	28,71	31,36
17.07.2022	13:30	45	46	1	0,02	29,32	30,66
17.07.2022	13:45	43	48	5	0,10	29,89	29,27
17.07.2022	14:00	49	55	6	0,11	29,90	29,76
17.07.2022	14:15	39	50	11	0,22	29,92	29,09
17.07.2022	14:30	43	48	5	0,10	30,91	29,89
17.07.2022	14:45	45	46	1	0,02	30,91	28,32
17.07.2022	15:00	42	44	2	0,05	30,59	27,43
17.07.2022	15:15	45	44	0	0,00	30,57	29,30
17.07.2022	15:30	41	45	4	0,09	31,02	30,49
17.07.2022	15:45	42	44	2	0,05	31,32	28,49
17.07.2022	16:00	40	43	3	0,07	30,96	30,09
17.07.2022	16:15	45	44	0	0,00	30,54	29,27
17.07.2022	16:30	43	44	1	0,02	30,08	30,30
17.07.2022	16:45	43	43	0	0,00	29,72	31,05
17.07.2022	17:00	40	44	4	0,09	29,81	30,11
17.07.2022	17:15	37	44	7	0,16	29,70	32,10
17.07.2022	17:30	45	44	0	0,00	29,16	33,38
17.07.2022	17:45	45	52	7	0,14	27,58	34,90
17.07.2022	18:00	43	49	6	0,12	25,20	39,38
17.07.2022	18:15	47	51	4	0,08	23,82	44,08
17.07.2022	18:30	46	49	3	0,06	22,83	46,05
17.07.2022	18:45	48	46	0	0,00	22,01	47,86
17.07.2022	19:00	51	54	3	0,06	21,13	51,40
17.07.2022	19:15	51	51	0	0,00	20,64	54,23
17.07.2022	19:30	47	52	5	0,10	20,49	55,85
17.07.2022	19:45	46	50	4	0,08	20,06	57,08
17.07.2022	20:00	45	47	2	0,04	19,72	59,57
17.07.2022	20:15	46	48	2	0,04	19,25	60,78
17.07.2022	20:30	46	54	8	0,15	18,94	62,41
17.07.2022	20:45	46	52	6	0,12	18,50	63,88
17.07.2022	21:00	50	53	3	0,06	17,89	65,99
17.07.2022	21:15	50	52	2	0,04	16,98	68,75
17.07.2022	21:30	50	51	1	0,02	16,42	70,59
17.07.2022	21:45	48	53	5	0,09	15,76	71,96
17.07.2022	22:00	51	52	1	0,02	15,43	73,01
17.07.2022	22:15	47	54	7	0,13	14,77	73,07
17.07.2022	22:30	47	48	1	0,02	12,51	79,66
17.07.2022	22:45	46	50	4	0,08	11,89	82,79
17.07.2022	23:00	45	49	4	0,08	11,72	83,36
17.07.2022	23:15	47	50	3	0,06	11,76	83,28
17.07.2022	23:30	49	50	1	0,02	11,40	83,81
17.07.2022	23:45	48	50	2	0,04	10,84	84,58

Date	Time	Fo	Fm	Fv	Fv/Fm	Temperature [°C]	Relative Humidity [%]
18.07.2022	00:00	49	51	2	0,04	10,74	86,23
18.07.2022	00:15	43	54	11	0,20	11,34	85,49
18.07.2022	00:30	46	53	7	0,13	10,74	85,46
18.07.2022	00:45	49	53	4	0,08	10,54	85,97
18.07.2022	01:00	47	52	5	0,10	10,33	85,82
18.07.2022	01:15	50	51	1	0,02	9,73	87,94
18.07.2022	01:30	52	50	0	0,00	10,02	87,51
18.07.2022	01:45	50	53	3	0,06	10,48	87,05
18.07.2022	02:00	49	51	2	0,04	10,37	86,42
18.07.2022	02:15	50	53	3	0,06	9,66	86,28
18.07.2022	02:30	49	51	2	0,04	9,11	88,84
18.07.2022	02:45	47	54	7	0,13	9,74	87,90
18.07.2022	03:00	50	54	4	0,07	9,56	87,96
18.07.2022	03:15	47	53	6	0,11	9,58	86,93
18.07.2022	03:30	47	52	5	0,10	8,91	88,98
18.07.2022	03:45	48	54	6	0,11	9,03	88,22
18.07.2022	04:00	45	56	11	0,20	9,49	87,97
18.07.2022	04:15	48	54	6	0,11	9,30	87,92
18.07.2022	04:30	48	48	0	0,00	10,15	87,17
18.07.2022	04:45	46	52	6	0,12	10,71	84,83
18.07.2022	05:00	48	52	4	0,08	10,83	83,72
18.07.2022	05:15	48	48	0	0,00	10,88	83,50
18.07.2022	05:30	46	48	2	0,04	10,89	83,33
18.07.2022	05:45	48	50	2	0,04	11,03	84,15
18.07.2022	06:00	47	48	1	0,02	11,38	84,01
18.07.2022	06:15	46	51	5	0,10	11,30	82,24
18.07.2022	06:30	45	56	11	0,20	11,51	83,33
18.07.2022	06:45	50	54	4	0,07	11,88	83,81
18.07.2022	07:00	51	52	1	0,02	12,15	84,00
18.07.2022	07:15	49	52	3	0,06	12,57	84,73
18.07.2022	07:30	50	51	1	0,02	13,11	84,14
18.07.2022	07:45	49	53	4	0,08	13,52	84,09
18.07.2022	08:00	50	52	2	0,04	13,96	83,24
18.07.2022	08:15	48	55	7	0,13	14,45	82,04
18.07.2022	08:30	54	55	1	0,02	14,99	80,77
18.07.2022	08:45	57	52	0	0,00	15,63	79,11
18.07.2022	09:00	53	54	1	0,02	16,25	76,31
18.07.2022	09:15	45	57	12	0,21	17,43	73,78
18.07.2022	09:30	51	55	4	0,07	20,20	64,82
18.07.2022	09:45	52	54	2	0,04	23,37	52,92
18.07.2022	10:00	51	53	2	0,04	25,24	47,41
18.07.2022	10:15	49	54	5	0,09	26,77	43,79
18.07.2022	10:30	54	53	0	0,00	26,73	44,46
18.07.2022	10:45	47	50	3	0,06	27,44	37,17
18.07.2022	11:00	50	50	0	0,00	27,83	36,02
18.07.2022	11:15	51	54	3	0,06	28,82	34,34
18.07.2022	11:30	45	52	7	0,14	29,85	32,44
18.07.2022	11:45	51	50	0	0,00	30,06	30,89
18.07.2022	12:00	47	52	5	0,10	30,40	30,08
18.07.2022	12:15	47	47	0	0,00	31,28	30,16
18.07.2022	12:30	45	49	4	0,08	32,15	31,05
18.07.2022	12:45	51	48	0	0,00	32,47	30,21
18.07.2022	13:00	47	47	0	0,00	32,48	29,94
18.07.2022	13:15	49	46	0	0,00	32,69	30,47
18.07.2022	13:30	45	48	3	0,06	32,70	32,00
18.07.2022	13:45	45	48	3	0,06	32,54	30,86
18.07.2022	14:00	46	46	0	0,00	32,83	30,86
18.07.2022	14:15	45	48	3	0,06	32,73	31,22
18.07.2022	14:30	44	48	4	0,08	32,36	28,38
18.07.2022	14:45	48	49	1	0,02	32,52	30,60
18.07.2022	15:00	48	47	0	0,00	33,37	30,47
18.07.2022	15:15	50	48	0	0,00	33,51	28,99
18.07.2022	15:30	49	48	0	0,00	33,42	28,67
18.07.2022	15:45	47	46	0	0,00	33,33	27,98
18.07.2022	16:00	44	46	2	0,04	33,16	28,01
18.07.2022	16:15	45	46	1	0,02	32,88	29,18
18.07.2022	16:30	45	47	2	0,04	33,00	30,90
18.07.2022	16:45	47	47	0	0,00	31,77	34,51
18.07.2022	17:00	46	46	0	0,00	31,23	32,23
18.07.2022	17:15	47	46	0	0,00	30,13	35,48
18.07.2022	17:30	46	50	4	0,08	29,82	34,36
18.07.2022	17:45	44	50	6	0,12	28,29	37,73
18.07.2022	18:00	50	54	4	0,07	26,49	42,86
18.07.2022	18:15	47	52	5	0,10	25,92	46,33
18.07.2022	18:30	47	50	3	0,06	25,10	48,54
18.07.2022	18:45	50	50	0	0,00	24,32	52,10
18.07.2022	19:00	49	47	0	0,00	23,82	54,21
18.07.2022	19:15	48	55	7	0,13	22,82	55,42
18.07.2022	19:30	49	53	4	0,08	22,04	57,88
18.07.2022	19:45	53	52	0	0,00	21,60	59,68
18.07.2022	20:00	48	53	5	0,09	21,06	61,88
18.07.2022	20:15	48	50	2	0,04	20,72	62,27
18.07.2022	20:30	50	53	3	0,06	20,33	62,54
18.07.2022	20:45	49	46	0	0,00	19,77	64,57
18.07.2022	21:00	54	51	0	0,00	19,36	64,72
18.07.2022	21:15	50	52	2	0,04	19,00	64,86
18.07.2022	21:30	45	52	7	0,14	18,49	67,01
18.07.2022	21:45	51	53	2	0,04	18,01	68,53
18.07.2022	22:00	53	54	1	0,02	17,34	70,85
18.07.2022	22:15	47	53	6	0,11	16,92	72,24
18.07.2022	22:30	47	51	4	0,08	15,03	74,85
18.07.2022	22:45	49	51	2	0,04	13,79	78,64
18.07.2022	23:00	47	55	8	0,15	13,45	80,38
18.07.2022	23:15	44	53	9	0,17	13,11	81,72
18.07.2022	23:30	46	57	11	0,19	13,20	82,34
18.07.2022	23:45	50	54	4	0,07	13,02	84,03

Appendix 4 Data of the PAM measurements (dark experiment) of *Nostoc commune* at the sun-exposed location **2/2**

Date	Time	Fo	Fm	Fv	Fv/Fm	Temperature [°C]	Relative Humidity [%]
19.07.2022	00:00	51	54	3	0,06	12,77	84,09
19.07.2022	00:15	49	54	5	0,09	12,40	84,95
19.07.2022	00:30	51	54	3	0,06	12,41	85,93
19.07.2022	00:45	51	51	0	0,00	12,31	85,42
19.07.2022	01:00	51	51	0	0,00	12,04	86,63
19.07.2022	01:15	50	53	3	0,06	11,81	86,63
19.07.2022	01:30	52	55	3	0,06	11,71	87,24
19.07.2022	01:45	50	55	5	0,09	11,87	86,92
19.07.2022	02:00	48	56	8	0,14	11,84	87,27
19.07.2022	02:15	52	54	2	0,04	11,76	86,86
19.07.2022	02:30	53	54	1	0,02	11,47	87,71
19.07.2022	02:45	47	55	8	0,15	11,35	87,62
19.07.2022	03:00	50	56	6	0,11	10,88	88,12
19.07.2022	03:15	48	57	9	0,16	10,69	89,45
19.07.2022	03:30	50	55	5	0,09	11,04	88,07
19.07.2022	03:45	53	55	2	0,04	10,83	88,61
19.07.2022	04:00	52	56	4	0,07	10,52	88,91
19.07.2022	04:15	54	56	2	0,04	10,27	89,80
19.07.2022	04:30	55	53	0	0,00	11,68	87,62
19.07.2022	04:45	53	57	4	0,07	12,26	84,53
19.07.2022	05:00	51	57	6	0,11	12,08	84,14
19.07.2022	05:15	54	58	4	0,07	12,17	83,91
19.07.2022	05:30	52	57	5	0,09	12,18	83,44
19.07.2022	05:45	50	57	7	0,12	12,12	84,03
19.07.2022	06:00	53	54	1	0,02	12,26	83,89
19.07.2022	06:15	52	56	4	0,07	12,44	84,17
19.07.2022	06:30	51	55	4	0,07	12,51	85,16
19.07.2022	06:45	50	55	5	0,09	12,89	84,67
19.07.2022	07:00	54	56	2	0,04	13,29	84,50
19.07.2022	07:15	56	55	0	0,00	13,65	84,56
19.07.2022	07:30	55	56	1	0,02	14,04	86,62
19.07.2022	07:45	50	56	6	0,11	14,63	84,87
19.07.2022	08:00	55	56	1	0,02	15,12	83,92
19.07.2022	08:15	54	56	2	0,04	15,55	83,04
19.07.2022	08:30	52	56	4	0,07	16,07	82,09
19.07.2022	08:45	52	56	4	0,07	16,74	79,88
19.07.2022	09:00	51	60	9	0,15	17,48	76,52
19.07.2022	09:15	56	57	1	0,02	18,58	73,92
19.07.2022	09:30	53	61	8	0,13	21,49	62,86
19.07.2022	09:45	49	57	8	0,14	24,59	52,93
19.07.2022	10:00	52	58	6	0,10	26,21	47,98
19.07.2022	10:15	50	55	5	0,09	27,27	44,87
19.07.2022	10:30	53	61	8	0,13	28,38	44,04
19.07.2022	10:45	54	53	0	0,00	29,01	44,74
19.07.2022	11:00	52	54	2	0,04	29,40	42,55
19.07.2022	11:15	50	54	4	0,07	29,79	42,70
19.07.2022	11:30	52	57	5	0,09	30,53	40,73
19.07.2022	11:45	50	56	6	0,11	31,31	35,31
19.07.2022	12:00	53	65	12	0,19	31,80	36,18
19.07.2022	12:15	49	56	7	0,13	32,24	32,19
19.07.2022	12:30	53	56	3	0,05	32,87	32,58
19.07.2022	12:45	55	52	0	0,00	33,54	31,46
19.07.2022	13:00	54	54	0	0,00	33,61	30,48
19.07.2022	13:15	51	53	2	0,04	33,72	30,50
19.07.2022	13:30	57	52	0	0,00	33,74	32,58
19.07.2022	13:45	51	54	3	0,06	34,35	32,36
19.07.2022	14:00	54	53	0	0,00	33,66	31,21
19.07.2022	14:15	52	55	3	0,06	33,45	32,56
19.07.2022	14:30	55	57	2	0,04	33,68	30,85
19.07.2022	14:45	56	53	0	0,00	33,84	30,81
19.07.2022	15:00	54	53	0	0,00	33,88	31,90
19.07.2022	15:15	57	53	0	0,00	33,83	33,37
19.07.2022	15:30	56	50	0	0,00	33,94	33,61
19.07.2022	15:45	53	52	0	0,00	34,72	32,70
19.07.2022	16:00	56	51	0	0,00	34,66	32,92
19.07.2022	16:15	51	51	0	0,00	34,04	31,84
19.07.2022	16:30	52	51	0	0,00	33,66	33,65
19.07.2022	16:45	50	50	0	0,00	33,71	34,68
19.07.2022	17:00	52	53	1	0,02	33,61	35,77
19.07.2022	17:15	52	51	0	0,00	33,23	36,24
19.07.2022	17:30	53	54	1	0,02	32,19	39,23
19.07.2022	17:45	53	54	1	0,02	31,01	41,56
19.07.2022	18:00	55	57	2	0,04	28,77	47,51
19.07.2022	18:15	56	68	12	0,18	27,57	50,98
19.07.2022	18:30	56	59	3	0,05	26,45	53,52
19.07.2022	18:45	57	62	5	0,08	25,66	56,28
19.07.2022	19:00	59	60	1	0,02	25,10	58,39
19.07.2022	19:15	59	59	0	0,00	24,61	59,31
19.07.2022	19:30	60	65	5	0,08	24,16	60,74
19.07.2022	19:45	59	62	3	0,05	23,73	62,62
19.07.2022	20:00	56	64	8	0,13	23,36	63,92
19.07.2022	20:15	58	63	5	0,08	22,91	65,92
19.07.2022	20:30	62	63	1	0,02	22,52	66,81
19.07.2022	20:45	60	64	4	0,06	22,20	67,50
19.07.2022	21:00	60	64	4	0,06	21,68	68,21
19.07.2022	21:15	63	64	1	0,02	21,02	69,10
19.07.2022	21:30	61	62	1	0,02	20,33	70,49
19.07.2022	21:45	62	58	0	0,00	19,77	71,73
19.07.2022	22:00	59	60	1	0,02	19,06	74,12
19.07.2022	22:15	60	64	4	0,06	17,55	78,93
19.07.2022	22:30	55	59	4	0,07	16,64	83,08
19.07.2022	22:45	51	57	6	0,11	16,31	84,49
19.07.2022	23:00	54	57	3	0,05	16,31	84,44
19.07.2022	23:15	51	59	8	0,14	16,21	84,82
19.07.2022	23:30	57	57	0	0,00	16,21	84,92
19.07.2022	23:45	53	55	2	0,04	15,83	85,09
20.07.2022	00:00	52	58	6	0,10	15,35	87,01

Appendix 5 Data of the PAM measurements (ambient light) of *Nostoc commune* at the shaded location **1/2**

Date	Time	Fs	Fm'	ΦPS2	PAR [lx]	Temperature [°C]	Relative Humidity [%]
21.07.2023	00:00	449	996	0,55	0,00	15,72	96,32
21.07.2023	00:15	486	1064	0,54	0,00	15,61	96,49
21.07.2023	00:30	494	1071	0,54	0,00	15,46	96,29
21.07.2023	00:45	499	1069	0,53	0,00	15,35	96,43
21.07.2023	01:00	511	1098	0,54	0,00	15,18	98,02
21.07.2023	01:15	528	1105	0,52	0,00	15,03	98,20
21.07.2023	01:30	528	1102	0,52	0,00	14,90	98,34
21.07.2023	01:45	530	1097	0,52	0,00	14,75	98,39
21.07.2023	02:00	533	1090	0,51	0,00	14,62	98,42
21.07.2023	02:15	540	1086	0,50	0,00	14,50	98,47
21.07.2023	02:30	538	1085	0,50	0,00	14,43	98,51
21.07.2023	02:45	544	1082	0,50	0,00	14,38	98,64
21.07.2023	03:00	589	1176	0,50	0,00	14,22	98,54
21.07.2023	03:15	612	1197	0,49	0,00	14,17	98,71
21.07.2023	03:30	618	1202	0,49	0,00	14,13	98,77
21.07.2023	03:45	616	1197	0,49	0,00	14,04	98,74
21.07.2023	04:00	626	1200	0,48	0,00	14,12	98,87
21.07.2023	04:15	656	1240	0,47	0,00	14,04	98,97
21.07.2023	04:30	669	1237	0,46	0,00	14,10	98,95
21.07.2023	04:45	682	1236	0,45	0,00	14,06	99,05
21.07.2023	05:00	719	1257	0,43	0,00	14,05	99,21
21.07.2023	05:15	712	1292	0,45	107,68	13,99	99,22
21.07.2023	05:30	696	1365	0,49	225,66	14,13	99,34
21.07.2023	05:45	701	1436	0,51	318,00	14,09	99,33
21.07.2023	06:00	703	1486	0,53	405,19	14,14	99,36
21.07.2023	06:15	707	1515	0,53	512,87	14,20	99,42
21.07.2023	06:30	727	1545	0,53	738,53	14,39	99,47
21.07.2023	06:45	729	1545	0,53	697,51	14,49	99,50
21.07.2023	07:00	788	1648	0,52	1148,82	14,71	99,62
21.07.2023	07:15	795	1650	0,52	1230,91	14,92	99,61
21.07.2023	07:30	796	1654	0,52	1271,94	15,10	99,68
21.07.2023	07:45	808	1659	0,51	1641,20	16,22	99,91
21.07.2023	08:00	817	1658	0,51	5251,80	17,81	99,40
21.07.2023	08:15	815	1642	0,50	5908,28	18,31	98,88
21.07.2023	08:30	795	1637	0,51	3938,84	18,16	99,11
21.07.2023	08:45	791	1650	0,52	2215,59	18,06	99,37
21.07.2023	09:00	786	1644	0,52	2215,59	18,12	99,76
21.07.2023	09:15	796	1637	0,51	4923,56	20,21	99,29
21.07.2023	09:30	779	1594	0,51	16411,89	21,55	98,14
21.07.2023	09:45	753	1558	0,52	8862,40	22,59	97,80
21.07.2023	10:00	717	1511	0,53	6893,00	23,09	92,83
21.07.2023	10:15	647	1372	0,53	6236,52	23,68	86,18
21.07.2023	10:30	567	1221	0,54	5087,66	23,29	83,20
21.07.2023	10:45	499	1116	0,55	3610,60	22,78	84,45
21.07.2023	11:00	466	1042	0,55	4102,98	22,83	83,35
21.07.2023	11:15	406	882	0,54	3610,60	22,99	84,08
21.07.2023	11:30	409	847	0,52	4923,56	23,31	81,19
21.07.2023	11:45	407	833	0,51	5087,66	23,64	82,19
21.07.2023	12:00	404	811	0,50	5251,80	24,01	80,10
21.07.2023	12:15	388	785	0,51	4595,32	23,96	77,03
21.07.2023	12:30	394	823	0,52	3610,60	23,95	78,32
21.07.2023	12:45	386	817	0,53	3610,60	23,86	78,82
21.07.2023	13:00	390	836	0,53	3118,26	23,73	82,44
21.07.2023	13:15	383	796	0,52	5251,80	24,80	78,82
21.07.2023	13:30	390	817	0,52	5908,28	25,43	75,39
21.07.2023	13:45	385	783	0,51	7221,25	25,81	78,45
21.07.2023	14:00	392	785	0,50	6893,00	25,81	78,76
21.07.2023	14:15	378	785	0,52	6893,00	25,70	79,24
21.07.2023	14:30	385	772	0,50	7549,44	26,18	76,87
21.07.2023	14:45	378	795	0,53	4431,22	25,85	79,28
21.07.2023	15:00	382	779	0,51	6893,00	25,91	79,57
21.07.2023	15:15	378	747	0,49	5251,80	26,34	78,35
21.07.2023	15:30	375	741	0,49	6893,00	26,34	75,47
21.07.2023	15:45	370	755	0,51	6893,00	26,06	78,67
21.07.2023	16:00	377	755	0,50	5908,28	24,75	81,95
21.07.2023	16:15	366	728	0,50	3610,60	24,04	83,87
21.07.2023	16:30	364	694	0,48	4595,32	24,42	85,15
21.07.2023	16:45	371	701	0,47	5908,28	24,84	83,91
21.07.2023	17:00	378	711	0,47	6564,76	24,88	83,15
21.07.2023	17:15	387	705	0,45	6893,00	24,82	83,52
21.07.2023	17:30	382	725	0,47	5251,80	24,39	85,05
21.07.2023	17:45	388	724	0,46	5580,04	24,37	84,44
21.07.2023	18:00	390	717	0,46	5580,04	24,30	84,88
21.07.2023	18:15	388	747	0,48	3938,84	23,58	86,65
21.07.2023	18:30	393	784	0,50	2954,12	23,10	88,30
21.07.2023	18:45	395	788	0,50	2954,12	22,79	88,05
21.07.2023	19:00	387	831	0,53	1969,44	22,15	89,23
21.07.2023	19:15	390	844	0,54	1805,30	21,75	90,72
21.07.2023	19:30	389	850	0,54	1887,35	21,49	92,21
21.07.2023	19:45	382	862	0,56	1559,11	21,25	92,90
21.07.2023	20:00	370	878	0,58	1066,77	20,83	93,77
21.07.2023	20:15	362	870	0,58	615,46	20,41	94,73
21.07.2023	20:30	352	836	0,58	179,49	20,06	95,37
21.07.2023	20:45	344	799	0,57	15,39	19,88	96,08
21.07.2023	21:00	338	779	0,57	0,00	19,66	96,25
21.07.2023	21:15	328	765	0,57	0,00	19,55	96,41
21.07.2023	21:30	318	758	0,58	0,00	19,48	96,73
21.07.2023	21:45	323	746	0,57	0,00	19,48	96,69
21.07.2023	22:00	326	742	0,56	0,00	19,48	96,39
21.07.2023	22:15	333	739	0,55	0,00	19,51	96,45
21.07.2023	22:30	333	744	0,55	0,00	19,45	96,55
21.07.2023	22:45	332	734	0,55	0,00	19,38	96,67
21.07.2023	23:00	329	725	0,55	0,00	19,32	96,84
21.07.2023	23:15	335	724	0,54	0,00	19,15	97,03
21.07.2023	23:30	337	728	0,54	0,00	19,05	96,59
21.07.2023	23:45	335	707	0,53	0,00	18,90	96,77

Date	Time	Fs	Fm'	ΦPS2	PAR [lx]	Temperature [°C]	Relative Humidity [%]
22.07.2023	00:00	342	719	0,52	0,00	18,71	97,27
22.07.2023	00:15	335	715	0,53	0,00	18,56	97,52
22.07.2023	00:30	334	705	0,53	0,00	18,52	97,51
22.07.2023	00:45	338	706	0,52	0,00	18,51	97,38
22.07.2023	01:00	341	706	0,52	0,00	18,05	97,45
22.07.2023	01:15	337	699	0,52	0,00	17,68	97,58
22.07.2023	01:30	342	703	0,51	0,00	17,50	97,62
22.07.2023	01:45	342	700	0,51	0,00	17,22	97,43
22.07.2023	02:00	344	704	0,51	0,00	16,93	97,20
22.07.2023	02:15	342	695	0,51	0,00	16,75	97,38
22.07.2023	02:30	346	696	0,50	0,00	16,55	97,40
22.07.2023	02:45	350	706	0,50	0,00	16,45	97,46
22.07.2023	03:00	350	705	0,50	0,00	16,31	97,35
22.07.2023	03:15	351	710	0,51	0,00	16,13	97,34
22.07.2023	03:30	365	731	0,50	0,00	16,00	97,10
22.07.2023	03:45	367	730	0,50	0,00	15,82	96,91
22.07.2023	04:00	368	731	0,50	0,00	15,73	97,09
22.07.2023	04:15	373	735	0,49	0,00	15,64	97,02
22.07.2023	04:30	378	740	0,49	0,00	15,53	97,10
22.07.2023	04:45	378	727	0,48	0,00	15,42	96,84
22.07.2023	05:00	383	723	0,47	0,00	15,34	97,06
22.07.2023	05:15	388	746	0,48	25,63	15,19	96,99
22.07.2023	05:30	374	797	0,53	102,58	15,22	97,23
22.07.2023	05:45	383	883	0,57	451,31	15,29	97,08
22.07.2023	06:00	393	912	0,57	738,53	15,50	97,10
22.07.2023	06:15	415	963	0,57	1107,79	15,87	97,75
22.07.2023	06:30	422	958	0,56	1559,11	16,12	97,22
22.07.2023	06:45	429	943	0,55	1641,20	16,39	97,24
22.07.2023	07:00	434	938	0,54	1559,11	16,50	96,70
22.07.2023	07:15	434	920	0,53	1641,20	16,61	97,00
22.07.2023	07:30	433	907	0,52	1805,30	16,85	96,98
22.07.2023	07:45	438	892	0,51	2051,49	18,05	97,43
22.07.2023	08:00	437	858	0,49	5580,04	19,69	92,98
22.07.2023	08:15	446	857	0,48	5908,28	19,96	91,51
22.07.2023	08:30	444	857	0,48	3610,60	19,70	93,34
22.07.2023	08:45	439	850	0,48	2625,88	19,63	93,91
22.07.2023	09:00	435	848	0,49	2461,78	19,61	94,91
22.07.2023	09:15	433	839	0,48	4595,32	21,62	91,25
22.07.2023	09:30	416	793	0,48	6893,00	22,93	85,23
22.07.2023	09:45	389	740	0,47	14442,44	24,37	83,46
22.07.2023	10:00	370	731	0,49	6236,52	24,99	79,04
22.07.2023	10:15	364	712	0,49	6236,52	24,98	78,48
22.07.2023	10:30	356	714	0,50	4595,32	24,38	82,27
22.07.2023	10:45	346	710	0,51	3446,50	23,66	85,02
22.07.2023	11:00	348	708	0,51	3938,84	23,50	86,73
22.07.2023	11:15	346	710	0,51	3446,50	23,30	86,76
22.07.2023	11:30	341	703	0,52	3446,50	23,47	86,24
22.07.2023	11:45	340	701	0,52	3118,26	23,44	85,97
22.07.2023	12:00	341	684	0,50	3446,50	23,53	86,27
22.07.2023	12:15	335	657	0,49	4102,98	24,29	82,42
22.07.2023	12:30	329	632	0,48	4923,56	24,95	80,55
22.07.2023	12:45	318	604	0,47	5087,66	25,06	78,94
22.07.2023	13:00	315	627	0,50	3610,60	24,77	80,71
22.07.2023	13:15	315	631	0,50	4431,22	25,36	79,50
22.07.2023	13:30	297	611	0,51	5908,28	26,05	77,47
22.07.2023	13:45	300	605	0,50	6236,52	26,60	75,73
22.07.2023	14:00	287	595	0,52	6564,76	26,93	74,82
22.07.2023	14:15	289	578	0,50	6564,76	26,85	75,08
22.07.2023	14:30	284	564	0,50	6564,76	27,31	74,43
22.07.2023	14:45	275	564	0,51	6564,76	27,36	73,50
22.07.2023	15:00	271	560	0,52	6236,52	27,47	73,60
22.07.2023	15:15	264	553	0,52	6236,52	27,44	74,24
22.07.2023	15:30	259	546	0,53	6236,52	27,61	72,30
22.07.2023	15:45	254	536	0,53	6236,52	27,67	71,75
22.07.2023	16:00	248	525	0,53	6564,76	27,79	70,35
22.07.2023	16:15	249	513	0,52	6893,00	27,99	70,80
22.07.2023	16:30	264	382	0,31	6893,00	28,69	67,17
22.07.2023	16:45	184	304	0,40	7221,25	29,27	69,44
22.07.2023	17:00	197	344	0,43	7221,25	29,36	68,60
22.07.2023	17:15	200	384	0,48	6893,00	28,95	71,37
22.07.2023	17:30	205	398	0,49	5908,28	28,37	73,80
22.07.2023	17:45	210	406	0,48	3938,84	26,91	79,20
22.07.2023	18:00	210	424	0,51	2379,73	25,73	83,03
22.07.2023	18:15	218	440	0,51	2051,49	24,92	85,93
22.07.2023	18:30	224	456	0,51	1887,35	24,42	88,77
22.07.2023	18:45	229	476	0,52	1723,25	24,04	89,79
22.07.2023	19:00	228	483	0,53	1641,20	23,67	90,70
22.07.2023	19:15	230	484	0,53	1641,20	23,38	91,24
22.07.2023	19:30	228	492	0,54	1805,30	23,12	91,62
22.07.2023	19:45	224	510	0,56	1107,79	22,53	92,99
22.07.2023	20:00	225	525	0,57	738,53	21,96	94,08
22.07.2023	20:15	226	531	0,57	564,14	21,47	94,66
22.07.2023	20:30	217	530	0,59	323,09	20,96	95,23
22.07.2023	20:45	209	496	0,58	87,19	20,55	95,96
22.07.2023	21:00	208	480	0,57	15,39	20,22	96,14
22.07.2023	21:15	197	466	0,58	0,00	19,95	96,47
22.07.2023	21:30	191	459	0,58	0,00	19,71	96,46
22.07.2023	21:45	191	451	0,58	0,00	19,57	96,55
22.07.2023	22:00	194	457	0,58	0,00	19,43	96,56
22.07.2023	22:15	194	459	0,58	0,00	19,35	96,47
22.07.2023	22:30	196	461	0,58	0,00	19,24	96,63
22.07.2023	22:45	188	452	0,58	0,00	19,08	96,64
22.07.2023	23:00	193	457	0,58	0,00	18,93	96,67
22.07.2023	23:15	193	457	0,58	0,00	18,81	96,89
22.07.2023	23:30	193	457	0,58	0,00	18,88	96,94
22.07.2023	23:45	198	450	0,56	0,00	18,82	96,97

Appendix 6 Data of the PAM measurements (ambient light) of *Nostoc commune* at the shaded location **2/2**

Date	Time	Fs	Fm'	ΦPS2	PAR [lx]	Temperature [°C]	Relative Humidity [%]
23.07.2023	00:00	201	452	0,56	0,00	18,62	96,96
23.07.2023	00:15	207	466	0,56	0,00	18,47	97,11
23.07.2023	00:30	202	455	0,56	0,00	18,39	97,07
23.07.2023	00:45	202	461	0,56	0,00	18,40	97,07
23.07.2023	01:00	205	465	0,56	0,00	18,60	96,94
23.07.2023	01:15	206	472	0,56	0,00	18,60	97,22
23.07.2023	01:30	210	474	0,56	0,00	18,58	96,94
23.07.2023	01:45	212	479	0,56	0,00	18,67	97,20
23.07.2023	02:00	211	478	0,56	0,00	18,84	98,07
23.07.2023	02:15	216	481	0,55	0,00	19,16	99,89
23.07.2023	02:30	279	558	0,50	0,00	18,70	99,91
23.07.2023	02:45	328	613	0,47	0,00	18,41	99,77
23.07.2023	03:00	312	591	0,47	0,00	18,07	99,63
23.07.2023	03:15	318	601	0,47	0,00	17,88	99,63
23.07.2023	03:30	311	596	0,48	0,00	17,82	99,58
23.07.2023	03:45	298	585	0,49	0,00	17,63	99,58
23.07.2023	04:00	291	569	0,49	0,00	17,15	99,22
23.07.2023	04:15	266	552	0,52	0,00	16,75	99,19
23.07.2023	04:30	310	616	0,50	0,00	16,63	99,32
23.07.2023	04:45	306	610	0,50	0,00	16,54	99,55
23.07.2023	05:00	315	614	0,49	0,00	16,63	99,51
23.07.2023	05:15	317	623	0,49	15,39	16,42	99,46
23.07.2023	05:30	309	670	0,54	138,46	16,41	99,52
23.07.2023	05:45	293	686	0,57	435,92	16,45	99,61
23.07.2023	06:00	294	714	0,59	482,09	16,23	99,60
23.07.2023	06:15	290	713	0,59	820,58	16,61	99,91
23.07.2023	06:30	299	708	0,58	1395,01	17,04	99,96
23.07.2023	06:45	297	686	0,57	2133,54	17,66	99,99
23.07.2023	07:00	292	685	0,57	1969,44	17,83	99,99
23.07.2023	07:15	297	678	0,56	1723,25	18,05	99,98
23.07.2023	07:30	300	637	0,53	3446,50	18,51	99,94
23.07.2023	07:45	285	653	0,56	1395,01	18,62	99,91
23.07.2023	08:00	293	623	0,53	4923,56	19,99	99,56
23.07.2023	08:15	296	601	0,51	6893,00	20,40	98,81
23.07.2023	08:30	278	588	0,53	2215,59	19,82	99,50
23.07.2023	08:45	279	562	0,50	3446,50	20,00	99,81
23.07.2023	09:00	254	519	0,51	3610,60	20,25	99,97
23.07.2023	09:15	230	454	0,49	4595,32	21,06	99,45
23.07.2023	09:30	221	448	0,51	5580,04	21,89	99,26
23.07.2023	09:45	226	453	0,50	6564,76	22,81	98,93
23.07.2023	10:00	228	444	0,49	5908,28	23,29	98,74
23.07.2023	10:15	221	432	0,49	6564,76	23,12	98,66
23.07.2023	10:30	219	430	0,49	4595,32	22,90	98,46
23.07.2023	10:45	218	410	0,47	5908,28	22,69	97,02
23.07.2023	11:00	213	396	0,46	7221,25	23,58	91,31
23.07.2023	11:15	207	372	0,44	7877,68	24,29	82,09
23.07.2023	11:30	204	359	0,43	7877,68	24,69	81,01
23.07.2023	11:45	203	351	0,42	7549,44	24,91	80,77
23.07.2023	12:00	201	340	0,41	9190,64	25,29	76,48
23.07.2023	12:15	190	325	0,42	8534,16	24,34	81,94
23.07.2023	12:30	207	387	0,47	4431,22	23,80	87,68
23.07.2023	12:45	202	346	0,42	10175,36	25,48	82,61
23.07.2023	13:00	190	314	0,40	9190,64	25,75	78,33
23.07.2023	13:15	190	314	0,40	9518,88	25,83	80,50
23.07.2023	13:30	191	332	0,43	6893,00	25,59	77,57
23.07.2023	13:45	193	333	0,42	6893,00	25,69	78,33
23.07.2023	14:00	189	342	0,45	5908,28	25,99	78,79
23.07.2023	14:15	195	329	0,41	9190,64	26,25	80,45
23.07.2023	14:30	185	309	0,40	10175,36	26,17	80,76
23.07.2023	14:45	196	341	0,43	6893,00	25,65	81,48
23.07.2023	15:00	199	354	0,44	6564,76	25,68	82,99
23.07.2023	15:15	197	365	0,46	5908,28	25,21	81,65
23.07.2023	15:30	204	369	0,45	6893,00	25,15	82,60
23.07.2023	15:45	200	365	0,45	6893,00	25,65	82,38
23.07.2023	16:00	200	362	0,45	6893,00	26,43	81,25
23.07.2023	16:15	188	341	0,45	8534,16	26,77	78,90
23.07.2023	16:30	192	356	0,46	5908,28	25,73	80,91
23.07.2023	16:45	197	370	0,47	3446,50	25,69	82,95
23.07.2023	17:00	202	367	0,45	6564,76	26,39	81,23
23.07.2023	17:15	199	366	0,46	3446,50	25,79	82,56
23.07.2023	17:30	192	350	0,45	4923,56	26,06	82,22
23.07.2023	17:45	195	346	0,44	7221,25	25,90	80,76
23.07.2023	18:00	197	381	0,48	2625,88	24,58	85,94
23.07.2023	18:15	199	378	0,47	3446,50	24,00	85,71
23.07.2023	18:30	202	388	0,48	1887,35	22,77	87,18
23.07.2023	18:45	202	397	0,49	1805,30	21,99	88,45
23.07.2023	19:00	207	407	0,49	2051,49	21,90	89,22
23.07.2023	19:15	206	414	0,50	2051,49	21,92	90,59
23.07.2023	19:30	204	435	0,53	779,55	21,53	92,37
23.07.2023	19:45	202	441	0,54	820,58	21,32	93,20
23.07.2023	20:00	199	446	0,55	738,53	20,83	93,75
23.07.2023	20:15	193	428	0,55	292,31	20,34	94,42
23.07.2023	20:30	189	422	0,55	169,24	20,14	95,08
23.07.2023	20:45	184	413	0,55	20,54	20,02	95,07
23.07.2023	21:00	175	403	0,57	0,00	19,92	95,27
23.07.2023	21:15	159	378	0,58	0,00	19,89	96,26
23.07.2023	21:30	164	374	0,56	0,00	19,64	97,27
23.07.2023	21:45	157	367	0,57	0,00	19,32	99,21
23.07.2023	22:00	141	316	0,55	0,00	19,12	99,43
23.07.2023	22:15	153	336	0,55	0,00	19,02	99,48
23.07.2023	22:30	204	431	0,53	0,00	18,85	99,43
23.07.2023	22:45	202	423	0,52	0,00	18,76	99,51
23.07.2023	23:00	169	363	0,53	0,00	18,79	99,35
23.07.2023	23:15	194	414	0,53	0,00	18,59	99,30
23.07.2023	23:30	210	447	0,53	0,00	18,35	99,27
23.07.2023	23:45	161	340	0,53	0,00	18,18	99,25

Date	Time	Fs	Fm'	ΦPS2	PAR [lx]	Temperature [°C]	Relative Humidity [%]
24.07.2023	00:00	192	386	0,50	0,00	18,00	99,27
24.07.2023	00:15	205	421	0,51	0,00	17,81	99,29
24.07.2023	00:30	205	416	0,51	0,00	17,64	99,47
24.07.2023	00:45	206	420	0,51	0,00	17,92	99,85
24.07.2023	01:00	210	417	0,50	0,00	18,04	99,83
24.07.2023	01:15	203	413	0,51	0,00	17,84	99,60
24.07.2023	01:30	204	409	0,50	0,00	17,90	99,92
24.07.2023	01:45	204	405	0,50	0,00	17,66	99,60
24.07.2023	02:00	201	401	0,50	0,00	17,49	99,87
24.07.2023	02:15	203	392	0,48	0,00	17,75	100,00
24.07.2023	02:30	204	390	0,48	0,00	17,87	100,00
24.07.2023	02:45	195	381	0,49	0,00	17,88	99,98
24.07.2023	03:00	192	375	0,49	0,00	17,71	99,89
24.07.2023	03:15	190	376	0,50	0,00	17,62	99,90
24.07.2023	03:30	193	367	0,47	0,00	17,50	99,98
24.07.2023	03:45	188	365	0,49	0,00	17,66	100,00
24.07.2023	04:00	190	364	0,48	0,00	17,74	100,00
24.07.2023	04:15	186	360	0,48	0,00	17,82	100,00
24.07.2023	04:30	198	382	0,48	0,00	17,78	100,00
24.07.2023	04:45	198	382	0,48	0,00	17,83	100,00
24.07.2023	05:00	197	379	0,48	0,00	17,81	100,00
24.07.2023	05:15	201	378	0,47	0,00	17,89	100,00
24.07.2023	05:30	207	388	0,47	20,54	17,93	100,00
24.07.2023	05:45	200	403	0,50	87,19	17,99	100,00
24.07.2023	06:00	199	430	0,54	179,49	18,00	100,00
24.07.2023	06:15	202	438	0,54	92,34	18,06	100,00
24.07.2023	06:30	204	437	0,53	138,46	18,07	100,00
24.07.2023	06:45	212	448	0,53	184,63	18,08	100,00
24.07.2023	07:00	212	449	0,53	307,70	18,21	100,00
24.07.2023	07:15	218	450	0,52	1230,91	18,63	100,00
24.07.2023	07:30	227	439	0,48	902,67	18,69	100,00
24.07.2023	07:45	221	436	0,49	1805,30	18,93	100,00
24.07.2023	08:00	199	386	0,48	2051,49	19,03	100,00
24.07.2023	08:15	207	383	0,46	1969,44	19,33	100,00
24.07.2023	08:30	208	354	0,41	3118,26	19,97	100,00
24.07.2023	08:45	205	339	0,40	2461,78	19,83	99,94
24.07.2023	09:00	202	325	0,38	5251,80	19,90	99,90
24.07.2023	09:15	204	319	0,36	2954,12	20,66	99,83
24.07.2023	09:30	182	294	0,38	4923,56	21,26	99,09
24.07.2023	09:45	184	296	0,38	5251,80	22,26	98,16
24.07.2023	10:00	189	296	0,36	6236,52	22,73	94,73
24.07.2023	10:15	193	300	0,36	6564,76	24,81	86,68
24.07.2023	10:30	183	279	0,34	6893,00	24,96	84,94
24.07.2023	10:45	176	281	0,37	3938,84	22,87	90,83
24.07.2023	11:00	184	293	0,37	4431,22	23,35	89,27
24.07.2023	11:15	178	261	0,32	6893,00	22,92	89,75
24.07.2023	11:30	182	285	0,36	3118,26	22,37	92,43
24.07.2023	11:45	173	282	0,39	3938,84	22,53	92,01
24.07.2023	12:00	168	262	0,36	6236,52	23,36	90,04
24.07.2023	12:15	166	254	0,35	6564,76	23,11	89,96
24.07.2023	12:30	175	285	0,39	2954,12	22,89	89,72
24.07.2023	12:45	170	259	0,34	6893,00	23,65	88,43
24.07.2023	13:00	161	253	0,36	6893,00	23,74	85,82
24.07.2023	13:15	167	259	0,36	4923,56	23,72	87,96
24.07.2023	13:30	160	255	0,37	9518,88	24,27	86,34
24.07.2023	13:45	166	281	0,41	5908,28	23,87	87,63
24.07.2023	14:00	170	278	0,39	3446,50	24,52	87,05
24.07.2023	14:15	163	270	0,40	3938,84	24,42	86,11
24.07.2023	14:30	166	266	0,38	8534,16	25,21	83,07
24.07.2023	14:45	160	254	0,37	6236,52	25,01	84,08
24.07.2023	15:00	160	266	0,40	2215,59	23,31	84,46
24.07.2023	15:15	162	267	0,39	5087,66	24,50	83,72
24.07.2023	15:30	162	259	0,38	7221,25	24,96	81,47
24.07.2023	15:45	163	278	0,41	5087,66	24,69	81,56
24.07.2023	16:00	160	274	0,42	1969,44	24,44	80,55
24.07.2023	16:15	164	278	0,41	3118,26	24,02	85,42
24.07.2023	16:30	163	280	0,42	4431,22	24,44	85,14
24.07.2023	16:45	159	286	0,44	2051,49	23,35	86,94
24.07.2023	17:00	161	290	0,45	4595,32	24,65	83,92
24.07.2023	17:15	161	287	0,44	4431,22	24,83	83,33
24.07.2023	17:30	149	261	0,43	4102,98	24,86	82,54
24.07.2023	17:45	164	294	0,44	2954,12	23,95	83,60
24.07.2023	18:00	161	297	0,46	1969,44	23,02	89,25
24.07.2023	18:15	161	308	0,48	1559,11	22,51	91,04
24.07.2023	18:30	165	310	0,47	1395,01	22,03	92,34
24.07.2023	18:45	173	329	0,47	1312,96	21,68	92,74
24.07.2023	19:00	169	339	0,50	1148,82	21,39	93,82
24.07.2023	19:15	167	343	0,51	1025,75	21,04	94,13
24.07.2023	19:30	168	350	0,52	902,67	20,69	94,79
24.07.2023	19:45	166	351	0,53	625,70	20,21	95,12
24.07.2023	20:00	162	345	0,53	507,73	19,73	95,03
24.07.2023	20:15	153	334	0,54	374,41	19,32	96,10
24.07.2023	20:30	135	327	0,59	241,05	18,91	95,58
24.07.2023	20:45	139	316	0,56	92,34	18,55	96,04
24.07.2023	21:00	135	312	0,57	20,54	18,24	96,29
24.07.2023	21:15	136	310	0,56	0,00	17,98	96,57
24.07.2023	21:30	141	314	0,55	0,00	17,78	96,58
24.07.2023	21:45	130	307	0,58	0,00	17,59	96,87
24.07.2023	22:00	130	304	0,57	0,00	17,46	96,76
24.07.2023	22:15	133	305	0,56	0,00	17,32	97,01
24.07.2023	22:30	132	303	0,56	0,00	17,15	96,41
24.07.2023	22:45	132	298	0,56	0,00	17,01	97,20
24.07.2023	23:00	137	297	0,54	0,00	16,89	96,86
24.07.2023	23:15	136	298	0,54	0,00	16,76	97,18
24.07.2023	23:30	134	296	0,54	0,00	16,55	96,86
24.07.2023	23:45	134	290	0,55	0,00	16,50	96,44
24.07.2023	00:00	133	289	0,54	0,00	16,54	97,56

Appendix 7 Data of the pilot cultivation experiments. Initial and final masses (after 21 days) were measured and the effective gain was calculated as: $\frac{(final\ mass - initial\ mass)}{initial\ mass}$. Tested substrate (pilot experiment 1) and tested irrigation interval (pilot experiment 2) are highlighted in blue.

Pilot experiment 1 - Substrates						
Substrate: Marble chippings				Substrate: Glass beads		
Initial dry mass [mg]	Final dry mass [mg]	Effective gain [%]		Initial dry mass [mg]	Final dry mass [mg]	Effective gain [%]
1,97	2,50	26,81		2,69	2,48	-7,52
1,98	3,19	60,67		2,92	2,53	-13,34
2,07	3,64	75,94		2,29	2,99	30,46
1,13	2,32	104,77		0,94	1,05	12,13
2,20	2,31	4,58		2,91	1,81	-37,85
2,41	3,02	25,58		2,80	3,14	11,95
2,65	2,55	-3,59		2,69	0,98	-63,69
2,73	3,83	40,54		1,32	1,83	38,97
2,86	2,78	-2,63		1,45	2,60	78,54
3,42	4,18	22,23		2,20	3,48	58,63

Pilot experiment 2 - Interval						
Substrate: 1,5 h				Substrate: 3 h		
Initial dry mass [mg]	Final dry mass [mg]	Effective gain [%]		Initial dry mass [mg]	Final dry mass [mg]	Effective gain [%]
1,21	1,56	29,33		0,92	2,40	160,33
1,30	2,13	63,67		0,94	1,90	101,17
1,34	2,55	89,73		1,01	1,24	22,82
1,18	1,65	39,31		1,08	1,81	67,84
1,27	2,03	59,42		1,11	1,18	6,59
1,17	1,90	62,10		2,11	3,28	55,28
1,26	1,92	51,94		1,17	1,29	10,80
1,29	2,13	65,40		1,37	1,33	-2,56
1,30	2,24	72,44		1,66	1,85	11,01
1,11	1,15	3,51		1,83	3,07	67,98

Appendix 8 Data of main experiment 1. Initial and final masses (after 21 days) were measured and the effective gain was calculated as: $\frac{(final\ mass - initial\ mass)}{initial\ mass}$. Highlighted in gray are the irrigation methods utilized, while the blue shades denote the media used.

Sprinkler								
BG11_diluted_1_to_10			BG11_N0			Rainwater		
Initial dry mass [mg]	Final dry mass [mg]	Effective gain [%]	Initial dry mass [mg]	Final dry mass [mg]	Effective gain [%]	Initial dry mass [mg]	Final dry mass [mg]	Effective gain [%]
1,07	1,85	72,43	1,18	1,08	-9,04	0,51	0,86	68,55
0,93	3,53	279,35	0,84	0,58	-31,11	0,37	0,26	-31,08
0,46	0,60	30,15	0,64	0,80	25,16	0,60	0,63	5,21
0,75	2,48	231,77	0,64	0,66	2,99	0,71	1,40	97,03
0,80	2,25	180,63	0,61	0,62	1,47	0,61	0,58	-4,46
1,07	1,46	36,26	0,40	0,16	-61,29	0,82	1,15	40,49
1,01	1,18	16,44	0,75	0,58	-23,54	0,70	0,74	4,99
0,54	0,46	-15,19	0,64	0,73	14,89	0,46	0,43	-6,32
0,47	1,40	196,81	0,89	0,41	-53,66	0,85	0,93	8,94
1,08	1,82	68,02	0,69	0,22	-67,45	1,10	0,93	-14,98
1,51	4,29	183,91	0,88	0,54	-38,11	0,35	0,43	24,57
1,66	2,75	65,86	0,53	0,95	80,30	0,74	0,72	-2,04
0,98	1,48	51,13	0,50	1,81	263,91	0,72	0,69	-3,76
0,84	1,16	37,93	0,51	0,39	-23,44	0,53	0,69	29,57
0,57	1,01	78,13	1,25	1,20	-3,76	1,04	0,98	-6,15
1,32	2,12	60,61	0,81	2,86	252,84	0,42	0,43	2,86
0,55	0,87	59,05	1,19	5,73	382,07	0,87	0,97	11,10
1,00	2,10	108,76	0,97	4,11	323,15	0,92	0,93	1,97
0,51	3,67	619,61	0,66	0,46	-30,11	1,00	1,03	3,20
0,73	1,25	71,63	0,99	2,34	137,77	0,74	0,78	5,83
1,07	2,12	97,76	0,53	2,77	424,39	0,49	0,68	38,32
0,75	0,88	17,24	0,55	0,63	15,17	1,00	1,08	7,71
1,24	1,69	36,01	1,03	1,15	12,39	1,05	1,55	48,23
0,48	0,83	73,13	0,86	1,42	64,65	1,03	1,15	11,37
1,00	1,39	39,20	1,02	0,77	-24,31	0,78	0,99	27,09
0,75	1,53	104,55	1,00	3,12	213,65	0,59	0,62	5,08
0,93	1,94	109,73	0,85	1,00	17,83	0,48	0,52	10,32
0,70	1,07	52,14	1,05	0,89	-14,90	0,67	0,90	33,58
0,94	1,90	102,56	0,64	0,75	16,59	0,90	2,18	142,92
0,99	1,78	79,07	0,47	1,05	124,26	0,48	1,02	114,29

Lift without substrate								
BG11_diluted_1_to_10			BG11_N0			Rainwater		
Initial dry mass [mg]	Final dry mass [mg]	Effective gain [%]	Initial dry mass [mg]	Final dry mass [mg]	Effective gain [%]	Initial dry mass [mg]	Final dry mass [mg]	Effective gain [%]
0,76	0,45	-41,11	0,99	0,88	-10,66	0,68	1,00	47,63
1,31	0,85	-35,04	1,00	0,59	-40,72	0,82	0,96	17,42
1,11	0,70	-37,01	1,07	0,83	-22,57	0,62	0,44	-28,64
1,06	0,52	-51,51	0,58	0,55	-6,36	0,33	0,64	94,55
1,05	0,68	-35,62	0,68	1,98	192,33	0,38	0,72	88,16
1,30	0,83	-36,29	0,80	2,06	156,80	1,09	1,11	1,37
0,90	0,51	-43,62	0,65	2,33	258,22	0,81	0,32	-60,52
0,69	0,52	-24,57	0,49	0,49	0,00	0,38	0,77	100,00
0,75	0,59	-20,54	0,89	1,05	18,06	0,91	1,13	24,01
0,60	0,51	-15,73	0,77	1,16	51,57	0,71	0,80	13,44
0,61	0,41	-32,13	0,81	1,20	48,03	0,55	1,01	82,64
0,45	0,38	-14,35	0,97	0,60	-38,04	0,47	0,42	-10,30
1,23	0,82	-33,12	0,73	0,52	-28,37	1,25	0,84	-33,28
0,76	0,29	-61,99	0,94	1,71	81,55	0,53	0,45	-14,86
0,96	0,40	-58,77	0,53	0,74	39,47	0,55	0,98	79,56
1,02	0,54	-47,17	0,91	0,56	-38,46	0,97	0,52	-46,60
0,73	0,31	-57,49	1,11	0,76	-31,29	0,62	0,47	-23,86
0,89	0,56	-36,79	0,69	0,96	40,58	0,79	1,11	40,25
1,19	0,64	-46,43	0,73	0,68	-6,04	0,42	0,56	31,21
1,33	0,80	-39,77	1,06	0,85	-19,59	1,02	0,55	-46,53
1,33	0,75	-43,90	0,41	0,20	-50,62	0,78	0,74	-5,13
0,72	0,39	-45,67	0,60	0,45	-25,00	1,19	0,93	-21,90
0,81	0,35	-56,33	0,90	2,46	171,57	0,91	0,40	-56,07
0,70	0,42	-39,71	0,69	0,57	-17,80	0,35	0,84	139,09
1,22	1,26	3,53	0,41	0,20	-50,12	1,14	1,15	0,79
0,51	0,50	-1,78	0,87	3,75	330,05	0,82	0,38	-53,58
0,93	0,75	-19,29	0,72	0,56	-23,02	0,67	0,34	-49,85
1,15	1,17	1,48	0,65	0,48	-26,31	0,44	0,55	25,51
1,06	0,89	-16,27	0,66	0,53	-19,05	1,01	0,79	-21,70
0,55	0,50	-9,29	1,10	1,11	1,00	1,05	0,67	-36,35

Appendix 9 Data of main experiment 2. Initial and final masses (after 21 days) were measured and the effective gain was calculated as: $\frac{(final\ mass - initial\ mass)}{initial\ mass}$. Highlighted in gray are the irrigation methods utilized, while the blue shades denote the media used. Removed* indicates that this colony was removed due to degradation during the experiment to reduce contamination.

Sprinkler								Submerged		
BG11				BG11_N0				BG11		
Initial dry mass [mg]	Final dry mass [mg]	Effective gain [%]		Initial dry mass [mg]	Final dry mass [mg]	Effective gain [%]		Initial dry mass [mg]	Final dry mass [mg]	Effective gain [%]
1,35	3,03	125,04		1,13	2,78	147,38		1,78	1,51	-15,38
1,22	1,20	-1,80		1,14	0,74	-34,74		0,82	1,00	22,03
1,46	1,07	-26,19		1,86	1,59	-14,18		1,28	0,93	-27,29
1,19	1,16	-2,36		1,04	1,22	17,61		0,72	0,69	-5,11
1,62	1,07	-33,95		1,40	1,49	6,44		0,97	1,19	22,84
1,23	0,70	-43,44		0,75	0,31	-58,93		0,96	1,33	39,02
1,58	1,37	-13,39		1,77	1,62	-8,27		0,97	1,10	13,86
1,13	0,67	-40,20		1,80	1,38	-23,65		1,34	1,87	39,30
1,51	0,88	-41,55		1,80	3,34	85,52		0,91	1,76	93,28
0,93	1,22	31,04		1,28	2,28	77,54		1,10	1,11	1,37
1,19	0,70	-41,21		0,75	0,47	-36,73		1,95	1,93	-0,57
0,84	1,06	26,37		1,19	1,99	67,76		1,15	0,89	-22,39
1,32	1,54	16,73		1,01	3,08	204,55		2,18	2,00	-8,05
1,87	1,78	-5,02		1,81	3,62	100,72		1,49	1,86	24,41
0,69	0,61	-11,68		1,18	2,74	132,63		0,89	1,82	103,70
0,91	1,12	22,64		1,09	1,47	34,53		0,93	2,16	133,69
0,81	0,68	-15,49		0,87	1,53	76,52		0,94	1,15	22,65
1,67	1,76	5,02		1,44	3,97	176,38		1,44	1,62	12,12
1,51	1,30	-14,35		0,76	3,01	296,45		1,29	1,11	-13,76
0,87	0,78	-10,89		1,41	2,79	97,38		1,73	1,27	-26,79
1,35	0,85	-36,81		1,45	1,76	21,38		1,79	1,14	-36,29
1,39	1,35	-2,59		0,86	2,83	229,87		1,69	1,50	-11,39
1,92	1,90	-1,30		1,30	removed*			1,81	1,01	-44,09
1,28	1,15	-9,64		1,73	2,29	32,70		1,41	1,29	-8,50
1,61	0,94	-41,18		1,39	3,61	159,71		1,02	1,05	2,64
1,93	1,26	-34,44		1,15	1,41	21,96		1,26	1,18	-6,82
0,68	0,38	-43,81		0,93	1,14	22,10		1,43	1,22	-14,24
1,35	1,02	-24,93		1,59	removed*			1,10	0,70	-36,75
0,63	0,37	-41,46		1,35	1,29	-4,73		2,35	3,84	63,60
1,30	0,66	-48,96		1,27	1,09	-13,80		1,38	1,27	-8,03
1,48	0,84	-42,96		1,76	1,35	-23,62		1,20	1,32	10,43
1,52	1,35	-11,62		1,16	0,43	-63,36		1,24	1,37	9,99
1,74	1,61	-7,38		1,49	1,15	-22,58		0,97	0,83	-14,26
1,10	0,43	-60,53		1,51	0,68	-55,33		1,16	1,42	22,40
1,02	0,64	-37,04		1,39	2,47	77,54		0,88	0,58	-33,94
0,78	0,64	-18,15		1,18	0,69	-42,15		1,69	2,21	31,02
1,09	1,04	-4,58		1,20	1,56	30,43		0,77	1,84	137,60
1,56	1,12	-28,52		1,07	1,34	25,33		0,88	1,14	28,39
0,90	0,70	-22,36		1,27	1,28	1,02		0,88	1,43	62,17
1,42	1,10	-22,87		0,90	0,96	6,50		2,32	1,45	-37,66

* degraded colony removed to prevent contamination

Lift								Submerged		
BG11				BG11_N0				BG11_N0		
Initial dry mass [mg]	Final dry mass [mg]	Effective gain [%]		Initial dry mass [mg]	Final dry mass [mg]	Effective gain [%]		Initial dry mass [mg]	Final dry mass [mg]	Effective gain [%]
1,59	1,28	-19,30		0,96	3,43	258,35		1,09	1,16	5,94
0,88	0,75	-14,71		1,39	1,87	34,37		1,08	2,70	149,26
1,26	1,65	30,77		1,12	0,78	-30,40		1,54	1,82	17,90
1,66	2,46	48,67		1,17	0,57	-51,75		1,73	1,17	-32,37
1,26	0,81	-35,40		1,20	0,71	-40,72		1,28	1,83	43,53
1,21	3,22	165,81		1,01	0,95	-5,83		1,16	1,84	59,26
1,23	0,86	-30,09		1,17	1,37	16,79		0,82	1,93	134,34
1,27	0,88	-30,50		1,39	0,62	-55,47		0,84	1,76	109,67
1,22	0,96	-21,49		0,79	1,32	66,46		0,81	2,82	249,07
1,50	8,18	445,93		1,52	7,86	418,00		1,60	3,67	129,07
1,76	1,17	-33,47		1,46	1,86	27,31		1,90	3,57	88,39
1,46	1,00	-31,27		1,92	1,58	-17,48		1,39	3,72	167,43
1,13	0,72	-36,68		1,97	1,62	-17,53		1,12	3,23	187,10
1,16	1,61	38,49		1,31	1,37	4,04		1,17	3,42	192,65
1,89	3,80	101,06		1,53	3,29	115,30		0,56	2,20	294,62
1,20	1,42	18,67		1,88	3,84	104,90		1,47	1,32	-10,30
1,00	0,98	-2,19		1,11	1,49	34,45		1,44	4,39	204,51
1,25	0,96	-23,26		1,27	2,48	95,51		0,99	2,17	119,80
1,79	2,60	45,39		1,21	1,50	23,80		1,96	3,26	66,07
1,26	1,91	51,15		1,67	1,12	-32,71		1,42	3,53	149,22
1,29	1,52	17,60		0,90	0,79	-12,11		2,21	1,81	-18,26
1,77	1,92	9,01		1,04	6,23	499,90		1,92	4,65	142,08
1,76	1,87	5,79		1,43	1,00	-29,83		1,50	1,42	-5,41
1,74	1,58	-8,82		1,46	0,84	-42,52		1,56	1,34	-14,53
1,61	0,79	-51,21		1,91	1,09	-43,08		1,99	1,63	-17,82
1,85	1,22	-33,78		1,47	2,75	86,84		1,44	4,05	181,00
1,50	0,90	-39,73		1,16	2,68	131,95		1,51	1,27	-15,73
0,90	removed*			1,25	0,40	-68,11		2,23	2,78	24,90
1,85	1,11	-39,89		0,76	0,30	-60,19		1,55	1,79	15,70
1,64	1,78	8,98		1,28	2,61	103,90		1,32	1,16	-11,77
1,78	0,29	-83,96		0,75	0,61	-19,01		1,83	1,88	3,01
0,90	0,83	-7,80		1,43	1,26	-11,71		0,70	1,94	176,39
1,24	0,66	-46,98		1,40	0,85	-39,01		0,93	2,41	158,52
1,18	1,25	5,96		1,21	6,85	468,22		2,01	2,46	22,44
1,95	5,23	167,64		1,54	0,86	-44,00		0,71	0,85	19,75
1,22	1,35	10,30		1,33	0,98	-26,40		1,08	2,20	103,61
1,11	1,26	13,36		1,25	0,88	-29,00		0,73	1,44	96,31
1,09	1,05	-3,86		1,39	0,93	-33,07		1,68	3,51	109,73
0,99	0,60	-40,04		1,67	2,98	78,82		1,66	5,17	210,76
1,49	0,67	-54,80		1,07	1,15	8,17		1,02	0,92	-9,42

Appendix 10 Data of main experiment 2. Initial and final masses (after 21 days) were measured and the effective gain was calculated as: $\frac{(final\ mass - initial\ mass)}{initial\ mass}$. Highlighted in gray are the irrigation methods utilized, while the blue shades denote the media used. For the Day & Night setting samples were illuminated 16 h followed by an 8 h dark period. Removed* indicates that this colony was removed due to degradation during the experiment to reduce contamination.

24 h Interval								
BG11_N/10			BG11_N0			BG11_N/10 (Day & Night)		
Initial dry mass [mg]	Final dry mass [mg]	Effective gain [%]	Initial dry mass [mg]	Final dry mass [mg]	Effective gain [%]	Initial dry mass [mg]	Final dry mass [mg]	Effective gain [%]
1,35	13,72	914,34	1,70	7,84	361,18	1,76	7,48	325,00
1,10	10,40	844,60	0,85	4,75	458,82	1,22	4,62	278,69
1,46	7,34	403,08	0,77	4,99	548,05	1,62	5,77	256,17
1,87	20,63	1003,80	1,15	8,64	651,30	0,92	6,48	604,35
1,17	8,78	651,71	1,69	6,64	292,90	1,40	7,62	444,29
1,74	9,75	460,34	1,12	8,42	651,79	1,22	9,36	667,21
1,51	removed*		1,21	3,33	175,21	1,67	8,27	395,21
1,06	10,60	899,06	1,43	2,85	99,30	1,66	11,17	572,89
1,23	3,65	196,03	0,94	7,56	704,26	1,19	5,26	342,02
0,55	9,75	1679,20	1,22	11,63	853,28	1,39	11,03	693,53
1,63	16,92	936,76	1,86	13,95	649,19	1,76	17,35	885,80
1,60	13,10	717,22	1,55	17,95	1058,06	1,23	7,21	486,18
2,19	2,43	11,01	0,90	5,66	528,89	0,81	6,15	659,26
1,20	removed*		0,83	15,41	1756,63	2,16	20,39	843,98
1,06	removed*		1,05	7,93	655,24	1,16	9,06	681,03
1,19	2,23	87,65	1,46	7,55	417,12	1,07	4,40	311,21
1,12	removed*		2,02	6,49	221,29	1,55	9,65	524,19
1,24	removed*		1,33	11,55	768,42	1,52	9,30	511,84
1,16	8,54	633,68	1,35	3,21	137,78	1,55	7,56	387,74
1,61	9,13	467,79	1,82	1,65	-9,34	1,76	5,83	231,25
1,41	removed*		1,55	15,39	892,90	2,02	2,18	7,92
1,52	removed*		1,34	6,06	352,24	1,86	3,60	93,55
1,10	7,20	555,74	1,15	2,45	113,04	1,64	15,15	823,78
1,59	18,98	1090,72	1,85	14,89	704,86	1,87	16,00	755,61
0,94	4,11	337,70	2,13	10,31	384,04	1,58	7,89	399,37
0,90	2,66	195,56	1,60	18,02	1026,25	2,56	9,12	256,25
1,31	3,13	138,20	1,92	13,64	610,42	2,06	7,15	247,09
1,90	8,12	327,82	1,75	8,32	375,43	1,90	7,35	286,84
2,03	5,91	191,56	1,27	8,49	568,50	1,54	11,35	637,01
2,21	11,83	435,78	1,02	5,27	416,67	1,75	7,83	347,43
1,28	13,43	949,22	1,87	0,00	-100,00	1,11	removed*	
1,67	11,20	572,67	2,15	0,00	-100,00	0,52	removed*	
0,91	5,48	500,88	1,29	5,73	344,19	1,45	removed*	
0,88	8,96	921,66	1,31	6,42	390,08	1,40	removed*	
0,90	removed*		1,34	10,50	683,58	0,95	removed*	
1,24	9,74	686,75	0,82	10,37	1164,63	1,94	removed*	
1,22	5,18	325,64	1,46	14,55	896,58	1,92	5,22	171,88
1,88	10,21	443,37	1,54	8,62	459,74	1,04	7,17	589,42
2,29	5,17	125,57	1,92	4,77	148,44	0,93	1,98	112,90
1,51	9,93	557,62	1,71	15,05	780,12	1,32	5,59	323,48

* degraded colony removed to prevent contamination

48 h Interval			Submerged					
BG11_N/10			BG11_N/10			BG11_N0		
Initial dry mass [mg]	Final dry mass [mg]	Effective gain [%]	Initial dry mass [mg]	Final dry mass [mg]	Effective gain [%]	Initial dry mass [mg]	Final dry mass [mg]	Effective gain [%]
0,94	3,40	260,17	1,26	1,77	40,48	1,27	1,54	21,26
0,96	4,87	408,88	1,92	2,28	18,75	1,80	1,29	-28,33
1,72	4,98	189,20	0,92	0,86	-6,62	2,20	3,15	43,18
1,95	5,91	203,70	1,55	1,64	5,81	1,17	1,75	49,57
1,73	4,65	168,48	1,88	1,38	-26,60	1,20	2,78	131,67
0,70	1,65	136,73	1,22	2,19	79,51	1,44	2,27	57,97
0,97	2,48	156,99	1,11	1,15	3,60	1,92	3,55	84,90
1,94	5,94	206,03	2,13	1,76	-17,37	1,00	0,98	-2,00
2,09	6,42	207,32	1,97	2,24	13,71	2,01	1,96	-2,49
1,37	4,39	219,97	1,18	2,65	124,58	1,28	2,75	114,17
1,93	3,49	81,20	1,18	3,04	157,63	2,16	0,76	-64,81
2,04	4,46	118,73	0,92	2,29	148,91	1,17	1,37	17,09
1,58	4,66	194,19	2,04	3,91	91,67	1,44	0,96	-33,40
1,38	5,99	335,00	2,00	4,09	104,50	1,12	1,16	3,57
1,77	13,68	674,63	2,14	4,04	88,79	1,36	0,89	-34,56
1,72	7,25	321,51	1,76	3,66	107,95	1,43	2,65	85,31
2,17	9,41	334,04	1,79	4,25	137,43	2,20	2,49	13,18
0,82	4,51	450,00	1,69	2,70	59,39	1,18	2,59	119,49
2,07	8,47	309,38	1,85	3,85	108,11	1,57	2,32	47,77
1,51	5,38	256,76	1,60	2,45	53,13	1,73	2,73	57,80
1,16	4,33	273,28	1,99	3,51	76,38	1,21	2,90	139,67
1,48	4,29	190,85	1,94	4,32	122,68	1,69	2,14	26,63
1,52	4,67	207,24	1,58	1,27	-19,62	1,16	1,81	56,03
1,10	3,45	212,50	2,03	1,59	-21,67	1,37	2,25	64,23
1,43	3,17	122,14	1,58	2,98	88,61	0,87	2,59	197,70
1,60	3,32	107,76	1,38	4,04	192,75	1,70	1,61	-5,29
1,13	8,85	682,49	1,26	2,46	95,24	1,55	3,54	128,65
1,22	5,23	328,17	1,77	3,86	118,08	1,50	2,49	66,00
1,26	3,56	183,21	1,78	1,17	-34,12	1,33	1,41	6,42
2,99	10,08	237,58	1,31	1,23	-6,11	1,66	2,78	67,47
1,51	6,97	360,67	1,73	1,80	4,05	0,72	2,32	222,22
1,38	5,53	299,86	1,65	1,12	-32,12	0,40	3,06	665,00
1,78	5,62	215,38	1,61	2,65	64,60	1,56	3,42	119,23
0,77	3,09	302,34	1,27	2,50	96,85	1,31	2,15	64,12
1,61	5,59	247,42	1,43	2,61	82,52	1,36	2,38	75,00
1,05	3,47	229,22	2,14	2,73	27,57	1,19	2,55	114,29
1,54	5,24	240,04	1,27	2,57	102,36	0,51	3,14	515,69
1,83	3,96	116,87	1,38	1,41	2,17	1,82	2,31	26,92
1,71	1,14	-33,37	1,21	0,67	-44,63	1,31	3,40	159,54
1,32	2,75	108,65	1,20	0,71	-40,83	1,88	1,81	-3,72

Appendix 11 Data from the PAM fluorescence measurements on a *Nostoc* colony which was submerged for 20 min with the constructed lift in $BG11_{N0}$ medium and afterwards let dry at air. Marble chippings were used as substrate and the run time was 24 h

First rehydration after longterm desiccation				Second rehydrateion after 24 h				Third rehydration after 48 h			
Time	Fs	Fm'	PSII	Time	Fs	Fm'	PSII	Time	Fs	Fm'	PSII
00:00	352	362	0,03	00:00	139	203	0,32	00:00	226	412	0,45
00:15	393	424	0,07	00:15	472	707	0,33	00:15	230	447	0,49
00:30	375	413	0,09	00:30	451	737	0,39	00:30	237	483	0,51
00:45	357	406	0,12	00:45	416	704	0,41	00:45	240	497	0,52
01:00	355	409	0,13	01:00	400	692	0,42	01:00	240	503	0,52
01:15	339	407	0,17	01:15	397	688	0,42	01:15	243	514	0,53
01:30	335	405	0,17	01:30	376	651	0,42	01:30	244	519	0,53
01:45	326	403	0,19	01:45	350	618	0,43	01:45	243	524	0,54
02:00	320	405	0,21	02:00	346	616	0,44	02:00	244	525	0,54
02:15	318	405	0,22	02:15	346	615	0,44	02:15	245	526	0,53
02:30	313	405	0,23	02:30	347	618	0,44	02:30	245	526	0,53
02:45	304	411	0,26	02:45	346	616	0,44	02:45	250	528	0,53
03:00	305	415	0,27	03:00	348	620	0,44	03:00	250	528	0,53
03:15	304	417	0,27	03:15	347	621	0,44	03:15	248	529	0,53
03:30	303	416	0,27	03:30	352	620	0,43	03:30	250	528	0,53
03:45	302	421	0,28	03:45	350	624	0,44	03:45	252	530	0,53
04:00	305	429	0,29	04:00	350	629	0,44	04:00	249	528	0,53
04:15	305	433	0,30	04:15	353	631	0,44	04:15	250	526	0,53
04:30	301	439	0,31	04:30	359	634	0,43	04:30	248	519	0,52
04:45	305	440	0,31	04:45	358	635	0,44	04:45	253	522	0,52
05:00	308	450	0,32	05:00	360	642	0,44	05:00	253	521	0,51
05:15	307	453	0,32	05:15	364	650	0,44	05:15	254	522	0,51
05:30	307	460	0,33	05:30	368	654	0,44	05:30	253	523	0,52
05:45	309	463	0,33	05:45	368	657	0,44	05:45	254	525	0,52
06:00	307	470	0,35	06:00	369	659	0,44	06:00	255	525	0,51
06:15	309	471	0,34	06:15	372	661	0,44	06:15	257	528	0,51
06:30	308	473	0,35	06:30	369	671	0,45	06:30	257	528	0,51
06:45	313	480	0,35	06:45	379	668	0,43	06:45	260	529	0,51
07:00	312	486	0,36	07:00	381	674	0,44	07:00	261	527	0,51
07:15	312	487	0,36	07:15	386	680	0,43	07:15	258	531	0,51
07:30	317	490	0,35	07:30	386	689	0,44	07:30	265	530	0,50
07:45	316	500	0,37	07:45	394	695	0,43	07:45	264	531	0,50
08:00	316	502	0,37	08:00	399	701	0,43	08:00	261	534	0,51
08:15	322	510	0,37	08:15	398	710	0,44	08:15	263	535	0,51
08:30	320	513	0,38	08:30	391	678	0,42	08:30	264	536	0,51
08:45	320	517	0,38	08:45	402	713	0,44	08:45	264	537	0,51
09:00	332	536	0,38	09:00	409	726	0,44	09:00	265	534	0,50
09:15	325	533	0,39	09:15	413	730	0,43	09:15	265	535	0,51
09:30	331	533	0,38	09:30	415	734	0,44	09:30	282	586	0,52
09:45	319	521	0,39	09:45	417	737	0,43	09:45	283	592	0,52
10:00	314	508	0,38	10:00	415	735	0,44	10:00	288	593	0,51
10:15	307	489	0,37	10:15	418	735	0,43	10:15	289	595	0,51
10:30	303	488	0,38	10:30	415	735	0,44	10:30	290	598	0,52
10:45	286	466	0,39	10:45	402	714	0,44	10:45	290	597	0,51
11:00	273	443	0,38	11:00	389	690	0,44	11:00	288	599	0,52
11:15	259	423	0,39	11:15	378	661	0,43	11:15	293	597	0,51
11:30	247	404	0,39	11:30	356	620	0,43	11:30	293	598	0,51
11:45	232	376	0,38	11:45	336	580	0,42	11:45	294	598	0,51
12:00	214	353	0,39	12:00	317	552	0,43	12:00	293	601	0,51
12:15	199	324	0,39	12:15	305	536	0,43	12:15	297	600	0,51
12:30	182	292	0,38	12:30	293	512	0,43	12:30	296	596	0,50
12:45	163	267	0,39	12:45	282	493	0,43	12:45	293	594	0,51
13:00	150	246	0,39	13:00	275	477	0,42	13:00	292	591	0,51
13:15	143	227	0,37	13:15	267	462	0,42	13:15	290	584	0,50
13:30	128	212	0,40	13:30	264	456	0,42	13:30	284	572	0,50
13:45	126	199	0,37	13:45	267	457	0,42	13:45	282	565	0,50
14:00	122	189	0,35	14:00	266	454	0,41	14:00	276	560	0,51
14:15	109	172	0,37	14:15	250	419	0,40	14:15	270	546	0,51
14:30	101	158	0,36	14:30	244	411	0,41	14:30	264	536	0,51
14:45	92	142	0,35	14:45	400	672	0,41	14:45	255	519	0,51
15:00	85	127	0,33	15:00	369	604	0,39	15:00	251	503	0,50
15:15	100	141	0,29	15:15	343	545	0,37	15:15	245	486	0,50
15:30	125	188	0,34	15:30	305	458	0,33	15:30	240	476	0,50
15:45	115	170	0,32	15:45	272	381	0,29	15:45	233	462	0,50
16:00	97	146	0,34	16:00	243	326	0,26	16:00	224	444	0,50
16:15	82	117	0,30	16:15	221	286	0,23	16:15	215	427	0,50
16:30	65	84	0,23	16:30	213	266	0,20	16:30	212	416	0,49
16:45	49	55	0,11	16:45	210	258	0,19	16:45	205	403	0,49
17:00	41	51	0,20	17:00	202	238	0,15	17:00	198	384	0,48
17:15	47	52	0,10	17:15	187	201	0,07	17:15	191	366	0,48
17:30	44	50	0,12	17:30	182	183	0,01	17:30	186	349	0,47
17:45	46	50	0,08	17:45	183	186	0,02	17:45	179	334	0,46
18:00	46	49	0,06	18:00	181	185	0,02	18:00	173	319	0,46
18:15	44	51	0,14	18:15	185	189	0,02	18:15	168	298	0,44
18:30	46	51	0,10	18:30	184	186	0,01	18:30	160	277	0,42
18:45	43	50	0,14	18:45	186	187	0,01	18:45	148	252	0,41
19:00	45	50	0,10	19:00	184	190	0,03	19:00	145	230	0,37
19:15	45	49	0,08	19:15	182	186	0,02	19:15	140	213	0,34
19:30	47	50	0,06	19:30	185	190	0,03	19:30	134	196	0,32
19:45	47	49	0,04	19:45	187	188	0,01	19:45	122	183	0,33
20:00	44	48	0,08	20:00	188	192	0,02	20:00	116	171	0,32
20:15	44	50	0,12	20:15	184	187	0,02	20:15	116	158	0,27
20:30	45	50	0,10	20:30	186	186	0,00	20:30	110	150	0,27
20:45	46	50	0,08	20:45	185	187	0,01	20:45	108	141	0,23
21:00	43	51	0,16	21:00	185	190	0,03	21:00	107	136	0,21
21:15	48	49	0,02	21:15	185	188	0,02	21:15	102	129	0,21
21:30	45	50	0,10	21:30	185	187	0,01	21:30	102	126	0,19
21:45	44	49	0,10	21:45	186	189	0,02	21:45	103	124	0,17
22:00	47	50	0,06	22:00	186	188	0,01	22:00	96	119	0,19
22:15	49	48	0,00	22:15	184	185	0,01	22:15	96	108	0,11
22:30	48	50	0,04	22:30	186	186	0,00	22:30	95	105	0,10
22:45	47	50	0,06	22:45	182	189	0,04	22:45	97	102	0,05
23:00	48	49	0,02	23:00	186	186	0,00	23:00	93	97	0,04
23:15	46	48	0,04	23:15	183	188	0,03	23:15	92	95	0,03
23:30	46	50	0,08	23:30	188	190	0,01	23:30	45	55	0,18
23:45	45	51	0,12	23:45	186	189	0,02	23:45	49	51	0,04
24:00	45	50	0,10	24:00	185	187	0,01	24:00	48	51	0,06